

Final Report

Reporting Date
31/12/2019

Project of
**Sri Lankan Wave Energy Resource Assessment
and Characterisation**

Prasanna Gunawardane

Matt Folley

Ravindu Lokuliyana

Nalin Wikramanayake

Harsha Ratnasooriya

Document Reference: WERSL-R-191231-RL

Document Version: B

Table of Contents

1.	Project Overview	1
2.	Objectives of the Project.....	2
3.	IEC Technical Specification (IEC TS 62600-101)	2
4.	Previously conducted wave resource studies in Sri Lanka	5
5.	Application of IEC TS 62600-101 to Sri Lanka	8
5.1	Class the resource assessment	9
5.2	Description of the study area.....	9
5.3	Boundary datasets	10
5.3.1	Bathymetry.....	11
5.3.2	Wave Data.....	13
5.4	Numerical Modelling	13
5.4.1	Selection of a third-generation wave model	16
5.4.2	SWAN model.....	17
5.4.3	Computational spatial grid.....	19
5.4.4	Unstructured grid for the model construction.....	19
5.4.5	Spatial input grids	21
5.4.6	Spectral input grid.....	21
5.4.7	Activation of physical processes.....	23
5.4.8	Output grids	24
6.	Model tuning and calibration	24
6.1	Model tuning with sensitivity analysis.....	24
6.2	Model calibration	26
6.3	Model Validation datasets.....	26
6.3.1	CCD-GTZ dataset	26
6.3.2	China Harbour Coperation dataset (SCSIO Project).....	27
6.3.3	GOW2 dataset.....	28
7.	Model validation	29
7.1	Model validation procedure	30
8.	Data analysis	33
9.	Presentation of results	34
9.1	Presentation of regional information.....	34
9.2	Presentation of information at study points.....	35

10.	Underlying assumptions.....	37
11.	Assessment of uncertainty	37
12.	Discussion.....	38
13.	Digital database.....	40
14.	Conclusions.....	41
15.	References.....	42
	Annex A : Sensitivity Analysis	
	Annex B : Model Validation	
	Annex C : Data Analysis	
	Annex D : Extent of Validation	
	Annex E : Presentation of Regional Information	
	Annex F : Presentation of Study Points	
	Annex G : Evaluation of Long-term Uncertainty	
	Annex H : User Manual : Model setup and implementation	

List of Figures

Figure 1: IEC TS 62600-101 Methodology	2
Figure 2: Study area of the wave resource assessment	10
Figure 3: Bathymetric contour map around Sri Lanka	12
Figure 4 : Developed Unstructured Grid around Sri Lanka.....	20
Figure 5: Spectral grid inputs used for the model construction	23
Figure 6: Location of CCD-GTZ buoy	27
Figure 7 : Observation deployment locations and topography	28
Figure 8 : Available GOW2 spectral data locations around Sri Lanka and selected validation points.....	29
Figure 9 : Model validation flow chart : IEC TS 62600-101:2015.....	31
Figure 10 : Example of the annual variation of the frequency wave spectrum	33
Figure 11: Study Points.....	36
Figure 12: Omni-directional wave power at 50 m water depth	39

List of Tables

Table 1: Classes of resource assessment.....	9
Table 2: Resolution of bathymetric data according to IEC standards	11
Table 3: Elements of suitable numerical models	14
Table 4: Statistics of the unstructured grid	20
Table 5: Specifications of the bathymetric and wind dataset	21
Table 6 : Specifications of two-dimensional wave spectral dataset	22
Table 7: Used physical processes and related authors	23
Table 8: Dataset profile, wind and wave dataset for Matara, Sri Lanka.....	28
Table 9 : Minimum validation requirements [54].....	31
Table 10: Summary of wave energy resource parameters to be archived and mapped.....	34
Table 11: Theoretical wave energy resourc potential of each province	40

Nomenclature

H_{mo}	Significant wave height
T_e	Energy Period
T_m	Mean wave period
T_z	Zero crossing period
T_p	Peak period
Θ	Mean wave direction
J	Wave power
J_θ	Directionally resolved wave power
$J_{\theta_{max}}$	Maximum time average wave power
$\theta_{J_{max}}$	Direction of maximum directionally resolved wave power
d	Directionality coefficient
m_n	Spectral moments of the n^{th} order
c_g	Group velocity
c_x	Propagation velocity in x space
c_y	Propagation velocity in y space
c_σ	Propagation velocity in σ space
c_θ	Propagation velocity in θ space
$S(\sigma, \theta)$	Source term in terms of energy density
$S(f, \theta)$	Variance density spectrum
RMSE	Root Mean Square Error
MAE	Mean Average Error
$b(e_p)$	Max acceptable weighted mean systematic error
$\sigma(e_p)$	Max acceptable weighted mean random error,

Acronyms

IEC	International Electro-technical Committee
TS	Technical Specification
PAS	Public Available Specifications
SWM	South West Monsoon Current
SW	southwest
NE	northeast
NMC	Northeast Monsoon Current
CCD	Coast Conservation Department -
WW3	WaveWatch 3
WAM	WAve Model
SWAN	Simulations WAves Neashore
ECMWF	European Centre for Medium-Range Weather Forecasts
NCEP	National Centres for Environmental Prediction
NOAA	National Oceanic and Atmospheric Administration
SCSIO	South China Sea Institute Of Oceanology
GEBCO	The General Bathymetric Chart of the Oceans
WEC	Wave Energy Convertor
MAE	Mean Average Error
ME	Maximum Error

1. Project Overview

Wave energy is one of the promising sources of renewable energy, and an island nation like Sri Lanka needs to achieve sustainable energy mix [1–4]. Worldwide there are a large number of companies developing wave energy technologies and are looking for potential deployment sites for both prototypes and commercial wave farms [6,7]. Amongst the many factors that may influence a company's choice of location is the availability of good quality data on the wave resource. Moreover, it is not only that the resource needs to be estimated, but it must also be characterised and presented in a way that allows it to be used effectively for calculation of the annual energy production for a particular technology [7]. The development of quality dataset for wave energy analysis typically addresses through a wave energy resource assessment which should conduct under a set of internationally recommended standards. As the interest in the exploitation of wave energy, there has been an explosion in the number of studies of the wave energy [9–18], but a limited number of them have followed specific standards.

Some of the established companies in the wave energy sector have already shown their interest on deploying wave energy convertors in Sri Lankan waters [19–21], but none of those projects have not been realized. One of the influential factors for such a drawback is the uncertainty on the annual energy production due to lack of reliable wave resource dataset. So that implementation of wave energy resource assessment under sets of international standards is a contemporary requirement to assess and characterise the available wave power around Sri Lanka. This requirement can be achieved by following the recently published International Electro-technical Committee (IEC) Technical Specification (TS 62600-101) that is designed specifically for the exploitation of wave energy [19].

This research project has specifically designed to assess and characterise the wave energy resource availability around Sri Lanka which has followed the standards of IEC TS 62600-101. This can catapult Sri Lanka into a small group of nations that can provide good quality wave resource data to prospective investors. Besides, the research project has not only assessed and characterised the wave resource but also identify the most promising areas for wave energy exploitation and the total technical wave energy resource of Sri Lanka. Finally, the project has produced illustrations of the use of the Sri Lankan wave resource that can be used to help promote Sri Lanka as a potential site for wave energy converter deployment.

2. Objectives of the Project

1. Produce wave resource data to IEC standards, which can be used by developers to assess the potential for their wave energy technologies in Sri Lanka.
2. Identify the most promising deployment locations for wave energy converters, based on the wave resource characteristics.
3. Calculate the mean annual energy production and its uncertainty for a wave energy converter deployed in Sri Lankan waters.
4. Estimate the available wave energy resource potential of Sri Lanka.

3. IEC Technical Specification (IEC TS 62600-101)

International Electro-technical Committee (IEC) is a well-recognised organisation for publishing international standards, Technical Specifications, Technical Reports, Public Available Specifications (PAS) and guides in different electrical and electronic fields. The IEC has recently published a Technical Specification (TS 62600-101) for the wave energy resource assessment and characterisation that is designed specifically for the exploitation of wave energy. This Technical Specification (TS) sets recommendations for wave resource assessments by describing the procedures for study planning and data collection, numerical modelling, data analysis, and technical report writing. The methodology which describes for wave energy resource assessment in IEC TS 62600-101 can be summarised into six major stages, as shown in Figure 1.

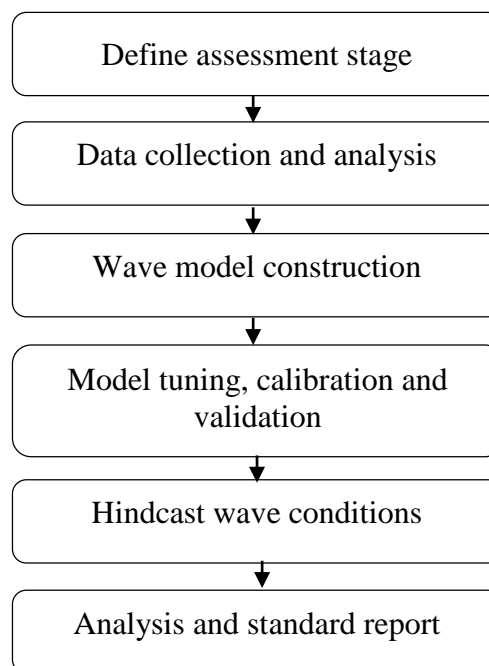


Figure 1: IEC TS 62600-101 Methodology

The first stage focuses on defining the appropriate assessment stage of the resource assessment. There are three main classes of resource assessments; Reconnaissance, Feasibility and Design, which are defined on the desired level of accuracy and uncertainties of wave energy resource parameter estimations. The Reconnaissance class is designed for the wave resource applications over large sea scale which would probably be the initial wave resource assessment of the particular area. This type of resource assessment identifies the locations which consist of high wave energy density. The Feasibility class can be considered as the refinement of Reconnaissance resource assessment which is designed to assess the wave energy potential of the identified sites. The Design class is considered as the most detailed assessment which delivers the in-depth analysis of wave energy potential of the specific site of interest. The overall effort and the accuracy level increase with each class of the wave resource assessment. In the Sri Lankan perspective, the required class of assessment should have to identify with respect to previously conducted studies.

The data collection and analysis involves collecting the required boundary and validation datasets for model development and validation. The principal boundary data required for a wave propagation model are bathymetry, the wave conditions on the boundaries of the modelled area, the strength and direction of marine currents and the meteorological conditions required to drive the wave generation and propagation. The model validation datasets typically obtain as wave measured or buoy datasets inside the model area, which are conducted for an appropriate period. These datasets would find from different sources, but the recommended resolutions which defined under standards should be satisfied for each dataset. As an example, if the resource assessment has followed the Reconnaissance study, the recommended spatial resolution of wind speed and direction over the specific model is 100 km. Similarly, recommended standards for other boundary and validation datasets are defined concerning the class of the assessment.

The third step involves the development of a wave propagation model. The numerical model features that are required to be considered, recommended and not permitted for each resource assessment classes are defined under Clause 7 of IEC TS 62600-101. The development of a numerical model is generally based on the output from a third-generation spectral wave model. A third-generation spectral wave model simulates the propagation of the action density across the ocean. These models also include source terms that allow the addition and subtraction of energy due to processes such as wind shear, white-capping, bottom-friction and wave breaking,

as well as terms that transfer energy within the wave spectrum to represent non-linear triad and quadrature interactions that occur in shallow and deep water respectively.

The next task focuses on model tuning, calibration and validation, which investigate the difference between wave model prediction and the validation datasets and modify the model to improve the fidelity of its predictions. The process of modification is an evidence-driven with modifications to the model being made based on the anticipated changes to the resource. This would form the basis of a structured tuning process where model parameters, such as bottom friction coefficient, are modified within reasonable limits to improve the accuracy of the resource prediction. The use of model calibration, where bias is removed from the resource prediction, has to be considered where it can be justified and shown to increase accuracy significantly. The developed model is said to be validated when the desired level and precision of recommended standards has reached with the comparison. This procedure deviates from conventional resource assessments where there is a specific process to follow on.

The final steps involve wave hindcasting using the validated wave model and reporting the results with a standard reporting format. IEC TS 62600-101 recommends to hindcasting the wave conditions over the study area for ten years or longer period with appropriate boundary conditions. IEC TS 62600-101 provides extensive details on how the wave resource should be reported for the spatial variation of the wave energy resource over the study area and the temporal variation at specific locations within the study area. It is also advised to store the main outputs of the resource assessment through an accessible, geo-referenced, digital database. Most importantly, this specification classifies the uncertainty of the wave resource assessment into four different types. (i) measurement uncertainty describes as the all uncertainties associated with the measured which are used to the validation of numerical model output. (ii) modelling uncertainty describes as the all uncertainties associated with the model outputs which address through the definition of the extent of validation of the numerical model. (iii) long term uncertainty is based on the long term variability of the wave climate over the study region for the selected time period. (iv) combined uncertainty describes a combination of above which proceed under the IEC/ISO Guide 98-3:2008 and/or the ASME 20-2009.

4. Previously conducted wave resource studies in Sri Lanka

Annual wave climate of Sri Lanka is affected by two monsoon periods; northeast (December-February) and southwest (May-September). Although the detailed wave analysis is not available for the monsoon periods, some studies clarify that the annual average wave power around the western coastal region of Sri Lanka consist of 10-15 kW/m while southern region has 15-20 kW/m [4]. It is also estimated that the annual average wave height ranges from 0.5-3 m in different periods where the 80% of 2-3 m heights occur during the June and July [23]. But all of these values are approximated according to the analysis of global wave models [24-25].

The directional wave climatic study that was conducted by Sri Lankan German Corporation under the project of CCD-GTZ (1994), can be considered as one of first comprehensive analysis of wave climatic data in Sri Lanka [26]. The numerical wave propagation model called “REFRAC” was used to transform the deep water wave measurements to locations along the southwest coast at shallower depths. The bathymetric data was defined by digitizing admiralty charts and physically recorded metocean buoy data were used as boundary conditions. The results of this study have been the basis for most of coastal engineering and wave resource studies in the following years [27–29].

The design and implementation of ‘WorldWaves’ wave model was another earliest wave resource assessment study which was applied Sri Lankan waters as a hypothetical case study. According to the reference, this package has the capability of calculating the wave conditions along the many coasts worldwide [25]. In-situ measurements, satellite measurements and numerical wave model data available in global scale have been used for the wave model construction which contains necessary information for the offshore wave and wind input in time series format.

Another study which was focused on the assessment of the variability of nearshore wave climate off the southern coast of Sri Lanka, using the MIKE 21 SW wave model [30], in a domain covering the entire southern coast and part of southeast coast of Sri Lanka [31]. The bathymetry used in this study was established by digitizing admiralty charts, which cover the entire south coast and part of the southeast coast as well. Here, the wave data at desired model locations were obtained through a wave transformation matrix approach with respect to three wave measured datasets.

Another application of a wave energy resource study can be found in [32], which was focused on a feasibility study of an ocean wave power generation for southern coast of Sri Lanka. Here, the modeled area was mainly selected by assuming the wave climate of northern and eastern parts of the country is restricted due to the geographical location of Sri Lanka. The available seasonal wave climatic data were modeled using WW3 wave model [33]. The paper further describes that the used model data was contained with wave directions, significant wave heights, peak periods and the wind data. But the sources of those data including bathymetry were not clearly specified in the research publication. Furthermore it addresses the feasibility of implementing wave energy power plants based on mechanical, electrical and sociological aspects by considering six different sites along the southern coast of Sri Lanka.

A wave energy resource assessment which was conducted for the Indian shelf seas also has consisted some information around Sri Lankan wave resource [14]. This study reveals that the southeast coast of India (northwest part of Sri Lanka) has less than 5 kW/m wave power. The WAM wave model [34], with ECMWF ERA-Interim global atmospheric re-analysis dataset [35], has used to define the boundary conditions for their model domain. The variations in wave power at 19 locations were studied with relevant model validation. The illustration related to the distribution of annual mean wave power indicates that the 15-20 kW/m range can be found at the south and southeast regions of Sri Lanka.

Another research which establishes an assessment of wave climate in southwest, south and southeast coasts of Sri Lanka, provides the annual wave power ranges over 100 kW/m for their study locations at 50 m water depth [36]. These estimates deviate from all other reference values which has the annual wave power of 5-20 kW/m. The wave model was developed using Delft 3D model [37] and TOPEX altimeter data [38] has used for the model calibration and validation.

A study based on climate change impacts on seasonal wave climate of the west coast of Sri Lanka is another type of wave resource study which focuses to set up and calibrate a wave model that is capable of predicting the off-shore wave climate around Sri Lanka [39]. Here the global wave model datasets of ECMWF [35], NCEP [40] and NOAA [41] were used as boundary condition data for model development and satellite altimetry TOPEX, JASON, SAR measurements were used to calibration and validation of the wave model which was developed from WW3 [33] and SWAN [42] third generation wave models.

Other than the above wave resource studies, the effectiveness of wave currents around Sri Lanka has addressed in previous studies which are more focused on South West Monsoon (SWM) [46-47]. In addition to that surface circulation and coastal upwelling patterns around Sri Lanka has analysed and demonstrated with satellite imagery and numerical simulations [48–50]. These studies further discuss the effect of the eastward flowing Southwest Monsoon Current (SMC) during the southwest (SW) monsoon and the westward flowing Northeast Monsoon Current (NMC) during the northeast (NE) monsoon. This research concludes that the consideration of current circulations which are not considered in previous studies would be important to the analysis of wave climate of Sri Lanka.

Some tidal resource studies show that the annual average tidal values around Sri Lankan water consist of the lower side where semi-diurnal tidal range lies between 0.1 -0.2 m and, semi-diurnal and spring tidal range lies between 0.4 - 0.6 m [51-54]. This is mainly due to Sri Lanka is situated near to the equator and the studies further state that the range is less in the northern part of the island and rapid changes can be found in the southeast. Since there aren't any specific on wave resource assessments around Sri Lankan region, some studies have considered the variations of the sea and swell separately for the Indian Ocean [55-56]. The southern Indian Ocean westerly swells mainly spread into Sri Lankan waters, and the effect becomes stronger in the southwest monsoon period [55].

5. Application of IEC TS 62600-101 to Sri Lanka

According to the previous review, most of the studies have considered offshore wave climate while few of them focused on the nearshore analysis. None of them has considered both nearshore and offshore wave climate of the whole Sri Lankan region which is particularly important for the wave resource studies as well as many other subjects including coastal engineering, metrological science..etc. The wave parameter values around Sri Lanka can be estimated using two of the above studies which were conducted for the Indian ocean and the global scale [14,25]. But they may have consisted of a higher level of uncertainty where they were not specifically designed for the Sri Lankan region. Moreover, only those two studies have used the measured datasets for the model validation while two other [36,39] used the satellite altimeter measurements. The wave hindcasting around Sri Lanka is another lacking part of those studies which is highly recommended in any wave resource assessment. None of these studies hasn't discussed the uncertainty estimations of the evaluation which is a compulsory requirement of the standards.

Since the previously conducted resource assessment studies have not satisfied the most of the basic requirements of wave resource assessment and the IEC TS 62600-101 standards, proper assessment of Sri Lankan wave energy resource is a much-needed element to address the weaknesses of previous evaluations and follow sets of internationally recommended standards. Because of that, this research has developed according to the IEC TS 62600-101 standards and this technical report discusses the following major topics.

- Class of the resource assessment
- Description of the study area
- Collection of boundary datasets
- Wave model construction
- Model tuning and calibration
- Model validation datasets
- Model validation
- Data analysis
- Presentation of results
- Underlying assumptions
- Assessment of uncertainty
- Discussion and conclusions

5.1 Class the resource assessment

The IEC-TS 62600-101 is intended to be applied across the range of assessment study types. Three main distinct types of studies, reconnaissance, feasibility and design, are defined to span a large region to detailed designed studies as described in Table 1.

Table 1: Classes of resource assessment

Class	Description	Uncertainty of wave energy resource study	Typical long-shore extent
Class 1	Reconnaissance	High	Greater than 300 km
Class 2	Feasibility	Medium	20 km to 500 km
Class 3	Design	Low	Less than 25 km

This study considers the whole Sri Lankan region which is having larger longshore extent (over 300 km) and probably be the first comprehensive analysis according to Table 1, the appropriate resource assessment is reconnaissance stage (Class 1) assessment. So that all the assessment features of this study has followed the recommended standards under Class 1 resource assessment.

5.2 Description of the study area

From IEC TS 62600-101:2015: Clause 6.2

“The study area is the area in which the wave resource is of interest and is to be assessed and characterised. The extent of the study area shall be declared. The main physiographic and oceanographic features of the study area shall be reviewed, especially those features that influence wave propagation and wave climate. When wave modelling is used to assess the resource, the model domain is the area across which the wave conditions are modelled. The model domain may extend beyond the study area. In this case, the extent of the model domain shall also be declared.”

The study area was specifically focused on Sri Lankan region as shown in Figure`2. Mainly, the study area can be considered as a subset of the model area which is used for the model construction (describe in Section 7). According to most of the references, deployments of the wave energy converters are typically suitable for the water depth between 20-100 m and distance of the coast less than 3 km. Thus the selected study area has covered the main physiographic and oceanographic features of the wave resource assessment.

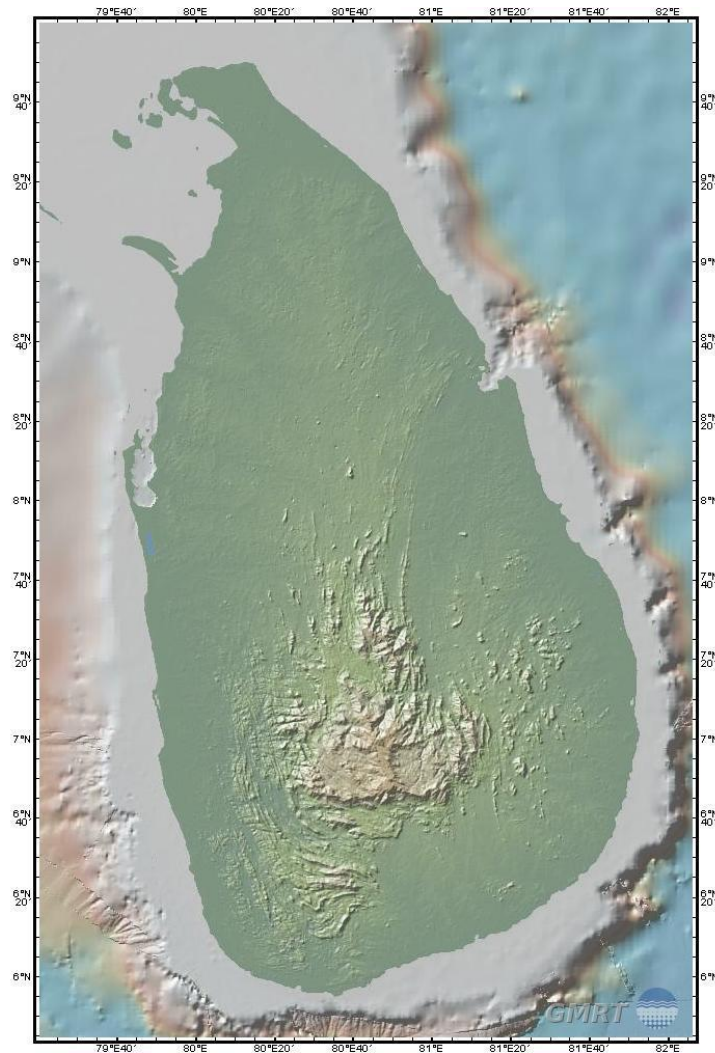


Figure 2: Study area of the wave resource assessment

5.3 Boundary datasets

The boundary and metocean data collection is a primary task of any wave resource assessment that needs to be completed during the initial stages of the project. These datasets are basically important for the development of the numerical model. According to the IEC TS 62600-101:2015: Clause 7.3, physically recorded metocean data, historical data predicted by a more extensive numerical model, or combination of the above can be used for the model development.

From IEC TS 62600-101:2015: Clause 7.3

“Boundary conditions for the numerical modeling should be defined using either,

- a) physically recorded metocean data,*
- b) historical data predicted by a more extensive numerical model, or*
- c) a combination of the above.*

...where wave data produced by previous modelling is used to define the boundary conditions for new numerical modelling, the data set should span a period of at least 10 years.”

The principal boundary data required for a wave propagation model are,

- bathymetry,
- the wave conditions on the boundaries of the model area,
- the strength and direction of marine currents and
- the meteorological conditions required to drive the wave generation and propagation.

These datasets come from a range of sources, with more than one source being available in some cases. There, most suitable sources of data have been identified, and most of the required data has been obtained from various resources. It was intended to use the best available high-resolution boundary data only within the study area. For this assessment, bathymetry, wind, and two-dimensional wave spectral data were used for the model construction, and the following section will describe the details of them.

5.3.1 Bathymetry

The term ‘bathymetry’ is generally referred to as the ocean's depth relative to sea level. The use of accurate bathymetry data is one of the essential need of any wave resource assessment. Again, these data can be found from different sources; measured, satellite, modelled data..etc.

From IEC TS 62600-101:2015: Clause 6.3

“The bathymetry of the model domain shall be described, and a bathymetric contour map shall be prepared. Where existing data sets are used, their source shall be provided. Existing bathymetric data sets will normally be employed in a Class 1 assessment. Depending on the quality of the bathymetric data that is available, new high-resolution bathymetric surveys may be required for higher class assessments.”

Based on the above clause, existing bathymetric data sets can be used in Class 1 (reconnaissance) assessment. Also, Table 2 further describes the required resolution of bathymetry data with respect to the class of assessment.

Table 2: Resolution of bathymetric data according to IEC standards

Class of assessment	1	2	3
Recommended maximum horizontal spacing of bathymetric data in water depths greater than 200 m	5 km	2 km	1 km

Recommended maximum percentage difference in water depth between adjacent bathymetric points in water depths less than 200 m	10 %	5 %	2 %
Recommended maximum horizontal spacing of bathymetric data in water depths less than 200 m	500 m	100 m	25 m
Recommended maximum horizontal spacing of bathymetric data in water depths less than 20 m	100 m	50 m	10 m

To obtain the possible resolutions, GEBCO 30 arc second interval grid [40] has used for the water depths over 200 m while digitized nautical charts [41] interpolated data has used for the water depth less than 200 m. This is a common practice in wave resource assessment when there is a lack of high-resolution bathymetric dataset. The selection of bathymetry resources has further described in WERSL-R-180701-RL-D Further Data Collection Report and the used bathymetric contour map for model construction is shown in Figure 3.

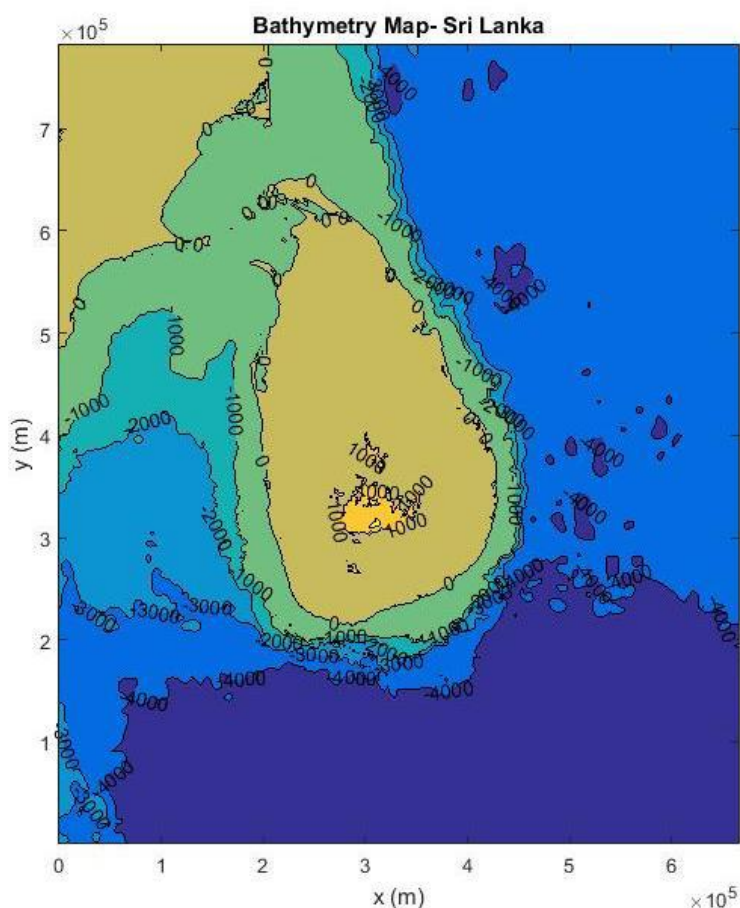


Figure 3: Bathymetric contour map around Sri Lanka

5.3.2 Wave Data

From IEC TS 62600-101:2015: Clause 6.4

“Existing data and study reports characterising wave conditions across the study area shall be collected, reviewed and described. Existing data may come from previous numerical simulations, physical measurements, earlier resource assessment studies or previous wave climate studies. The existing data and information may help guide the user in setting up the resource assessment, as it may describe key aspects of the wave resource including but not limited to seasonal variability, inter-annual variability, frequency of storms, prevalence of multimodal wave systems, expected spectral shape and the variability of dominant wave direction.”

Selection of existing wave data is essential as bathymetric data, but most importantly, these data should be operational for more than 10 years with the recommended spatial resolution of 100 km and temporal resolution of 3 hours. This was a somewhat challenging task where the available data resources haven't satisfy the recommended requirements. However, it was found that the best available sources of required wave data can be obtained from ECMWF - Interim dataset. The wind and two-dimensional wave spectral data were obtained from ECMWF Interim dataset which have interpolated spatial resolution of $0.25^{\circ} \times 0.25^{\circ}$ and $1.5^{\circ} \times 1.5^{\circ}$ respectively. All of these nonstationary datasets were obtained as timeseries data which have 6 hourly temporal resolution.

5.4 Numerical Modelling

Unlike wind, the random nature of ocean waves results in complicated behavior that is dependent on many parameters. Ocean wave characteristics can be determined through field measurements, numerical simulation, physical models and analytical solutions. Each of these methods has its own pros and cons, but the recent applications of numerical models can be considered as one of the promising techniques for the study of ocean waves. By using a numerical model for a certain area, wave energy converter deployment locations can be easily identified without the need to place multiple wave measuring instruments. However, the knowledge of average wave climate requires long term data which cannot be obtained through wave measuring instruments. A numerical wave model propagates the waves from where the wave resource data is known to the point of interests. In that case, the performance of the numerical wave model depends on how accurately the phenomena are expressed into the numerical schemes, so that more accurate wave parameters can be produced. Here, the concept

of numerical modelling related to Sri Lankan region has described together with the required input and output datasets. Furthermore, the model results and future usage will also be outlined.

From IEC TS 62600-101:2015: Clause 7.1

“The raw sea state data required for estimation of the wave energy resource shall be generated using suitable numerical models. The analysis of this data to provide a parametric representation of the sea states and wave climate”

Selecting a suitable numerical model is one of the most important requirements as it has significantly influenced for the all outcomes of the project. The IEC Technical Specification specifies the numerical model features described in Table 3, which are required for the selection of a suitable model.

Table 3: Elements of suitable numerical models

● Required to be considered ○ Recommended ○ Acceptable × Not permitted

Component: Description	Reconnaisance	Feasibility	Design
Boundary conditions			
Parametric boundary: Boundary conditions defined by parameters such as H_{m0} , T_e , θ_{Jmax} ^a	○	×	×
Hybrid boundary: Boundary conditions defined by wave spectrum with parametric directional parameters ^a	○	○	×
Spectral boundary: Boundary conditions defined by directional wave spectrum	●	●	●
Physical processes			
Wind-wave growth: Transfer of energy from the wind to the waves ^b	●	●	●
Whitecapping: Dissipation due to whitecapping included in model	●	●	●
Quadruplet interactions: Energy transfer due to quadruplet interactions included in model ^b	●	●	●
Wave breaking: Dissipation due to depth-induced wave breaking included in model	○	●	●
Bottom friction: Dissipation due to bed friction included in model	○	●	●

Triad interactions: Energy transfer due to triad interactions included in model ^c	○	●	●
Diffraction: Diffraction included in model ^{d, h}	●	●	●
Refraction: Refraction included in model	●	●	●
Effects of sea ice included in model	●	●	●
Water level variations (tides)	●	●	●
Wave reflections	●	●	●
Wave-current interactions	●	●	●
Wave set-up ^e	○	○	○
Numerics			
Parametric wave model	○	×	×
2nd generation spectral wave model	○	○	×
3rd generation spectral wave model	●	●	●
Mild-slope/parabolic/elliptical wave model ^e	○	○	○
Spherical coordinates ^f	●	○	○
Non-stationary solution	○	○	○
Minimum spatial resolution ^g	5 km	500 m	50 m
Minimum temporal resolution ^g	3 h	3 h	1 h
Minimum number of wave component frequencies in numerical model	25	25	25
Minimum number of azimuthal directions in numerical model	24	36	48
<p>^a An appropriate spectral shape and directional spreading function should be used.</p> <p>^b Importance of wind-wave growth and quadruplet interactions will depend on the geographical extent and their inclusion may be unnecessary for areas with small geographical extents.</p> <p>^c Importance of triad interactions will depend on water depth and their inclusion may be unnecessary for areas without shallow water.</p>			

- | | |
|---|---|
| d | Importance of diffraction will depend on the presence of islands, headlands and/or other obstructions and the inclusion of diffraction may be unnecessary for areas where these do not exist. |
| e | Recommended for shoreline wave energy converters. |
| f | The requirement for spherical coordinates will depend on the geographical extent and directional resolution; their use may be unnecessary for areas with small geographical extents. |
| g | Boundary conditions, wind fields, bathymetry and model computational grid/time steps should be defined to correctly reproduce the scale of variation of wave energy conditions in the study area with, at least, this resolution. |
| h | Diffraction in spectral wave models is based on a phase-averaged approximation that may not accurately model the effect of diffraction where the spatial resolution of the grid is too coarse. |

From IEC TS 62600-101:2015: Clause 7.2

“If a modelling feature is recommended then it is considered best practice, and should be included in the numerical model. If a modelling feature is acceptable then it may be used in the numerical model. If a modelling feature is not permitted then it shall not be used in the numerical model.”

Since our analysis is based on Class 1 resource assessment, the production of an appropriate model has focused on the **Reconnaissance** elements. The selection of an appropriate numerical model should satisfy all the above considerations and all recent models of the wave energy resource are based on the output from a third generation spectral wave model. A third generation spectral wave model simulates the propagation of the action density across the ocean. These models also include source terms that allow the addition and subtraction of energy due to processes such as wind shear, white-capping, bottom-friction and wave breaking, as well as terms that transfer energy within the wave spectrum to represent non-linear triad and quadrature interactions that occur in shallow and deep water respectively. This implies that the third generation wave models have the ability to cover the all major features of boundary conditions, physical processes and numerics referenced in Table 3.

5.4.1 Selection of a third-generation wave model

The wave climate changes in a complex way in space-time scales due to bathymetry, wave conditions on the boundaries, strength and direction of marine currents and meteorological conditions. As described in the previous section, the ocean wave characteristics were initially determined through field measurements, numerical simulation, physical models and analytical solutions. But the advancement of computer technology has enabled the development of

numerical models that allow significant enhancements in the understanding of waves. The most common practice nowadays is to use third-generation wave models for hindcast and forecast studies of long and short term wave resource assessments.

Most of the available wave models are applicable for both oceanic and coastal assessments. Some of well-known third generation wave models are WAM [31], WW3 [45], SWAN [39], MIKE21-SW [46] and TOMAWAC [47]. All of the wave models can be found as open source applications except MIKE21-SW. The principle behind the all third-generation model is solving the action balance density equation with a range of available source terms [48]. Each of these models uses different deterministic, and probabilistic approaches related to their applications. Their ability to reproduce wave conditions and provide spectral information for shallow or deep water locations, depends on the physical approaches used in the solvers within a specific wave model. While commonalities exist in some source terms, available options and parametrisations differ significantly within the models.

According to the previous analysis which was conducted under WERSL-R-181031-RL-B Model Construction Report, WAM model is not suitable for our requirement since it is designed for large area simulations. Similarly, TOMAWAC is not appropriate as it is primarily designed for shallow water mechanics. Mike21-SW satisfies the required capabilities with a user-friendly interface, but this expensive commercial package is beyond the project budget. WW3 and SWAN have similar features with minor differences and most importantly both of them are used for many recent wave energy assessment projects. With the advantage of familiarized background among the project team, SWAN third-generation wave model is selected for the model construction task of this project.

5.4.2 SWAN model

SWAN is a third-generation wave model for obtaining realistic estimates of wave parameters in coastal areas, lakes and estuaries from given wind, bottom and current conditions. However, SWAN can be used on any scale relevant for wind-generated surface gravity waves. The main goal of the SWAN model is to solve the spectral action balance equation without any a priori restrictions on the spectrum for the evolution of wave growth. This equation represents the effects of spatial propagation, refraction, shoaling, generation, dissipation and nonlinear wave-wave interactions. Following describes the terms of spectral action balance equation for Cartesian coordinates.

$$\frac{\partial}{\partial t} N + \frac{\partial}{\partial x} c_x N + \frac{\partial}{\partial y} c_y N + \frac{\partial}{\partial \sigma} c_\sigma N + \frac{\partial}{\partial \theta} c_\theta N = \frac{S}{\sigma}$$

The first term on the left-hand side represents the local rate of change of action density in time, the second and third term represent propagation of action in geographical space (with propagation velocities c_x and c_y in x and y space, respectively). The fourth term represents shifting of the relative frequency due to variations in depths and currents (with propagation velocity c_σ in σ space). The fifth term represents depth induced and current-induced refraction (with propagation velocity c_θ in θ space). The expressions for these propagation speeds are taken from linear wave theory. The term $S [= S(\sigma, \theta)]$ at the right-hand side of the action balance equation is the source term in terms of energy density, representing the effects of generation, dissipation, and nonlinear wave-wave interactions.

Based on the wave action balance equation with sources and sinks, the shallow water wave model SWAN is an extension of the deep water third-generation wave models. It incorporates the state-of-the-art formulations for the deep water processes of wave generation, dissipation and the quadruplet wave-wave interactions from the WAM model. In shallow water, these processes have been supplemented with the state-of-the-art formulations for dissipation due to bottom friction, triad wave-wave interactions and depth-induced breaking. SWAN is fully spectral (in all directions and frequencies) and computes the evolution of wind waves in coastal regions.

The following wave propagation processes are represented in SWAN:

- propagation through geographic space,
- refraction due to spatial variations in bottom and current,
- diffraction,
- shoaling due to spatial variations in bottom and current,
- blocking and reflections by opposing currents and
- transmission through, blockage by or reflection against obstacles.

The following wave generation and dissipation processes are represented in SWAN:

- generation by wind,
- dissipation by whitecapping,
- dissipation by depth-induced wave breaking,
- dissipation by bottom friction and
- wave-wave interactions in both deep and shallow water.

Thus, the SWAN third generation wave model satisfies all feature elements required under the IEC TS 62600-101.

5.4.3 Computational spatial grid

The first step of the model construction is to develop a required grid for the area of interest. This grid is known as the computational spatial grid on which SWAN performs all computations. In general, two types of grids are considered: structured and unstructured. Structured grids may be rectilinear and uniform or curvilinear. They always consist of quadrilaterals in which the number of grid cells that meet each other in an internal grid point is 4. In unstructured grids, this number can be arbitrarily (usually between 4 and 10). For this reason, the level of flexibility concerning the grid point distribution of unstructured grids is more significant compared to structured grids.

Unstructured grids may contain triangles or a combination of triangles and quadrilaterals (so-called hybrid grids). In the current version of SWAN, only triangular meshes can be employed. The use of unstructured grids in SWAN offers a good alternative to nested models not only because of the ease of optimal adaption of mesh resolution but also the modest effort needed to generate grids about complicated geometries, e.g. islands and irregular shorelines. This type of flexible meshes is particularly useful in coastal regions where the water depth varies greatly. As a result, this variable spatial meshing gives the highest resolution where it is most needed. The use of unstructured grids allows resolution of the model area with relatively high accuracy but with much fewer grid points than with regular grids. Because of these reasons, an unstructured grid is used for the model construction as described in the following section.

5.4.4 Unstructured grid for the model construction

In this project, the “Triangle mesh generator” is used to generate the required unstructured grid. Triangle is a well-known public-domain software for two-dimensional mesh generation through the construction of Delaunay triangulation [49]. For efficient generation of higher resolution grid in which areas where the bathymetry or evolution of the waves change rapidly, a graphical Matlab public-domain interface called BatTri used in accordance with the research requirements [50]. Figure 4 illustrates an unstructured grid around Sri Lankan region and Table 4 describes the statistics of it.

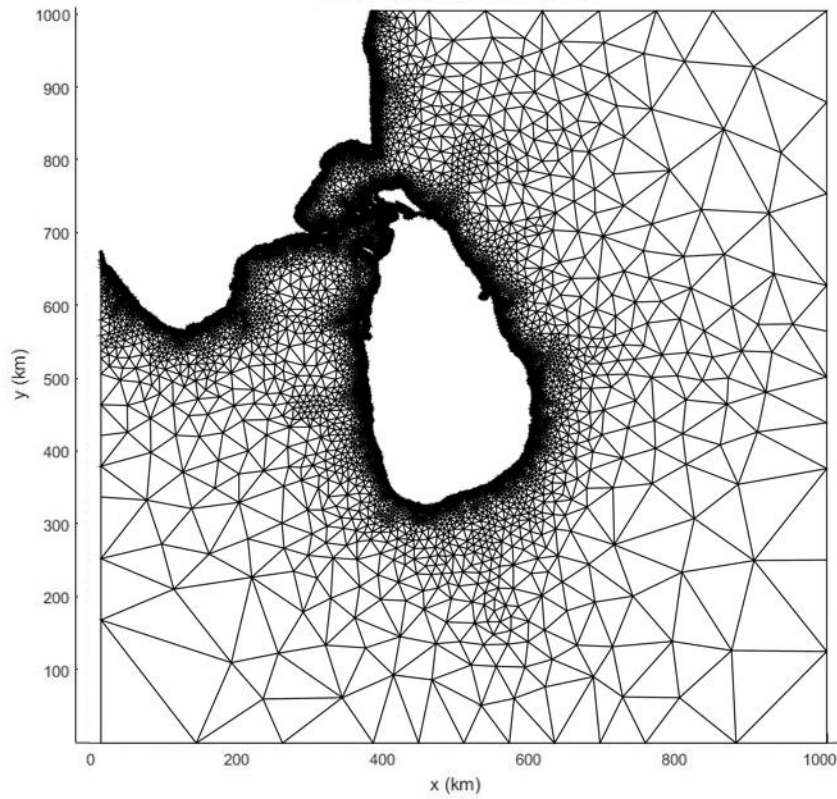


Figure 4 : Developed Unstructured Grid around Sri Lanka

Table 4: Statistics of the unstructured grid

Spatial coverage	Longitude range : 76.5 ⁰ W - 85.5 ⁰ E
	Latitude range : 3 ⁰ S - 12 ⁰ N
Input points	43018
Input triangles	82889
Input segments	3363
Mesh points	44018
Mesh triangles	84889
Mesh edges	128882
Mesh boundary edges	3097
Mesh segments	3363

5.4.5 Spatial input grids

As referenced in WERSL-R-180615-RL-D Further Data Collection Report, the selected boundary datasets for bathymetry and wind are used as spatial input grids for the final model construction. In the model running, wind dataset is considered as non-stationary computations and the bathymetry dataset is considered as a stationary computation. The required spatial inputs of water level and bottom friction are controlled by particular parameter values inside the model. Table 5 shows the details of used spatial input grids for stationary and non-stationary computations.

Table 5: Specifications of the bathymetric and wind dataset

	Bathymetric dataset	
Source	GEBCO	Nautical Charts
Grid resolution	30 arc second interval	15 arc second interval
Units	m	m
Spatial coverage:	Over 200 m water depths	Less than 200 m water depths
	Wind dataset	
Temporal range	2001-01-01 to 2019-01-01	
Source	ECMWF	
Parameters	U-component of wind V-component of wind	
Vertical levels	10 m specific height above ground	
Grid resolution	1.5° x 1.5°	
Units	ms ⁻¹	
Time interval	Every 6 hours	
Spatial coverage	Longitude range : 76.5°W - 85.5°E	
	Latitude range : 3°S - 12°N	

5.4.6 Spectral input grid

The computational spectral grid needs to be provided by the user. In frequency space, it is simply defined by a minimum and a maximum frequency and the frequency resolution which is proportional to the frequency itself. According to SWAN user manual, the frequency domain can be defined in number of ways. For our computational model, the frequency domain has been specified as lowest frequency, highest frequency and the number of frequencies. Similarly, in directional space, SWAN has the directional range of 360° unless the user specifies a limited directional range.

From IEC TS 62600-101:2015: Clause 7.2

“...A minimum of 25 wave frequency components and 24 to 48 directional components shall be used in the numerical model. Finer discretization in frequency and direction is recommended in order to improve the accuracy of the model output. It is recommended that the frequency range of the model output should cover at least 0.04 Hz to 0.5 Hz. The wave model may need to include computations at frequencies up to 2.0 Hz in order to adequately resolve important physical processes, such as wind-wave growth and white-capping.”

As described in WERSL-R-180615-RL-D Further Data Collection Report, the ECMWF ERA-Interim two-dimensional spectral dataset is used to define the computational spectral grid of the model. The dataset follows the requirements of the IEC Technical Specification and Table 6 describes the details of this dataset. The used spectral grid points for the model construction are illustrated in Figure 5.

Table 6 : Specifications of two-dimensional wave spectral dataset

Two-dimensional wave spectra dataset	
Temporal range	2001-01-01 to 2019-01-01
Source	ECMWF ERA-Interim
Parameters	Frequency domain and directional space
Frequency domain	
Lowest discrete frequency	0.0345 Hz
Highest discrete frequency	0.5473 Hz
Number of frequencies	30
Directional space	
Directional spreading	15°
Number of directions	24
Selected grid distance	1.5° longitude/latitude space
Units	m ² s radian ⁻¹
Time interval :	Every 6 hours

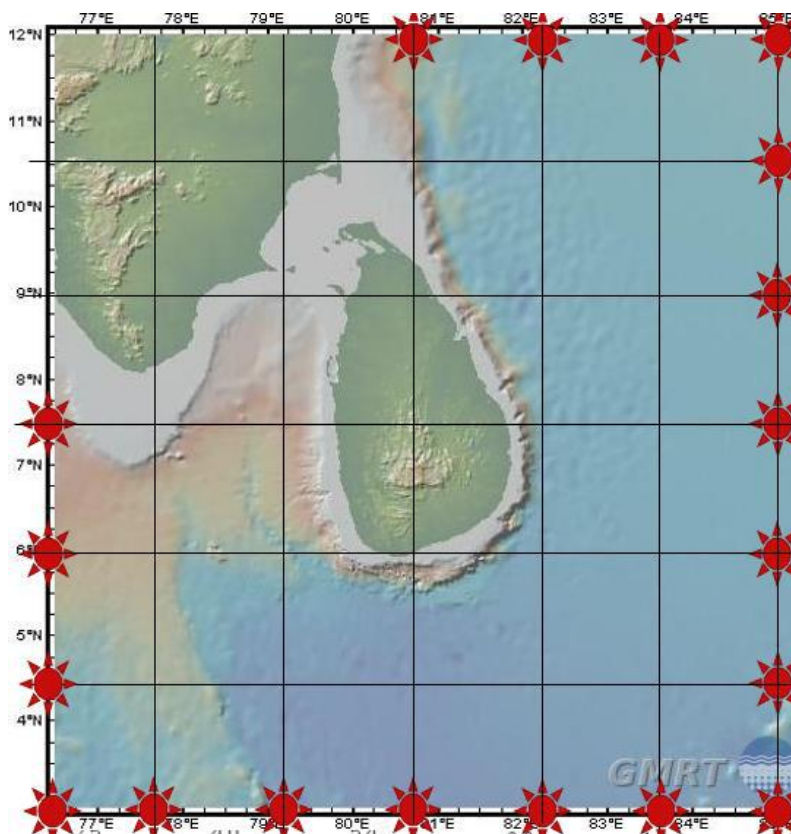


Figure 5: Spectral grid inputs used for the model construction

5.4.7 Activation of physical processes

SWAN contains several physical processes that add or subtract wave energy to or from the wave field. The included processes are wind input, whitecapping, bottom friction, depth-induced wave breaking, dissipation due to turbulence, obstacle transmission, nonlinear wave-wave interactions (quadruplets and triads) and wave-induced set-up. Whereas the input grid is unavailable (e.g. bottom friction), the user can control the required parameter by activating the related physical process. Table 7 shows the physical processes and related references that define these processes.

Table 7: Used physical processes and related authors

Physical process	Reference
Whitecapping: Dissipation due to whitecapping included in model	Komen <i>et al.</i> (1984)
Quadruplet interactions: Energy transfer due to quadruplet interactions included in model	Hasselmann <i>et al.</i> (1985)
Wave breaking: Dissipation due to depth-induced wave breaking included in model	Battjes and Janssen (1978)

Bottom friction: Dissipation due to bed friction included in model	JONSWAP (1973)
Triad interactions: Energy transfer due to triad interactions included in model	Eldeberky (1996)

5.4.8 Output grids

SWAN can provide outputs on a uniform, rectilinear spatial grids that are independent of the input grids and from the computational grid. An output grid can be specified by the user with an arbitrary resolution, but it is sensible to choose a resolution that is fine enough to show relevant spatial details, but not so fine as to result in an excessive amount of data storage. It must be pointed out that the information on an output grid is obtained from the computational grid by bi-linear interpolation (output always at computational time level). In nonstationary computations, outputs can be requested at regular intervals starting at a given time, but always at computational times. An initial model is developed to obtain the isolated location outputs and spatial distribution outputs. This isolated location outputs are useful for model validation task where the wave measured data (wave buoy data) is only available at particular locations.

6. Model tuning and calibration

From IEC TS 62600-101:2015: Clause 7.7

Model tuning refers to adjusting model parameters or settings (e.g. wave growth or dissipation terms such as bottom friction). Tuning of the model may involve adjusting model parameters to improve the accuracy of the model's predictions; however, the parameters shall not be assigned unreasonable values chosen solely to improve model accuracy.

According to the above clause, the model tuning and calibration process has significant impact on improving the accuracy of model predictions and outputs of final model validation. Following major steps were carried out to obtain the precise outcomes of this task.

6.1 Model tuning with sensitivity analysis

A useful first step the analysis of the most sensitive parameters in the model. The aim is to determine the rate of change in model output with respect to changes in model inputs (parameters). To undertake sensitivity analyses, it is necessary to identify key model parameters and to define the parameter precision required for the model tuning.

From IEC TS 62600-101:2015: Annex A, A.1

“Sensitivity studies are recommended in this Technical Specification as a method of determining whether a component of a numerical model has an insignificant effect on the estimation of the wave resource. If a model component is shown to have an insignificant effect then it can be omitted from the numerical model.”

Firstly, each of physical processes has excluded from the model one at a time and analysed the variations compared to the default model outputs. The statistical analysis of these types of measured and model datasets generally analyses based on the bias and the accuracy. This can be achieved by calculating the bias (mean error) and Root Mean Square Error (RMSE), considering the difference between the developed model values for a smaller computational domain. A complete analysis of sensitivity analysis described in Annex A.

According to the Table A.1, whitecapping dissipation and quadruplet wave-wave interaction have the marginal effect for the deviations of the model outputs and wave breaking has also small effect compared to other physical processes. As conclusions in of physical processes of the model, physical processes of whitecapping dissipation and quadruplet wave-wave interaction can be considered as the most sensitive parameters of the model. The analysis concludes that the most sensitive input parameters are wind speed, wind direction and bathymetry. But all of these parameter values are provided as external input grids to the model which means that the model sensitivity depends on the accuracy of those datasets. Furthermore all other manageable physical parameter values have not significantly influence for the model results within their range. Again, that implies the application of the default values of physical parameters will have mere influence for the validation model.

In order to decrease model response uncertainty and to make the risk on using the model results lower, the values of this model inputs should be as certain as possible. Low sensitivity of the observable to the other uncertain model coefficients says that model result variability is not growing significantly if the values of the coefficients are known within 10% range. Furthermore, it should be noted that since the model results do not change much, when the values of the coefficients vary, the calibration of this parameters can be difficult. Because of that, default parameter values of the SWAN physical processes are used for the final model validation.

6.2 Model calibration

From IEC TS 62600-101:2015: Clause 7.7

“Model calibration refers to adjusting model outputs to improve agreement with measurements. Measured data may also be used for calibration of the numerical model to improve the accuracy of the model’s predictions. Calibration of the model involves modification of the model output based on a function derived from the difference between the raw model output and a sub-set of the measured data. If model calibration is used this shall be reported, together with details of the calibration functions used and the changes in model uncertainties obtained. Measured data that is used for model calibration shall originate from time periods that are distinct from and non-overlapping with the time periods from which the validation data sets are drawn.”

Calibration and validation are typically performed by splitting the available observed data into two datasets: one for calibration, and another for validation. Here, the available data are most frequently split by time periods, carefully ensuring that the climate data used for both calibration and validation are not substantially different. Since there are limited wave measured data available in Sri Lankan region, all of them were used as model validation datasets. Because of that model calibration task have not been implemented at this stage. By using future wave measurements, the model can be calibrated to reduce model uncertainties.

6.3 Model Validation datasets

The selection of validation datasets mainly considers the available historical data sets that may be of use in validating a model of the Sri Lankan wave energy resource. Here, both measured and modeled data sources have been considered, which are adequate to validate the model. The available validation datasets around Sri Lanka for the model development consist primarily of metocean measurements which are possessed by a range of organizations. Three wave measured datasets are used for this validation process with the granted permission. Since those buoy datasets are available at the down south area, one of a global wave hindcast dataset had to use for further validation of other directions of the model. Following are the details of used validation datasets.

6.3.1 CCD-GTZ dataset

This wave measurement programme was governed by Coast Conservation Department (CCD) - Sri Lanka under the Sri Lankan-German Technical Assistant Programme in order to obtain a study on coast erosion management. The measurement device, a directional pitch and roll buoy

WAVEC was installed 8 km south off Galle harbour at about 70m water depth as shown in Figure 6.

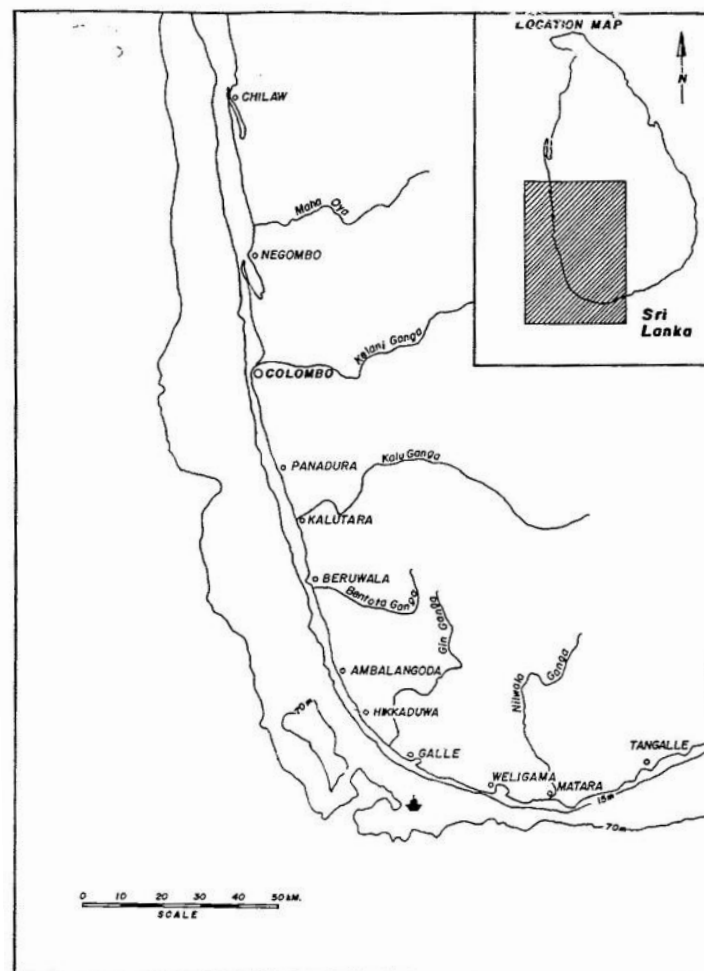


Figure 6: Location of CCD-GTZ buoy [51]

The dataset was measured in the period of March, 1989 to September, 1992 which has time-series parameter values of significant wave height (H_{m0}), average period by zero down crossing (T_z) and mean wave direction (Θ). Here measurements were recorded as the separate sea and swell components.

6.3.2 China Harbour Cooperation dataset (SCSIO Project)

The China Harbour Cooperation has granted access to a set of buoy data, which can be found in Science Data Bank (<http://www.sciencedb.cn/dataSet/handle/447>). In this study [52], wind and wave observational datasets were simultaneously collected in a nearshore area off Matara, Sri Lanka. Figure 7 shows the deployment locations of wave buoys and Table 8 describes the details of the dataset.

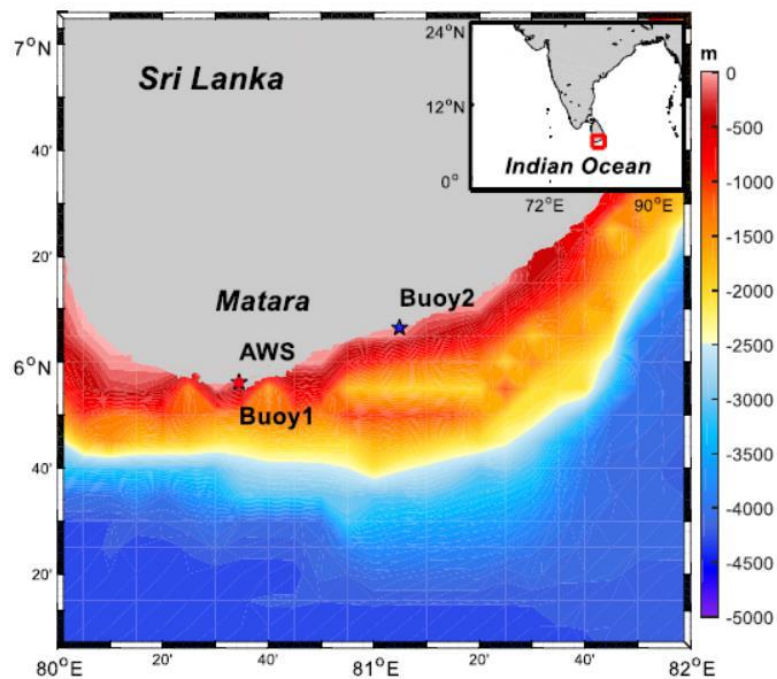


Figure 7 : Observation deployment locations and topography [52]

Table 8: Dataset profile, wind and wave dataset for Matara, Sri Lanka

Data name	Location	Deployment	Period	Frequency
Automated Weather Station (AWS)	5.936 N 80.575 E	Automated Weather Station	Nov 2012 – Jun 2014 Nov 2015 – Oct 2016	30 min
Buoy 1	5.934 N 80.574 E	Wave buoy (20m water depth)	Sep 2013 – Feb 2014	10 min
Buoy 2	6.106 N 81.080 E	Wave buoy (10m water depth)	Apr 2013 – Apr 2014	1 h

6.3.3 GOW2 dataset

The GOW2 dataset [53], a long-term wave hindcast covering the world coastline with improved resolution in coastal areas and along ocean islands. For developing the GOW2 hindcast, WW3 wave model is used in a multigrid two-way nesting configuration from 1979 onwards. The multigrid includes a global grid of 0.5° spatial resolution, specific grids configured for the Arctic and the Antarctic polar areas, and a grid of higher resolution (about 25 km) for all the coastal locations at a depth shallower than 200 m. Available outputs include

hourly sea state parameters (e.g. significant wave height, peak period, mean wave direction) and series of 3h spectra at more than 40000 locations in coastal areas.

Figure 8 shows the available spectral data points around the Sri Lankan region. Here, the highlighted points were selected as the validation data points which covers all four direction around the country.

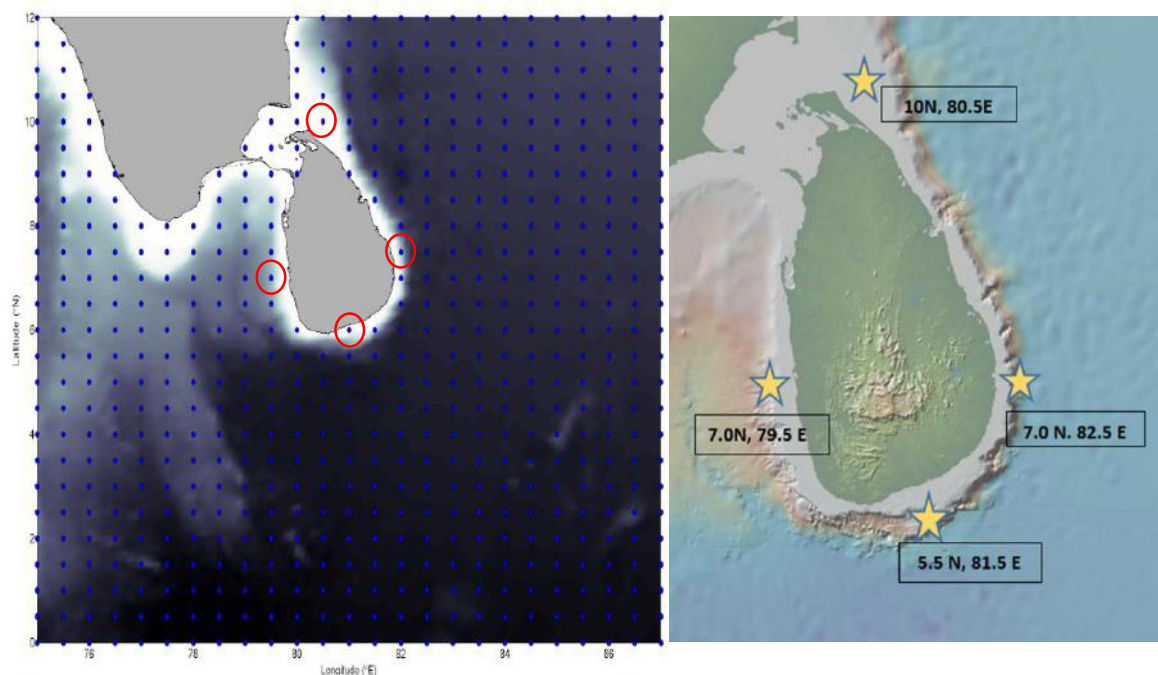


Figure 8 : Available GOW2 spectral data locations around Sri Lanka and selected validation points

7. Model validation

From IEC TS 62600-101:2015: Clause 7.6.1

“All numerical modelling shall be validated using measured wave data. The ability of the wave model to accurately predict the wave resource shall be assessed and confirmed. Whenever possible the numerical model output should be validated using data from one or more locations close to where wave energy converters might realistically be deployed. If this is not possible, because deployment locations are unknown or otherwise, the validation data should be from location(s) where the average water depth is close to the expected depths of future wave farm deployments”

Since one of the objective of this project is to identify the most promising locations for wave energy convertors and there are limited wave measured data available, the results of the numerical model is validated only for available wave buoy datasets.

For the final validation of the model, an area covering the whole Sri Lankan region was selected and validated with available wave measured and global wave model datasets. Next sections describes how the validation process has been conducted for the developed model by following the IEC TS 62600-101:2015 requirements.

7.1 Model validation procedure

From IEC TS 62600-101:2015: Clause 7.6.2 Validation data specification

“A validation data point is a single sea state measured at a particular location and time, and a validation data set consists of all validation data points associated with a particular location. To facilitate validation, the validation data set shall be used to construct an omni-directional H_{m0} - T_e scatter table showing the proportional frequency of occurrence of different sea states. The scatter table will comprise many cells or bins, each corresponding to a particular and unique small range of H_{m0} and T_e . Model error shall be evaluated by considering the data in each scatter table cell, and overall. To minimize the potential for correlation of error within a cell, validation data points within a single cell of the scatter table shall be derived from measurements separated by a minimum time period. A minimum separation period of 6 h is recommended.”

According to the above clause, H_{m0} and T_e are considered to be two main parameters of the model validation procedure. However, most of the validation datasets haven't consisted of direct measurement of energy period (T_e), but they are more often measured mean wave period (T_m) or zero crossing period (T_z). Due to this reason, the scatter tables which will use for the analysis of each validation datasets consist of $H_{m0} - T_m$ or $H_{m0} - T_z$ combinations. The validation procedure described in IEC TS 62600-101:2015 is summarized in Figure 9.

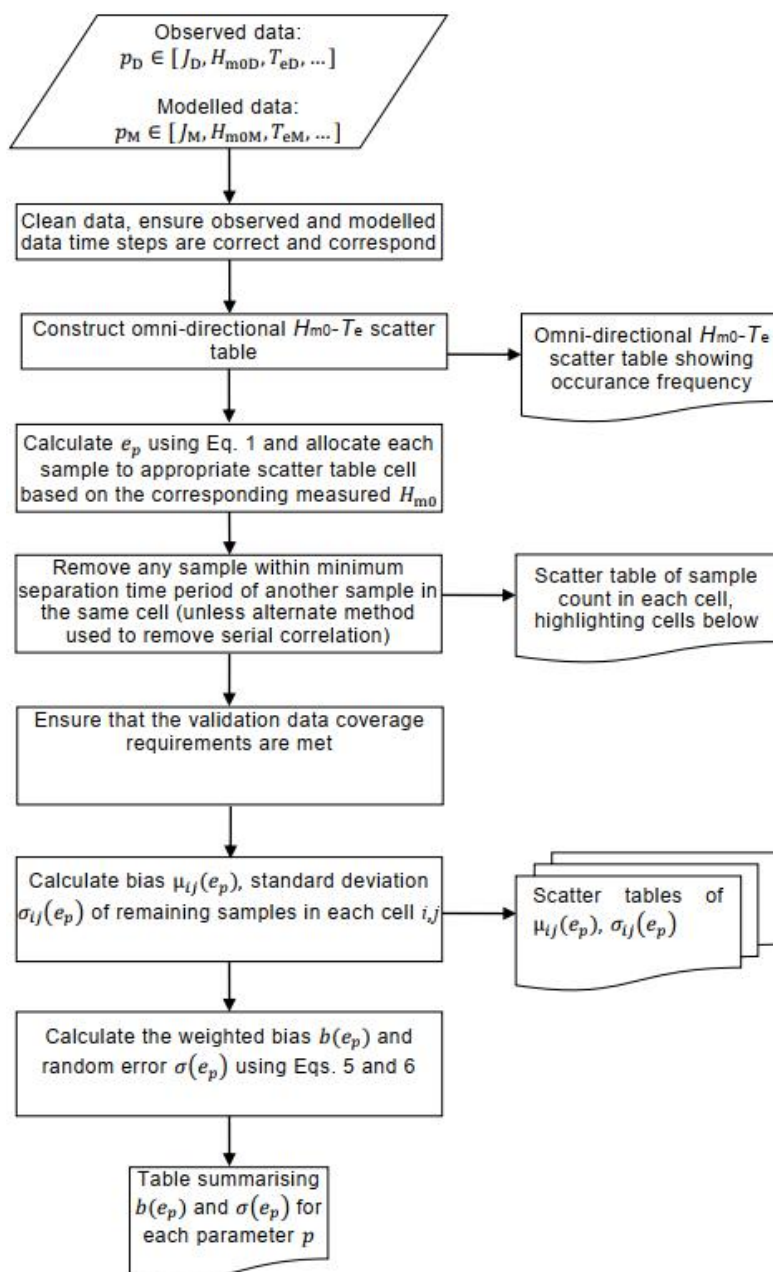


Figure 9 : Model validation flow chart : IEC TS 62600-101:2015 [54]

After following the above described procedure, Table 9 specifies the maximum acceptable weighted mean systematic and random errors for each key parameter for Class 01 resource assessment.

Table 9 : Minimum validation requirements [54]

	Class 1: Reconnaissance
Validation data coverage requirements	
Minimum number of validation data points to represent cell	3
Minimum coverage by validation data	90 %

Max acceptable weighted mean systematic error, $b(e_p)$	
Significant wave height, H_{mo}	10 %
Energy period, T_e	10 %
Omni-directional wave power, J	25 %
Max acceptable weighted mean random error, $\sigma(e_p)$	
Significant wave height, H_{mo}	15 %
Energy period, T_e	15 %
Omni-directional wave power, J	35 %

According to IEC TS 62600-101:2015, the numerical modelling output shall be considered to be successfully validated for a specific location and class of resource assessment when the criteria in Table 9 are satisfied.

A complete analysis on model validation is described under Annex B. According to that, all of the validation datasets were compared according to the minimum validation requirements of the IEC-TS 62600-101. Most of them are satisfied the minimum requirements except for few cases at the nearshore locations. This implies that the developed model has provided significantly accurate outputs at the offshore locations and consisted marginal deviations at the nearshore locations. Although the model has provided accurate outputs compared to the GOW2 hindcast dataset, the best option is to tune and calibrate the model using the wave measured datasets. The model can be further tuned and calibrated with the granted permission for other historical buoy datasets or future wave measurement programs. Also high resolution wind and bathymetric data, specially at the nearshore locations will also make significant improvements for the current model accuracy.

Since the model outputs at the validation points have satisfied the most of minimum validation requirements of the IEC-TS 62600-101, the developed model can be considered as a validated model with the available input grids. Because of that, this validated model can be used to assess and characterise the wave resource at other locations as well. The reporting of the Sri Lankan wave energy resource has completed in next section which will maximize the potential utility and user-friendliness of the wave resource assessment and characterisation making it easily accessible for any potential wave energy project developers.

8. Data analysis

The data analysis uses sea state data to produce characteristic parameters that are relevant to the performance of wave energy converters. For that, representation of the sea can be considered as one of the critical processes in a wave resource assessment where the behaviour of the ocean has very complex in nature. However, this phenomena is typically described by assuming a stationary, stochastic and homogeneous process. The most significant development in the representation of the sea is the definition of the sea using a spectrum. To understand the concept of the wave spectrum, it is first necessary to accept that the variation in water surface can be represented as the linear super-position of sinusoidal waves of different frequencies, amplitudes, directions and phases. Although this representation could be viewed as simply a change in the co-ordinate system (from the time-domain to the frequency-domain), it actually appears to be a reasonably good representation of the underlying physics. Indeed, the wave spectrum is now generally used to fully define any sea-state, with the assumption that there is a random phase between all of the individual wave components, which is a natural consequence of the assumption of linear super-position.

Here, the concept of directional variance density spectrum $S(f, \theta)$ displays how wave variances (or sea surface elevations) are distributed over different frequency bands (f) and propagation directions(θ).

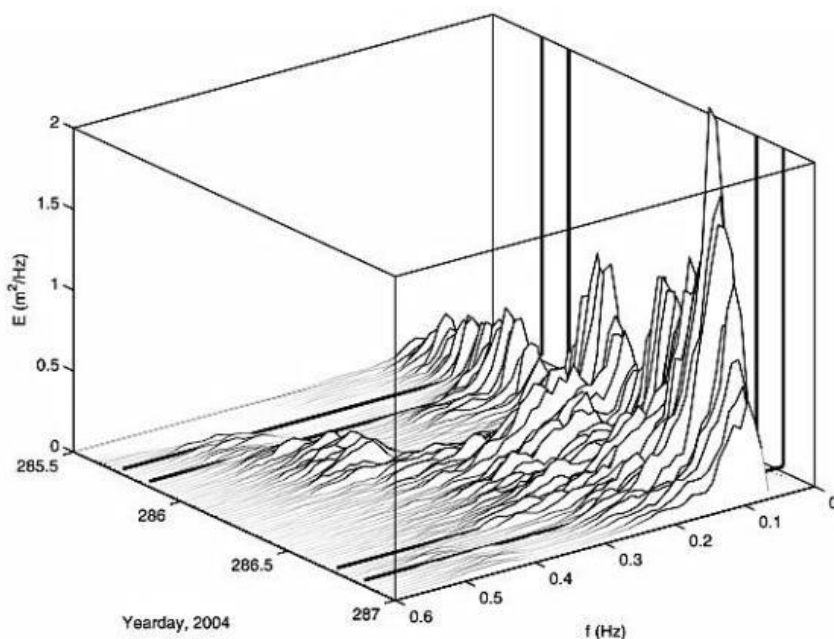


Figure 10 : Example of the annual variation of the frequency wave spectrum [55]

Estimates of many of important characterized wave parameters such as omni directional wave power(J), significant wave height(H_{mo}), mean wave period(T_m), energy period(T_e), zero-crossing period(T_z)...etc. can be described by using the above spectrum in a more precise way. Definitions of all used characterized parameters are described in Annex C according to the IEC TS 62600-101:2015.

9. Presentation of results

The validated model can be used to estimate the wave hindcast of wave resource parameters for the Sri Lankan region. According to IEC TS 62600-101, the numerical model dataset should span a period of at least 10 years. In this analysis, model outputs have been obtained for 18 years (2001-2018) and presented the results as,

- Regional information: a set of maps that illustrate the spatial variation of key wave resource parameters across the study area.
- Study points: a set of points which have detail analysis that further illustrates key properties of the wave resource

9.1 Presentation of regional information

From IEC TS 62600-101:2015: Clause 10.5

“..a set of maps shall be prepared and included in the report to illustrate the spatial variation of key wave resource parameters across the study area. The required and recommended parameters to be mapped are summarized in Table. The resolution of the maps shall be consistent with the resolution of the models used to generate the data.”

Table 10: Summary of wave energy resource parameters to be archived and mapped

● Required to be considered ○ Recommended

Parameter	Units	Class of assessment		
		Reconnaisa nce	Feasibilit y	Design
Annual mean omni-directional wave power	kW/m	●	●	●
Extent of successful model validation	-	●	●	●
Monthly variability of omni-directional wave power	kW/m		○	○
Annual mean significant wave height	m	○	○	○

Monthly variability of significant wave height	m		○	○
Annual mean energy period	s	○	○	○
Monthly variability of energy period	s		○	○
Annual mean spectral width	-		○	○
Monthly variability of spectral width	-			○
Annual mean of maximum directionally resolved wave power	kW/m		○	○

Considering the above requirements, following characterised wave resource parameters are used to represent as the regional information illustrated under Annex D.

- i. Annual mean omni-directional wave power
- ii. Annual mean significant wave height
- iii. Annual mean energy period

Although it is not required to represent the monthly variability for Class 1 resource assessment, those illustrations are presented for further understanding.

In IEC TS 62600-101 has not included a proper method to analyse the extent of model validation. So that a new methodology has been defined for the requirement which is described under Appendix E. This methodology was applied only for the study points since it is currently at the development stage.

9.2 Presentation of information at study points

A study point is a single location at which the wave resource is of interest and detailed wave resource characteristics have to be produced and reported. For these locations, the wave energy resource shall be characterized and reported in greater detail. A sufficient number of study points have been selected such that any significant spatial variability in the resource is represented. In this study, 10 study points with 50 m water depth have been selected which represents the all directions of Sri Lankan region as shown in Figure 11. The main reason for selecting the 50 m contour, because it is one of the recommended water depths for Wave Energy Converter deployment.

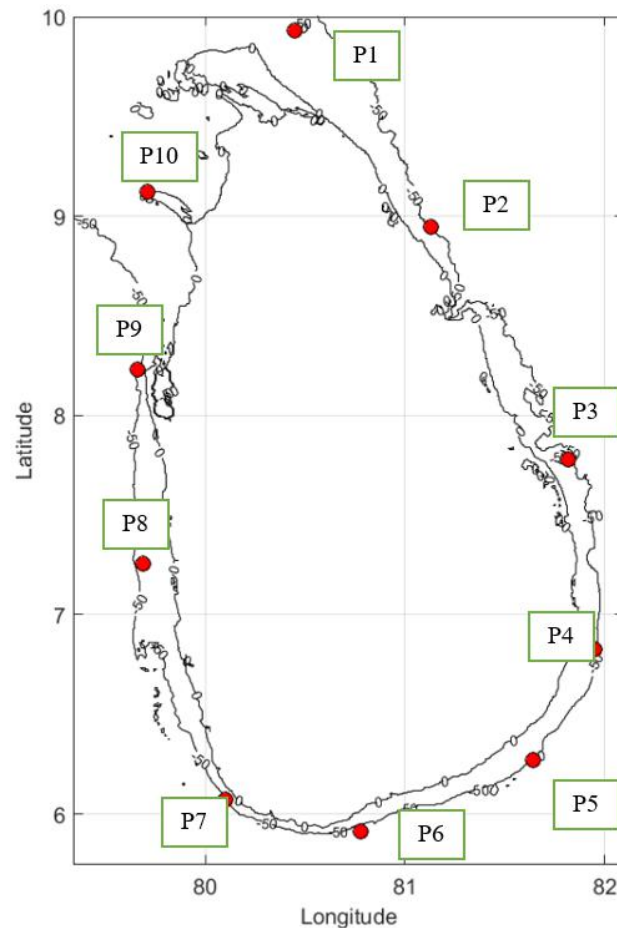


Figure 11: Study Points

As per the IEC TS recommendations, the following figures are required for the representation of the study points. The analysis of each study points has described under Annex F.

- Annual scatter table showing the proportional frequency of occurrence of sea states, parameterized in terms of the significant wave height, H_{m0} , and energy period, T_e . The dimensions of each bin in the scatter tables shall be no larger than 0.5 m and 1.0 s.
- Graphical and/or tabular presentation of the annual variation of the long-term monthly mean values of the following parameters:
 - ✓ significant wave height;
 - ✓ energy period;
 - ✓ omni-directional wave power
 - ✓ maximum directionally resolved wave power.
- Annual wave rose depicting the long-term joint distribution of:
 - ✓ maximum directionally resolved wave power and the direction of maximum directionally resolved power.

10. Underlying assumptions

This study has been carried out by considering the following assumptions.

- The interpolated resolution of input model datasets (bathymetry, wind and spectral dataset) are similar to the actual wave conditions around Sri Lankan region.
- The wave measured datasets which are used for the validation have properly calibrated.
- The used SWAN wave model bottom level, bottom friction and other physical parameters are identical to the real conditions of the study area.
- The nearshore model outputs are presented in 200 m -500 m grid resolution by assuming all points within the particular gridded region provide the nearest grid point parameter values.

11. Assessment of uncertainty

The purpose of the uncertainty analysis is to quantify the uncertainty of the wave resource estimates that are produced. According to IEC TS 62600-101 following categories of uncertainty have to be considered in any wave resource assessment.

- i. Measurement uncertainty
- ii. Modelling uncertainty
- iii. Uncertainty due to long-term variability
- iv. Combined uncertainty

The measurement uncertainty are the all uncertainties associated with the measured wave data that is used in the resource assessment for validation of the numerical model output. Since it assumes the wave devices are properly calibrated, this assessment doesn't include the measurement uncertainty. The modelling uncertainty is all uncertainties associated with the wave model outputs on which the resource estimates are based. This can be addressed through the concept of the extent of validation in numerical modelling. A complete analysis of this regard is described in Annex D.

The long-term uncertainty is related to the long-term variability of the wave climate over the study region. Further discussion of long-term uncertainty of the wave energy resource is provided in Annex G. So that the combined uncertainty can be defined as the combination of all above categories. It is also noted that the calculation of the uncertainty in the resource assessment is highly complex and considered that currently there are not enough definitive

procedures used for this clause to be overly prescriptive. It is also important to highlight that the provided spatial model outputs are not accurately presented within the 0-10 m water depths where that area consisted of higher uncertainty.

12. Discussion

Before drawing conclusions based on the project, the relevance and implications of both the results and the methods applied will discuss in this section. One of the main objectives of this project is to produce wave resource data to IEC TS 62600-101 standards which can be used by developers to assess the potential for their wave energy technologies in Sri Lanka. Since all the used methodologies follow the standards of IEC TS, the project itself presents a clear understanding and quality work towards any interested party who are working on the wave energy sector.

Another main objective focuses on identifying the most promising deployment locations for wave energy converters, based on the wave resource characteristics. According to the model results for 18 years of data, this can be analysed based on two categories; regional information (Annex E) and study points (Annex F). These information present that the maximum annual significant wave heights of 1.5-2.0 m can be obtained from the south coast, followed by southeast and southwest regions. The average H_{m0} range of 1.0-1.5 m can be found in west and east coasts, and the lowest values under 1 m present at the northern region. It is also important to highlight that the H_{m0} values develop up to 2.5 m at southern region during the southwest monsoon period (May-September).

The variation of omni-directional wave power (J) and directionally resolved wave power ($J_{\theta_{Jmax}}$) also presents a similar seasonal variation w.r.t. H_{m0} . The mean annual omni-directional wave power of south coast has consisted the highest range of 12-16 kW/m while the lowest range of 1-5 kW/m values can be found at the north, northwest and east regions of the country. The west coast has 5-6 kW/m wave power range. The monthly variation of J shows that the maximum range of 20-25 kW/m can be obtained at south coast during the southwest monsoon period. For further clarification, Figure 12 shows the variation of J in 50 m water depth around Sri Lanka. According to that, the highest wave energy resource can be found in Matara to Hambantota coastal region.

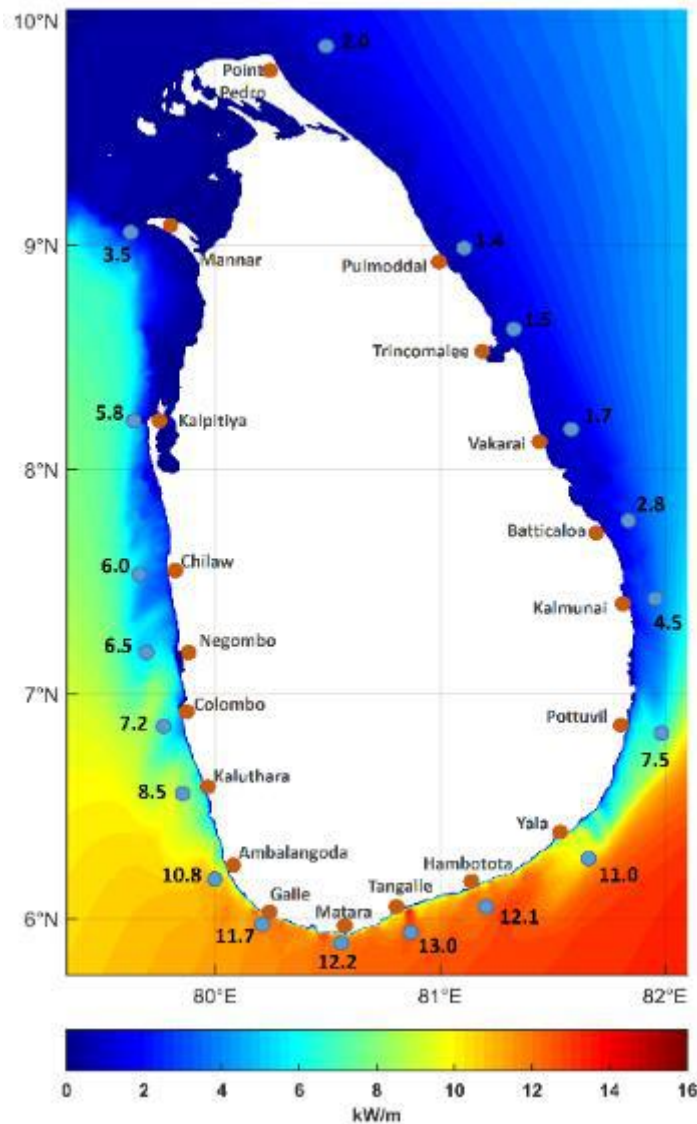


Figure 12: Omni-directional wave power at 50 m water depth

Despite the variation of omni-directional wave power, directionally resolved wave power ($J_{\theta_{Jmax}}$) has much influence for the wave energy converter (WEC) deployments. According to the study points analysis (Annex F) P5, P6 and P7 points (points at south coast) have consisted with consistent wave power where 40% the directionally spreading develop towards their main directions. The long-term uncertainty analysis shows that the mean annual variations of these points over 18 years also present less than 5% Mean Average Error (MAE) which is a crucial factor for the WECs deployments. The monthly variation of $J_{\theta_{Jmax}}$ follows similar seasonal variation towards the J where the maximum of 15-20 kW/m range can be obtained during June-August at P5, P6 and P7 study points.

The monthly variation of energy period (T_e) of Sri Lanka has deviated from the H_{m0} and J where the highest value range can be found during the February-April. The regional

information and study points show the mean annual energy period has the highest range of 9-12 s at the south, southwest and west coast regions. Despite other study points, P8 and P9 points (northwest region) show their highest variation of 8-9 s during March-April and October-November time period. For each study point, annual scatter tables are presented which show the proportional frequency of occurrence of sea states, parameterised in terms of the significant wave height, H_{m0} , and the energy period, T_e . The dimensions of each bin in the scatter tables shall be no larger than 0.5 m and 1.0 s. These details are significantly important to calculate the mean annual energy production and its uncertainty for a wave energy converter deployed in Sri Lankan waters. Finally, The theoretically available wave resource potential along the coasts of each province can be approximately calculated by using the regional information of omni-directional wave power plots.

Table 11: Theoretical wave energy resource potential of each province

	Province	Theoretical wave resource potential (TWh/year)
01	Northern province	2.65
02	Eastern province	4.35
03	Southern province	26.30
04	Western province	8.75
05	Northwestern province	5.25

13. Digital database

From IEC TS 62600-101:2015: Clause 10.4

“The main results/outputs of the resource assessment shall be stored in an accessible, geo-referenced, digital database. The main purpose of the database is to preserve the outputs of the resource assessment for future uses. The database shall include information for each model grid point (or MCP measurement site) where reliable estimates of the wave resource have been obtained. However, in some cases it may be necessary to exclude information for parts of the study area where reliable predictions could not be obtained due to limitations associated with the methodology, the boundary conditions, and the abilities of the wave model, the model resolution, or some other factor. Each location shall be clearly identified by the latitude, longitude and water depth below mean sea level.”

According to the above clause, a geo-referenced digital database has developed (included in the attached DVD) to assess the following characteristic parameter values around Sri Lanka.

1. Significant wave height
2. Energy Period

3. Omni-directional wave power

These parameter values can be obtained as mean annual, southwest and northeast monsoons and yearly (2001-2018) values with required longitude and latitude coordinates.

14. Conclusions

A good quality dataset obtained through internationally recommended standards for the Sri Lankan wave energy resource is an essential requirement to assess the wave energy potential and to attract potential wave energy developers. This particular requirement arises since the traditional wave resource studies are typically not adequate for a standardized assessment of wave energy capture potentials in wave energy converter deployment projects. This project has followed the International Electro-technical Committee Technical Specification (IEC TS 62600-101) standards which establish uniform methodologies for wave energy resource assessment and characterisation. The study has followed specifications defined under the Class 1, reconnaissance resource assessment of IEC TS 62600-101. The available boundary data of bathymetry, wind and spectral data have used to develop the wave model with required resolutions. A validated wave model that allows assessment of the Sri Lankan wave energy resource using SWAN third-generation wave model. Here, both measured and modelled data sources have been considered, which are adequate to validate the model. With that, the model outputs were obtained for 18 years (2001-2019) to assess and characterise the wave resource by identifying the most promising areas for wave energy exploitation with appropriate illustrations. The spatial attributes of significant wave height, energy period and omni-directional wave power have been obtained as mean annual, seasonal (southwest and northeast monsoons) and monthly variations. These datasets have also presented in a geo-referenced digital database which will be helpful for future wave energy projects in Sri Lanka. The highest wave energy potential can be found at the southern coast of Sri Lanka which covers the coastal area from Matara to Hambantota. The in-depth analysis of wave resource around Sri Lanka has presented using 10 study points which are significantly important to calculate the mean annual energy production and its uncertainty for a wave energy converter deployed in Sri Lankan waters. Finally, the findings of the project will help to promote Sri Lanka as the small group of nations that can provide good quality wave resource data to prospective investors. This project is a timely needed requirement to create an industry which can significantly contribute to the Sri Lankan economy in future. This will also make a door open to many researchers and local developers who are interested in the renewable energy industry where they can expand on the vision and commitment towards the wave energy field.

15. References

- [1] UNDP, “Sri Lanka: Rapid Assessment and Gap Analysis,” Report: *Sustainable Energy for all*, 2012.
- [2] D. Ranasinghe, “Strategic Importance of Blue Economy to Sri Lanka and Challenges,” *KDU IRC*, 2018
- [3] S. Sayanthan and N. Kannan, “Renewable energy resource of Sri Lanka ! A review,” *Int. Journal of Env. & Agri. Research*, vol. 3, no. 4, pp. 80–85, 2017.
- [4] J. Ratnasiri, “Alternative energy – prospects for Sri Lanka,” *Journal of the National Science Foundation of Sri Lanka*, 36, pp.89–114, 2008.
- [5] M. Folley, S.D.G.S.P. Gunawardane, “The development of marine renewable energy in Sri Lanka”, *National Energy Symposium*, Colombo, Sri Lanka, 2018.
- [6] E. Rusu and F. Onea, "A review of the technologies for wave energy extraction", *Clean Energy*, vol. 2, no. 1, pp. 10-19, 2018.
- [7] I. López, J. Andreu, S. Ceballos, I. M. De Alegría, and I. Kortabarria, “Review of wave energy technologies and the necessary power-equipment,” *Renew. Sustain. Energy Rev.*, vol. 27, pp. 413–434, 2013.
- [8] M. Folley, “The Wave Energy Resource BT - Handbook of Ocean Wave Energy,” A. Pecher and J. P. Kofoed, Eds. Cham: Springer International Publishing, 2017, pp. 43–79.
- [9] A. Akpınar and M. Kömürçü, "Wave energy potential along the south-east coasts of the Black Sea", *Energy*, vol. 42, no. 1, pp. 289-302, 2012.
- [10] G. Iglesias, R. Carballo, and C. Pen, “Offshore and inshore wave energy assessment : Asturias (N Spain),” *Energy*, vol. 35, no. 5, pp. 1964–1972, 2010.
- [11] M. G. Hughes and A. D. Heap, “National-scale wave energy resource assessment for Australia,” *Renew. Energy*, vol. 35, no. 8, pp. 1783–1791, 2010.
- [12] M. Gonçalves, P. Martinho, and C. G. Soares, “Assessment of wave energy in the Canary Islands,” *Renew. Energy*, vol. 68, pp. 774–784, 2014.
- [13] D. Mollison and M. Pontes, "Assessing the Portuguese wave-power resource", *Energy*, vol. 17, no. 3, pp. 255-268, 1992.
- [14] V. S. Kumar and T. R. Anoop, “Wave energy resource assessment for the Indian shelf seas,” *Renew. Energy*, vol. 76, pp. 212–219, 2015.
- [15] M. Gonçalves, P. Martinho and C. Guedes Soares, "Wave energy conditions in the western French coast", *Renew. Energy*, vol. 62, pp. 155-163, 2014.
- [16] R. Alonso, S. Solari and L. Teixeira, "Wave energy resource assessment in

- Uruguay", *Energy*, vol. 93, pp. 683-696, 2015.
- [17] R. Espindola and A. Araújo, "Wave energy resource of Brazil: An analysis from 35 years of ERA-Interim reanalysis data", *PLOS ONE*, vol. 12, no. 8, p. e0183501, 2017.
- [18] G. Kim, W. Mu, K. Soo, K. Jun, and M. Eun, "Offshore and nearshore wave energy assessment around the Korean Peninsula," *Energy*, vol. 36, no. 3, pp. 1460–1469, 2011.
- [19] "Finland company to help Lanka produce wave energy", *Daily News*, Available: <http://www.dailynews.lk/2017/10/11/local/130920/finland-company-help-lanka-produce-wave-energy>.
- [20] "Carnegie to harness Sri Lanka waves", *Marine Energy*, Available: <https://marineenergy.biz/2016/09/30/carnegie-to-harness-sri-lanka-waves/>.
- [21] "WERPO to make waves in Sri Lanka", *Marine Energy*, Available: <https://marineenergy.biz/2015/07/14/werpo-to-make-waves-in-sri-lanka/>.
- [22] International Electro-technical Committee, "IEC TS 62600-101 Wave Energy Resource Assessment and Characterisation," 2015.
- [23] K. D. R. J. Kumara, D. D. Dias, R. L. Nawagamuwa, and W. M. A. R. Weerasinghe, "Wave Energy Enhancement for Nearshore Electricity Generation," *Engineer: Journal of the Institution of Engineers* no. 2, pp. 43–52, 2018.
- [24] S. Barstow *et al.*, "WORLDWAVES : Fusion of data from many sources in a user-friendly software package for timely calculation of wave statistics in global coastal waters," Proc 13th ISOPE Conf. Oahu, Hawaii, USA, 2003.
- [25] S. Barstow, K. Belibassakis, T. Gerostathis, and G. Spaan, "WORLDWAVES : High quality coastal and offshore wave data within minutes for any global site" COPEDEC VI, Colombo, Sri Lanka, 2003.
- [26] "H. Scheffer, K.Fernando, "Direcional wave climate study south-west coast of Sri Lanka", CCD-GTZ Coast Conservation project, 1994.
- [27] N. Wikramanayake, P. P. Guneratne, M. M. G. S. Fernando, and I. Ratnayake, "The Coastal Wave Climate of Sri Lanka : Measurements and Modeling," COPEDEC VI, Colombo, Sri Lanka, 2003.
- [28] I. S. K. Wijayawardane, "Coastal Erosion : Investigations in the Southwest Coast of Investigations on Sediment Transport," International Conference on Sustainable Built Environments, Kandy, Sri Lanka, 2010
- [29] T. Thevasiyani and K. Perera, "Statistical analysis of extreme ocean waves in Galle , Sri Lanka," *Weather Clim. Extrem.*, vol. 5–6, pp. 40–47, 2014.
- [30] Danish Hydraulic Institute (DHI), "Mike 21 Wave Modelling," Scientific

documentation, 2015.

- [31] P. Gunaratna, D.P.L.Ranasinghe, and T.A.N.Sugandika, “Assessment of Neashore Wave Climate off Southern Coast of Sri Lanka” *Engineer: Journal of the Institution of Engineers, Sri Lanka*, 44(2), pp.33–42, 2011.
- [32] K. Amarasekara, G. Abeynayake, M. Fernando, and A. Arulampalam, “A prefeasibility study on ocean wave power generation for the southern coast of Sri Lanka : Electrical feasibility,” *Int. J. Distrib. Energy Resour. Smart Grids*, vol.10, pp.79–93, 2014.
- [33] H. L. Tolman, “User manual and system documentation of WAVEWATCH-III version 3.14,” *Tech. note*, no. 3.14, p. 220, 2009.
- [34] WAMDI Group, “The WAM model - A third generation ocean wave prediction model,” *Journal of Physical Oceanography*, vol. 18, no. 12. pp. 1775–1810, 1988.
- [35] “ECMWF ERA Interim dataset.”, *ECMWF*, Available: <https://www.ecmwf.int/en/forecasts/datasets/reanalysis-datasets/era-interim>.
- [36] V. Vithana, “Wave Energy Resource Assesment for the Southern Coast Of Sri Lanka Wave Energy Resource Assesment for The Southern Coast Of Sri Lanka,” 6th International Symposium-ACEP, 2018.
- [37] Delft3D , "Delft3D-FLOW User Manual" , 2014.”
- [38] “TOPEX altimeter data.” Available: <https://www.aviso.altimetry.fr/en/multimedia/publications-and-links/newsletter/newsletter03/tp-data.html>.
- [39] R. M. J. Bamunawala, S. S. L. Hettiarachchi, S. P. Samarawickrama, P. N. Wickramanayakkara, and R. Ranasinghe, “Climate Change Impacts on Seasonal Wave Climate of the Western Coast of Sri Lanka,” 3rd International Symposium-ACEP,, 2015.
- [40] “NCEP/NCAR Research Data Archive”, *NCEP/NCAR* Available: <https://rda.ucar.edu/>”
- [41] “National Oceanic and Atmospheric Administration.” Available: <https://www.noaa.gov/>.
- [42] SWAN, "SWAN Technical documentation," Delft University of Technology: Delft, 2016.
- [43] “Gridded Bathymetry Data”, *GEBCO* Available: https://www.gebco.net/data_and_products/gridded_bathymetry_data/.
- [44] “Admiralty Maritime Data Solutions”, *Admiralty Charts*, Available: <https://www.admiralty.co.uk/charts>.
- [45] Y. Luo, D. Wang, T. P. Gamage, and F. Zhou, “Wind and wave dataset for Matara , Sri Lanka,” *Earth Syst. Sci. Data*, pp. 131–138, 2018.

- [46] F. Schott, J. Reppin, J. Fischer, I. Meereskunde, and U. Kiel, “Currents and transports of the Monsoon Current releases,” *Int. J. Geophysical Research* vol. 99, 1994.
- [47] P. Physics, “Monsoon Response of the Sea around Sri Lanka : Generation of Thermal Domes and Anticyclonic Vortices,” *J. Physical Oceanography* pp. 1946–1960, 1998.
- [48] P. N. Vinayachandran, “Biological response of the sea around Sri Lanka to summer monsoon,” *Geophysical Research Letters* vol. 31, pp. 4–7, 2004.
- [49] K. K. A. S. Yapa, “Upwelling phenomena in the southern coastal waters of Sri Lanka during southwest monsoon period as seen from MODIS,” *Sri Lankan Journal of Physics* vol. 10, pp. 7–15, 2009.
- [50] A. De Vos, C. B. Pattiaratchi, and E. M. S. Wijeratne, “Surface circulation and upwelling patterns around Sri Lanka,” *Int. J. Biogeosciences* pp. 5909–5930, 2014.
- [51] P. L. Woodworth and V. N. Stepanov, “The Seasonal Cycle of Sea Level in Sri Lanka and Southern India,” *Western Indian Ocean J. Mar. Sci.* Vol. 7, No. 1, pp. 29–43, 2008 no. 2000.
- [52] U. Challenges and E. Economies, “Urbanization Challenges in Emerging Economies ,” *ASCE India Conference 2017* pp. 358–365.
- [53] E. M. S. Wijeratne and C. B. Pattiaratchi, “Sea Level Variability in Sri Lanka Waters,” *Conference: Understanding Sea-level Rise and Variability* p. 15, 2003.
- [54] K. W. Indika, E. M. S. Wijerathne, and G. W. A. R. Fernando, “Sea Level Variability in the West Coast of Sri Lanka,” *Project: Extream sea level chenge* , pp. 0–4, 2016.
- [55] C. W. Zheng, C. Y. Li, and J. Pan, “Propagation route and speed of swell in the Indian Ocean,” ,” *Int. J. Geophysical Research* pp. 1–24.

Annex A

Sensitivity Analysis

A.1 Study area

Here, an area covering the south coast of Sri Lanka was selected with respect to the availability of wave buoy datasets (Figure A.1). The main reason for choosing a small computational domain to save the computational time where the hundreds of computations had to carry out for the initial model tuning and calibration tasks.

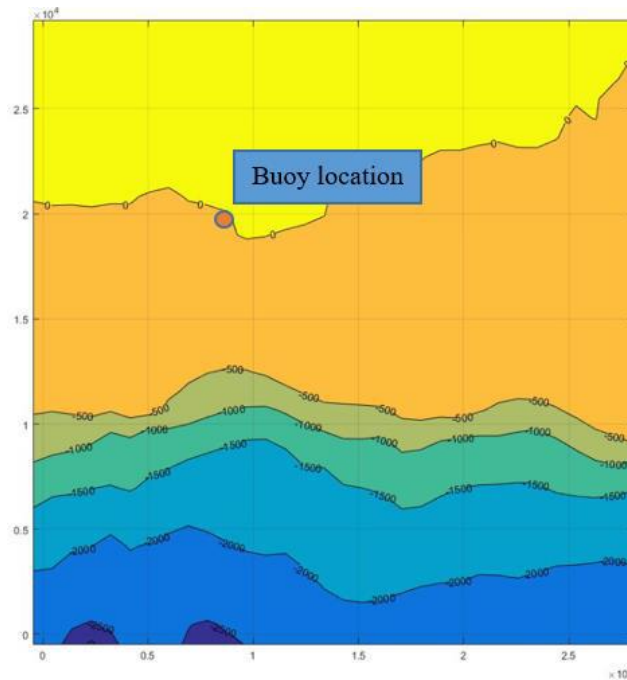


Figure A.1: Study area for the sensitivity analysis

A.2 Input and output grids for sensitivity analysis

Bathymetry, wind and two dimensional wave spectral data were employed as model input grids to obtain the outputs of the locations around the validation point. The output results of significant wave heights were analysed for five months (01.10.2013-28.02.2014) in 1 hour time intervals relative to the available wave buoy time period (3717 sea states). This buoy dataset was obtained from SCSIO project which was conducted by The China Harbour Corporation (Section 6.3.2).

Here, the boundaries defined under computational domain mainly cover the East, West and South regions of the selected area. The required data for 2D wave spectral data and wind data were obtained from ECMWF ERA-Interim in 6 hour time intervals with $0.125^\circ \times 0.125^\circ$ interpolated grid resolution. GEBCO 30 arc seconds grid resolution dataset was used as the

bathymetric dataset for the model development. The SWAN output spectral grids of Significant Wave Height (H_{m0}) have been obtained for the available buoy location.

A.3 Sensitivity analysis of physical processes of the model

To undertake the sensitivity analysis, following physical processes of the model were selected and compare with respect to the H_{m0} values of the default model.

- i. Whitecapping dissipation
- ii. Quadruplet wave-wave interaction
- iii. Wave breaking
- iv. Bottom friction
- v. Triad wave interaction
- vi. Diffraction

Here, each of the physical processes has excluded from the model one at a time and analysed the variations compared to the default model outputs. The statistical analysis of these types of measured and model datasets generally analyse based on the bias and accuracy. This can be achieved by calculating the Bias (mean error) and Root Mean Square Error (RMSE), considering the difference between the developed model values for the each case and the initial model outputs. Here, the analysis based on 4292 data points which were taken as hourly H_{m0} of the model.

The statistical analysis was based on the H_{m0} values of the initial model that include the period from five months (01.10.2013-28.02.2014) and contain 4292 records with 1 hour time interval. Following equations were used to calculate the results and Table 1 shows the bias and RMSE of excluded physical processes of the model with respect to the initial model outputs.

$$BIAS = \frac{\sum_{i=1}^n (H_{m0_{model,i}} - H_{m0_{initial\ model,i}})}{n}$$

$$RMSE = \sqrt{\frac{\sum_{i=1}^n (H_{m0_{model,i}} - H_{m0_{initial\ model,i}})^2}{n}}$$

Note: $H_{m0_{initial\ model,i}}$ is the significant wave height value of the initial model, $H_{m0_{model,i}}$ is the simulated significant wave height, n is the total number of seastates.

Following figures show that the H_{m0} variations of initial model outputs and the each of deactivated physical processes outputs.

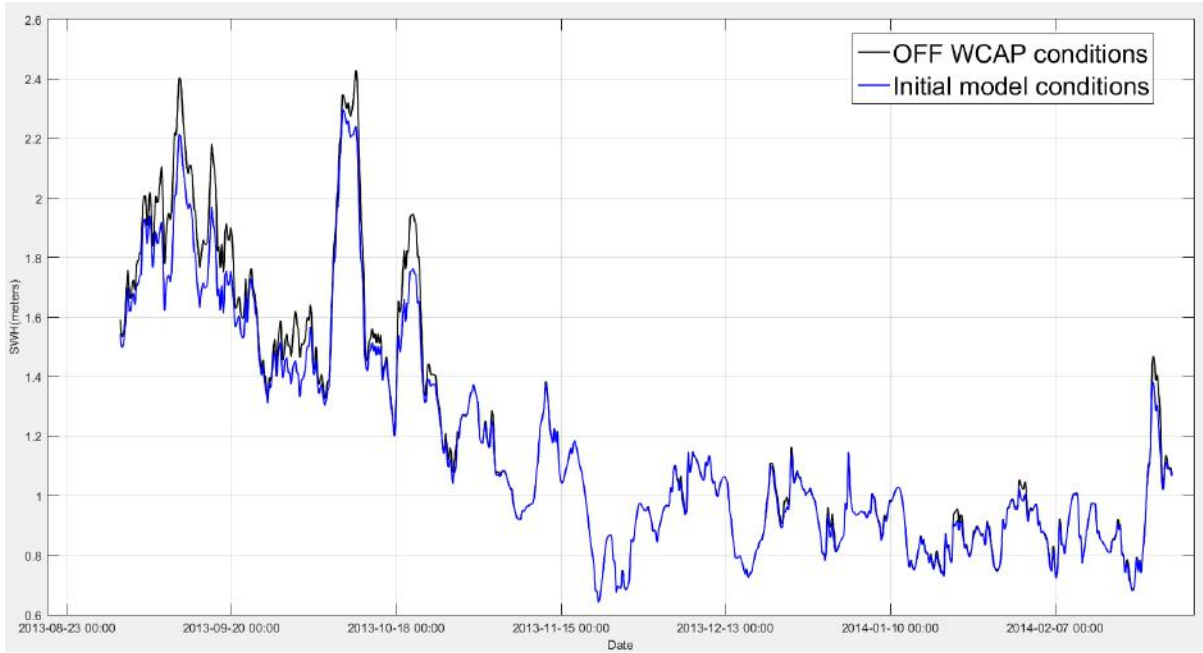


Figure A.2: H_{m0} variations of initial model outputs and deactivated whitecapping (WCAP) outputs

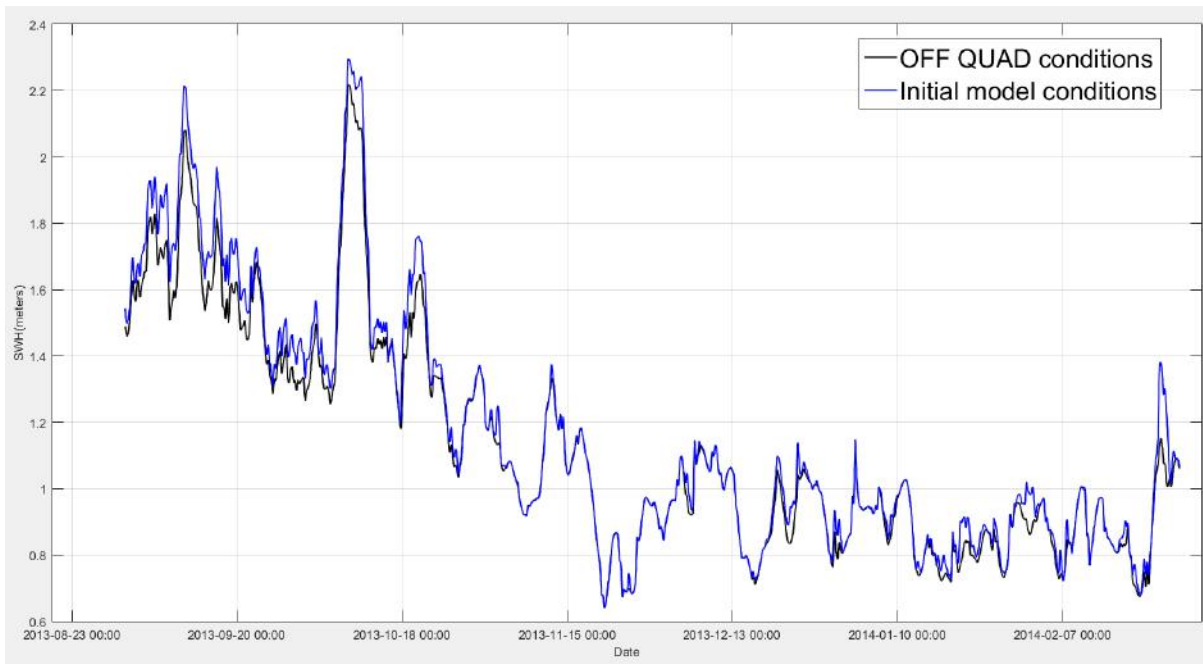


Figure A.3: H_{m0} variations of initial model outputs and deactivated quadruplet (QUAD) interactions

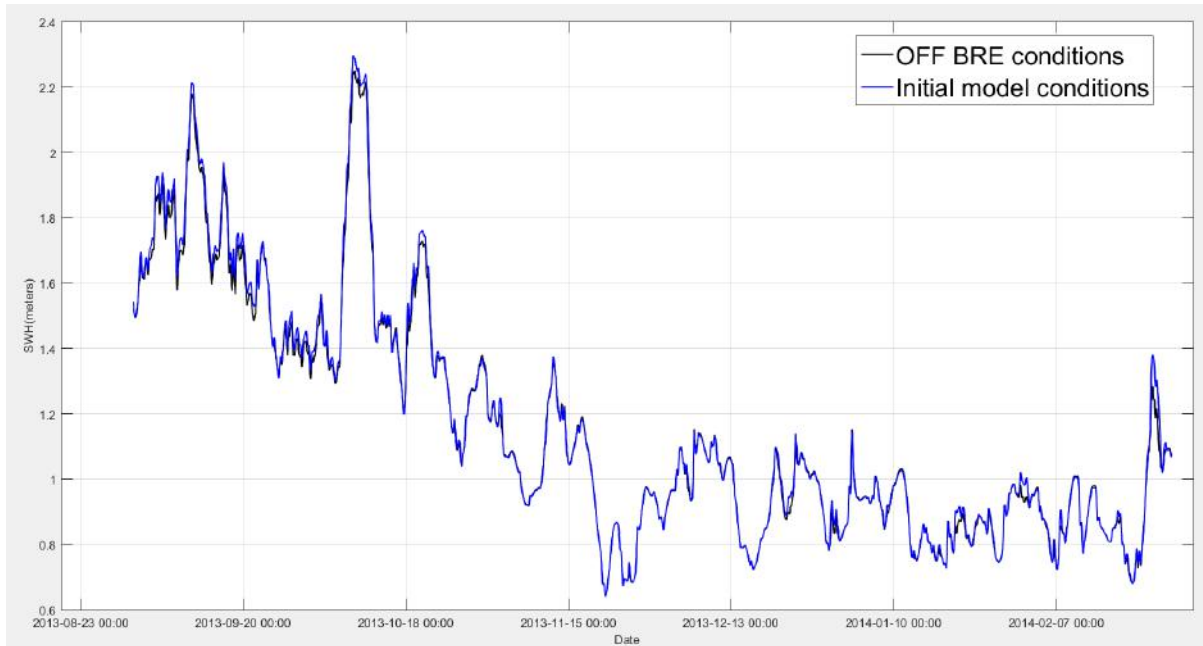


Figure A.4: H_{m0} variations of initial model outputs and deactivated wave breaking (BRE) conditions

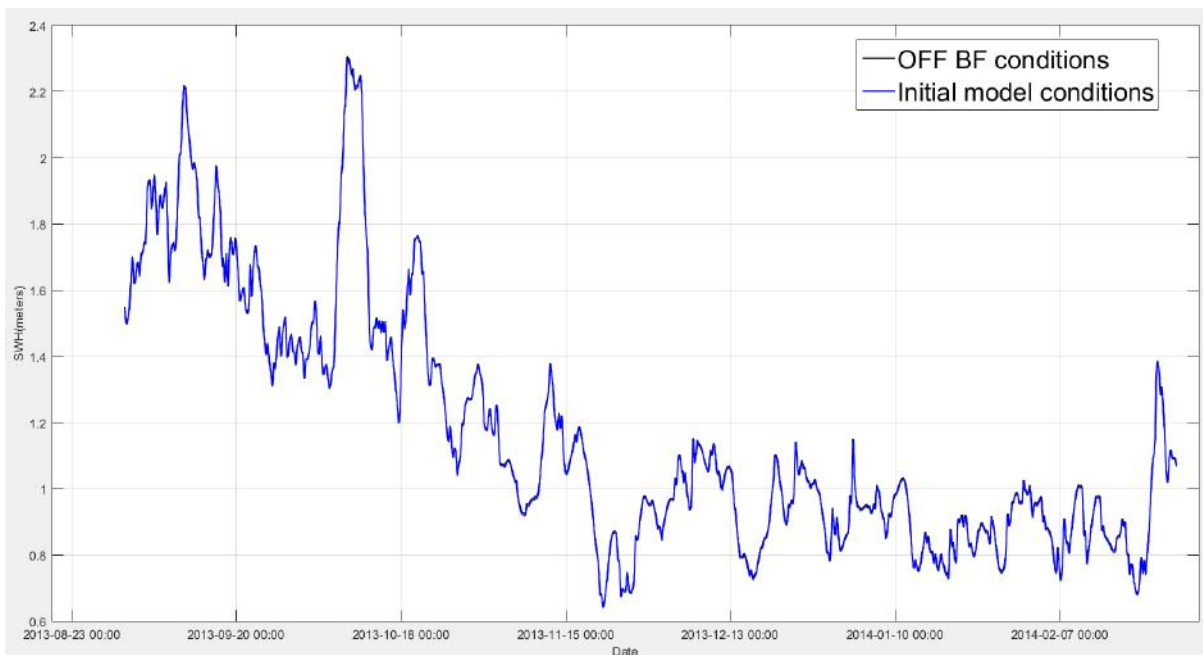


Figure A.5: H_{m0} variations of initial model outputs and deactivated bottom friction (BF) conditions

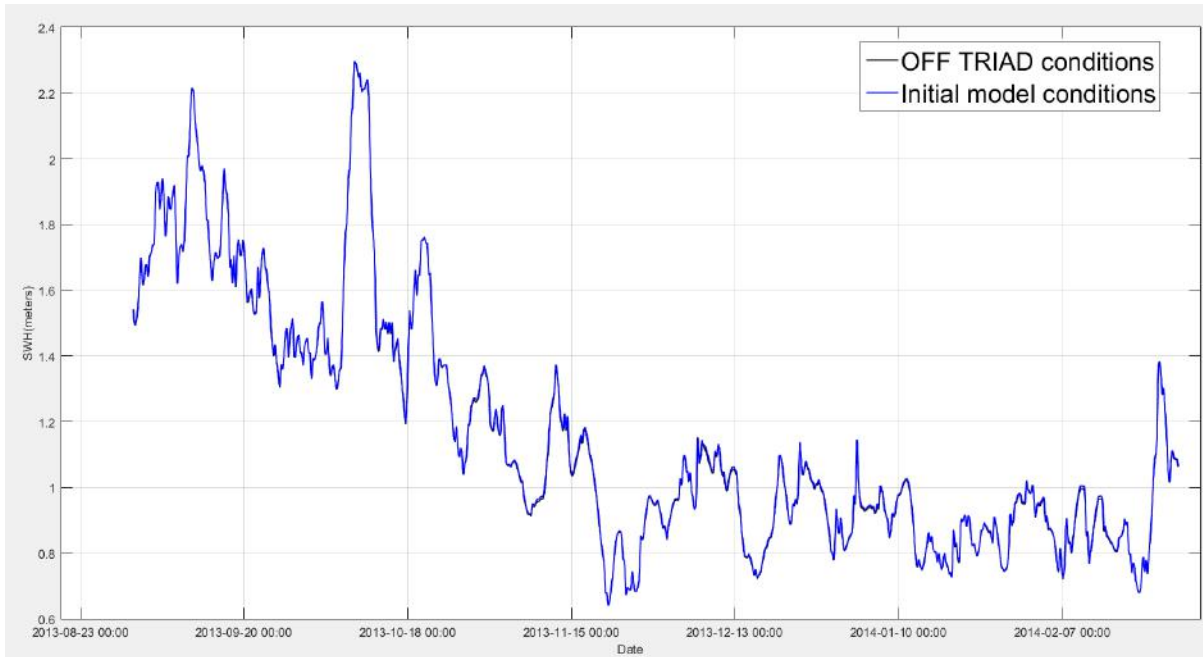


Figure A.6: H_{m0} variations of initial model outputs and deactivated triad (TRIAD) wave-wave interactions

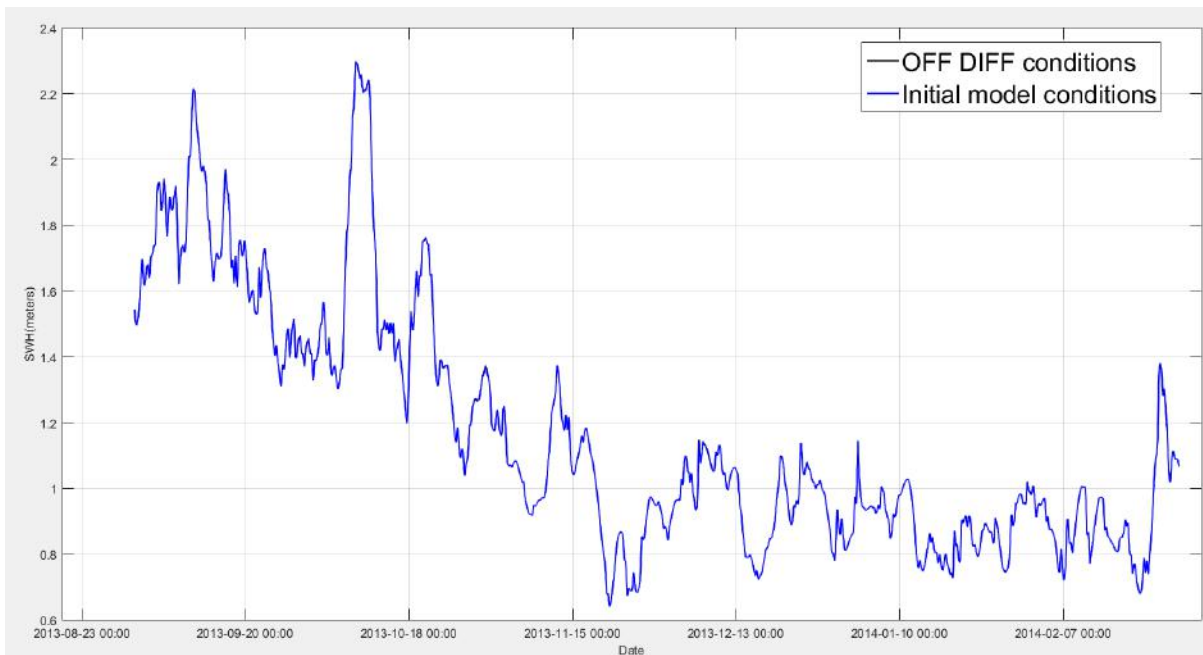


Figure A.7: H_{m0} variations of initial model outputs and deactivated diffraction (DIFF) conditions

The process has conducted for all excluded physical processes and compared the bias and RMSE as shown in Table A.1.

Table A.1: SWH deviation of the excluded physical processes of the model

No.	Excluded physical process	Bias (m)	RMSE (m)
01	Whitecapping dissipation	0.03	0.06
02	Quadruplet wave-wave interaction	-0.04	0.06
03	Wave breaking	-0.01	0.02
04	Bottom friction	0.01	0.01
05	Triad wave interaction	-0.01	0.01
06	Diffraction	0.00	0.01

A.4 Sensitivity analysis of parameter values of the physical processes

A set of simulations of selected uncertain inputs were implemented by setting a range of parameter values using the uniform distributions of the input parameters. Initially, 350 datasets were obtained by changing the default values of seven parameters of the SWAN computations by defining the maximum and minimum limits.

Here, more weights of uncertainty inputs have consisted with whitecapping dissipation and quadruplet wave-wave interactions by considering the previous sensitivity analysis results. Although the bottom friction and triad wave interaction haven't had the significant effects on model variations, those processes also included for the analysis which can be used for future publications. Other than that, results were obtained for water level variations to analyse the effect of bathymetry change for the model. Table A.2 and Table A.3 describe the uncertain parameters relevant to each physical processes and the selected ranges of them for the conducted simulations.

Table A.2: Selected parameters from the SWAN physical processes

	Physical Process	Selected parameters for the analysis
1	Whitecapping dissipation	Whitecapping dissipation rate coefficient
2	Quadruplet wave-wave interaction	Wind speed, Direction of the wind
3	Wave breaking	Proportionally coefficient of dissipation rate, Breaker index
4	Bottom friction	Bottom friction coefficient
5	Triad wave interaction	Proportionally coefficient of triad interaction
6	Bottom level	Water level

Table A.3: Limits of selected input parameters

	Input parameter	Default value	Min	Max	unit
a.	Whitecapping dissipation rate coefficient	2.36×10^{-5}	2.1×10^{-5}	2.6×10^{-5}	
b.	Wind speed	$\sqrt{u^2 + v^2}$	$0.5 \cdot \sqrt{u^2 + v^2}$	$1.5 \cdot \sqrt{u^2 + v^2}$	m/s
c.	Direction of the wind	$\text{atan2}(v,u)$	$\Phi - 20^\circ$	$\Phi + 20^\circ$	deg.
d.	Proportionally coefficient of dissipation rate	1.0	0.5	1.5	-
e.	Breaker index	0.73	0.6	1.0	-
	Bottom friction coefficient	3.8×10^{-2}	1.5×10^{-2}	7.0×10^{-2}	m^2/s^3
f.	Water level	0	-5	5	m

A.5 Results of uncertainty inputs

Different techniques can be used to analyse the uncertainty of the input parameters. Here, bias and RMSE were calculated and analysed of each of generated dataset with respect to the buoy measurements. Following sub sections will compare the bias and RMSE of obtained results of each case with appropriate figures.

The statistical analysis was based on the wave measurements that include the period from five months (01.10.2013-28.02.2014) and contain 3717 records with 1 hour time interval.

$$BIAS = \frac{\sum_{i=1}^n (H_{m0_{model,i}} - H_{m0_{buoy,i}})}{n}$$

$$RMSE = \sqrt{\frac{\sum_{i=1}^n (H_{m0_{model,i}} - H_{m0_{buoy,i}})^2}{n}}$$

Note: $H_{m0_{buoy,i}}$ is the measured significant wave height, $H_{m0_{model,i}}$ is the simulated significant wave height, n is the total number of datasets.

a. Whitecapping dissipation rate coefficient

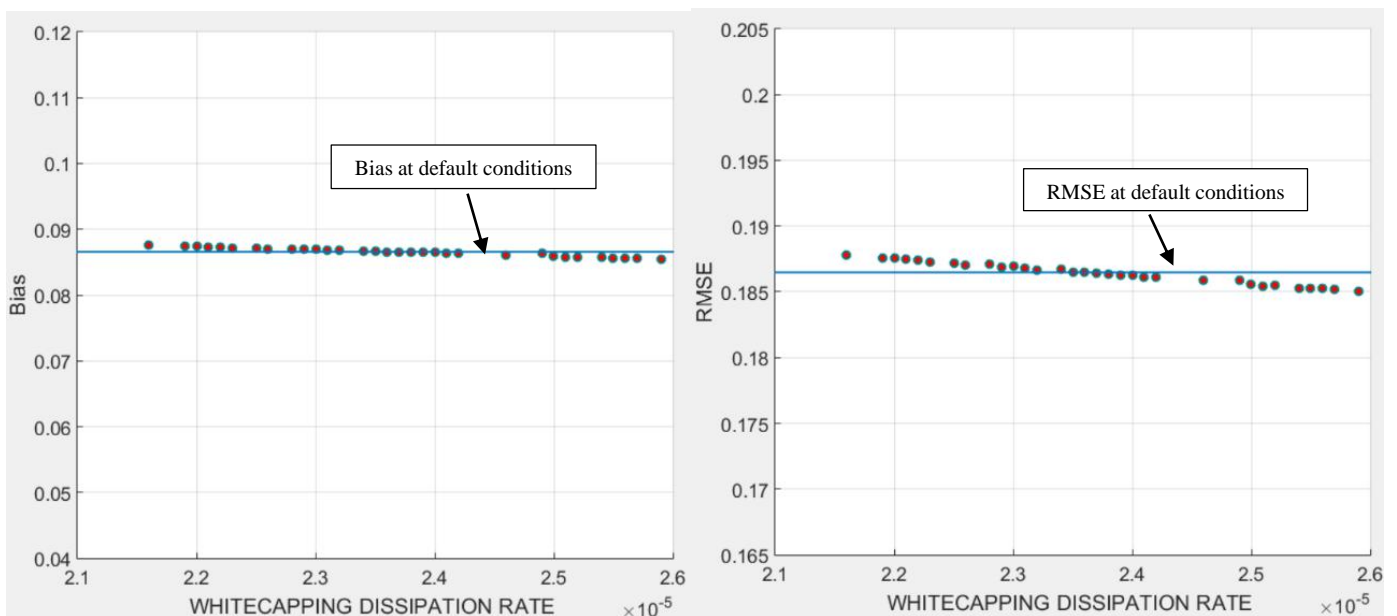


Figure A.8: Bias and RMSE variations at different whitecapping dissipation rates

b. Wind speed

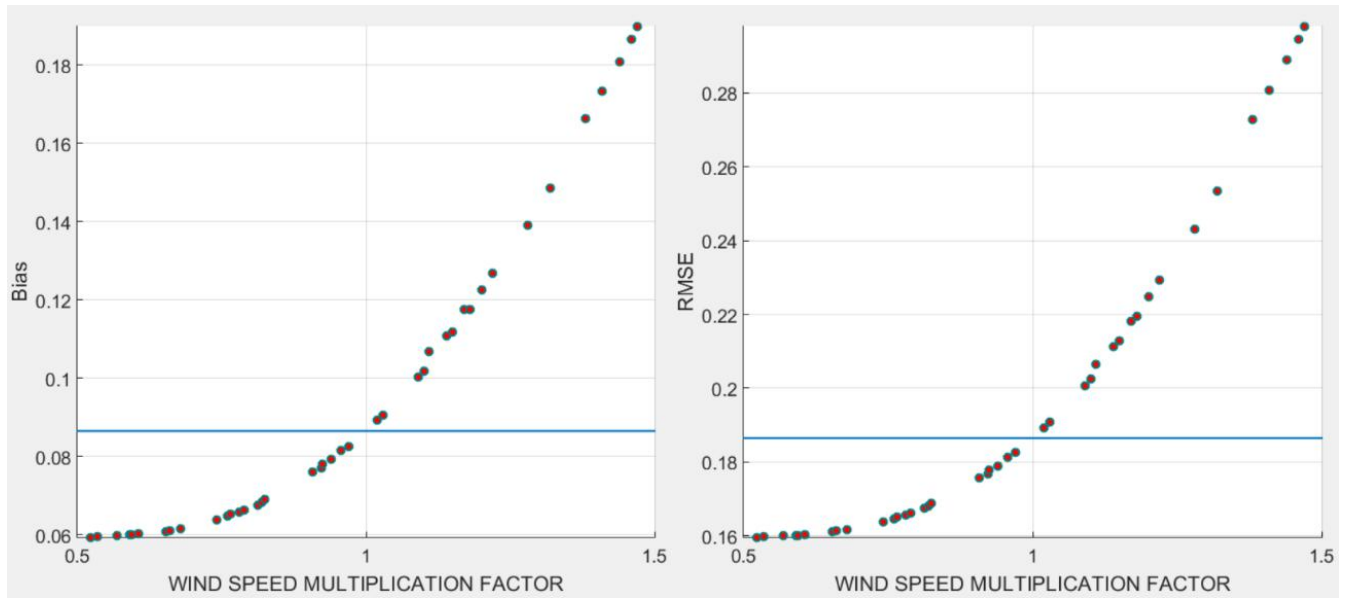


Figure A.9 : Bias and RMSE variations at different wind speeds

c. Direction of the wind

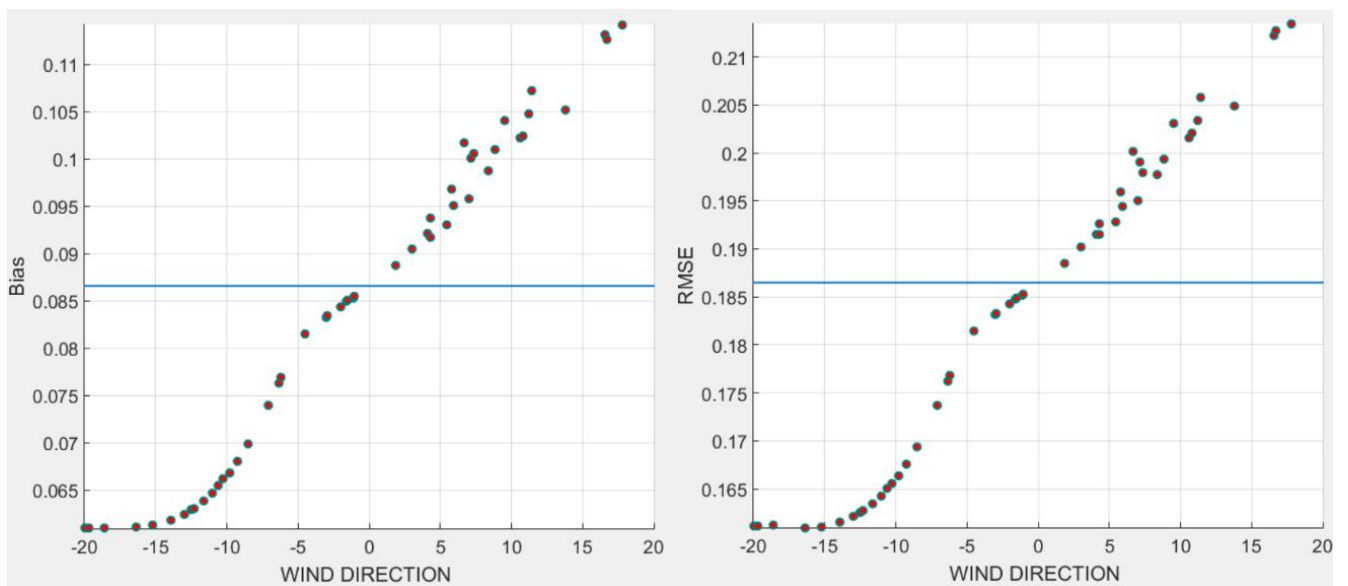


Figure A.10: Bias and RMSE variations at different wind directions

d. Proportionally coefficient of dissipation rate

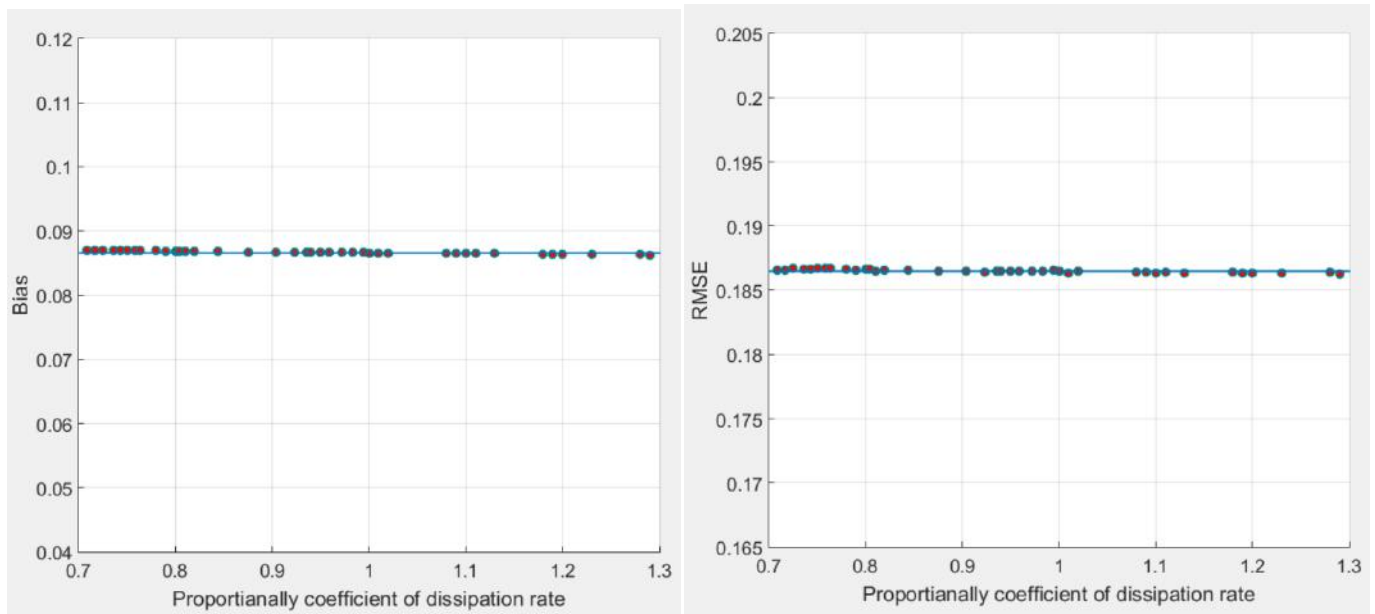


Figure A.11: Bias and RMSE variations at different proportionally coefficient of dissipation rates

e. Breaker index

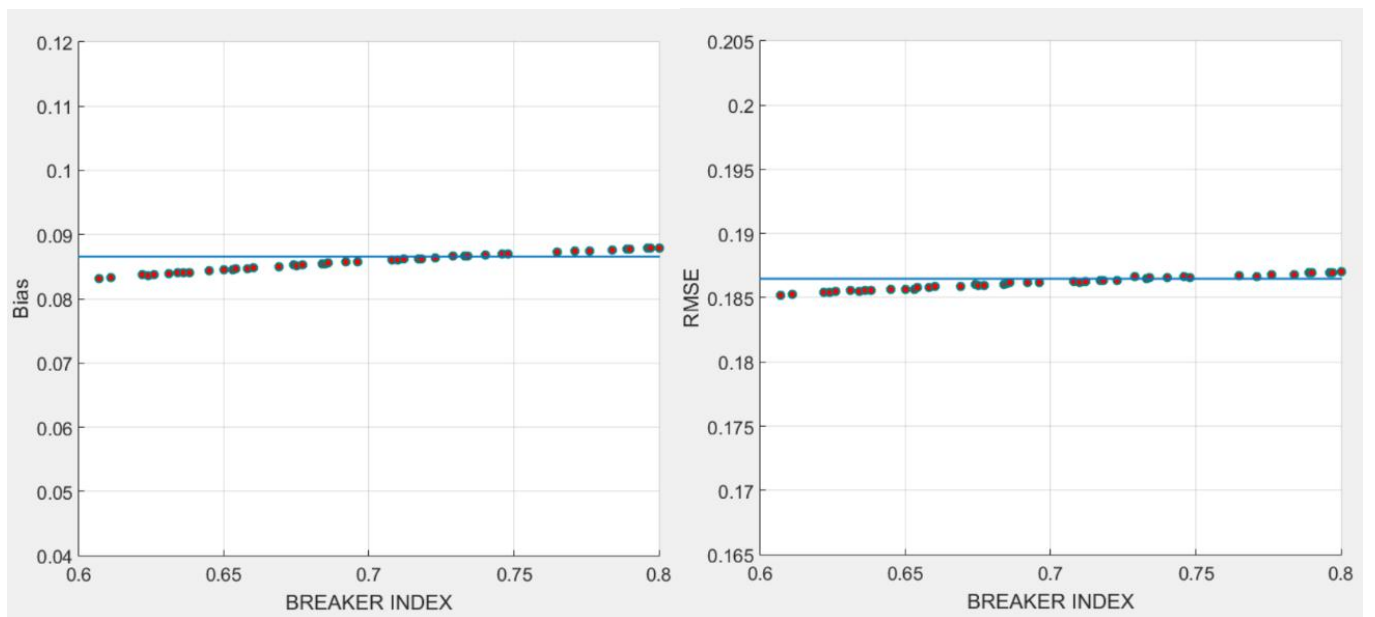


Figure A.12: Bias and RMSE variations at different breaker index values

f. Bottom friction coefficient

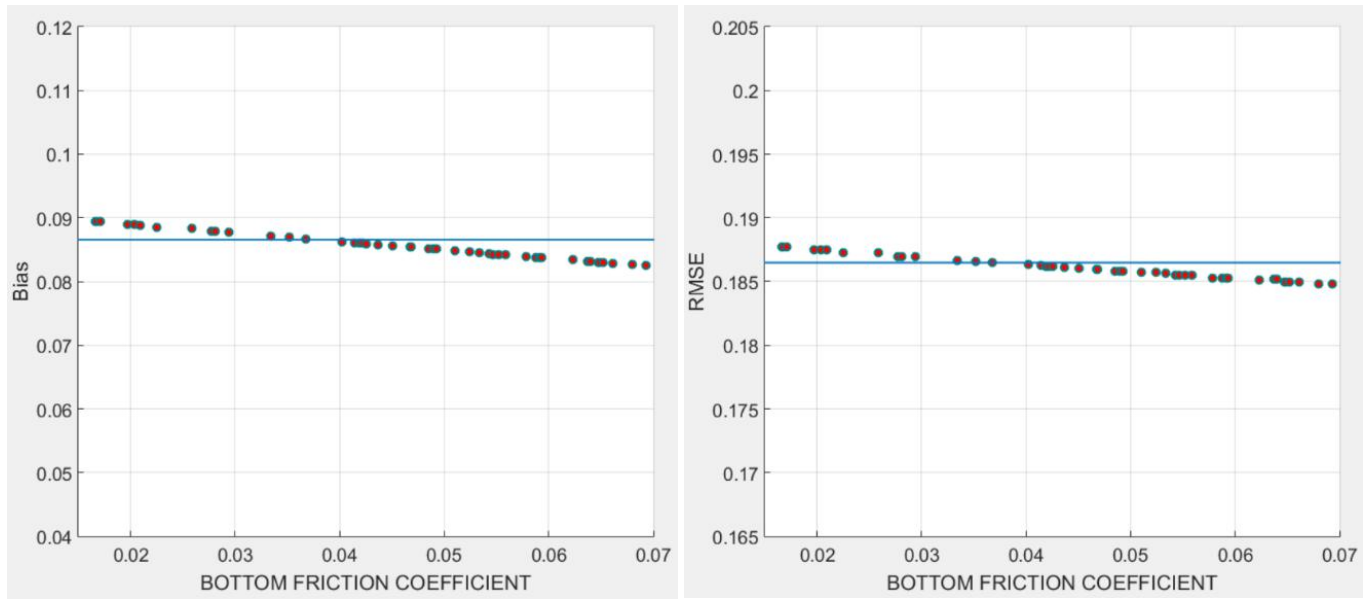


Figure A.13: Bias and RMSE variations at different bottom friction values

g. Water level/Bathymetry

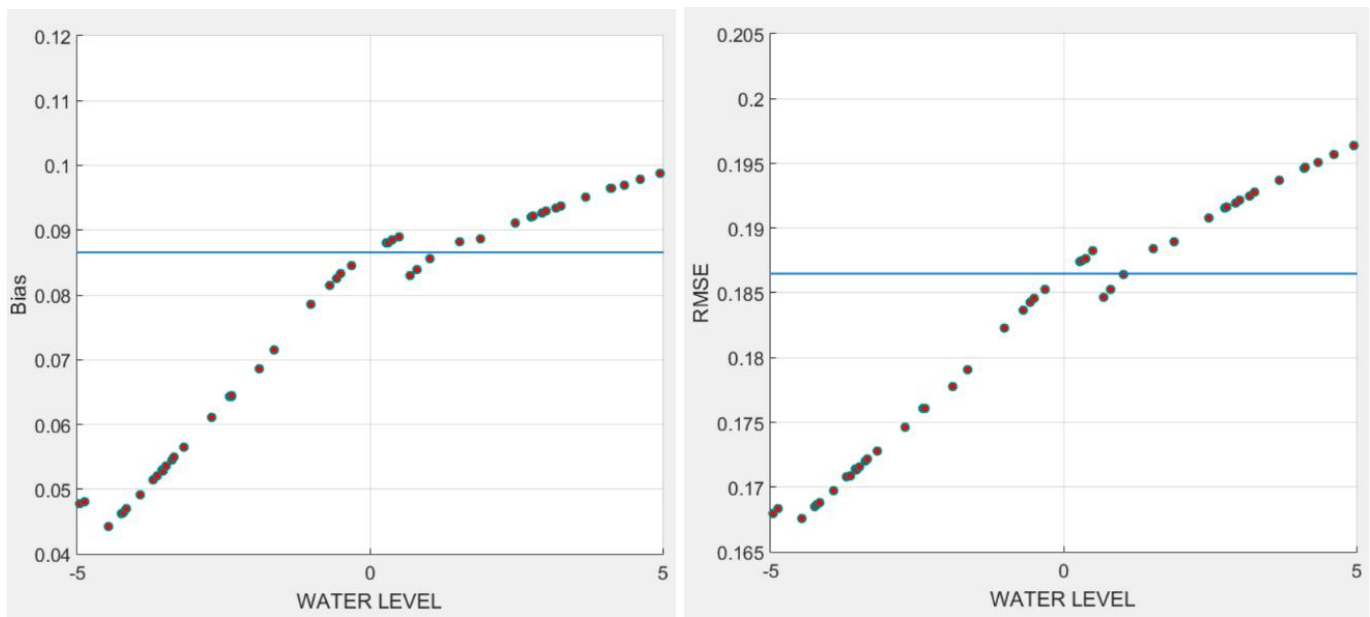


Figure A.14: Bias and RMSE variations at different bottom level values

Annex B

Model Validation

From IEC TS 62600-101:2015: Clause 7.6.3,

Procedure: Validation of numerical models

The data point value for parameter p derived from the wave measurements is denoted p_D and the corresponding value derived from the wave modelling is denoted p_M . For each represented cell the normalized error between measured and modelled values of parameter p shall be calculated as:

$$e_p = \begin{bmatrix} (p_{M_1} - p_{D_1})/p_{D_1} \\ \cdot \\ \cdot \\ \cdot \\ (p_{M_n} - p_{D_n})/p_{D_n} \end{bmatrix}$$

where p_{M_k} and p_{D_k} are values at coincident time-steps tk for $k = 1 \dots n$, and n is the number of measured/modelled parameter value pairs in the cell.

The error for each cell shall be separated into a systematic error, $\mu_{ij}(e_p)$ and a random error, $\sigma_{ij}(e_p)$. The systematic error, or bias, shall be defined as the mean of the errors in cell i, j , whilst the random error shall be defined as the standard deviation of the errors in cell i, j .

From the viewpoint of wave energy resource characterization, the significance of the systematic and random errors within any given cell can be related to their influence on the estimation of energy availability or production. For each cell i, j , the product of the proportional frequency of occurrence f_{ij} and mean incident wave power J_{ij} (where f_{ij} and J_{ij} are obtained over the duration of the resource assessment, not from the validation data set) gives a strong indication of the significance of any error and shall form the basis for computing the weighting factor, w_{ij} , as:

$$w_{ij} = J_{ij}f_{ij}$$

For those scatter table cells i, j where the requirements for a minimum number of validation data points is unmet (see Table 6), f_{ij} shall be set to zero. If a specific WEC technology is being considered, then the weighting factors may be scaled by the capture length L_{ij} associated with each cell (see IEC TS 62600-100), as:

$$w_{ij} = L_{ij} J_{ij} f_{ij}$$

In any case, the weighting matrix shall be normalized such that its sum is unity, as:

$$\hat{w}_{ij} = \frac{w_{ij}}{\sum_{i,j} w_{ij}}$$

The weighted mean systematic error (e_p) shall be calculated as the sum of the element-wise product of the normalized weighting matrix and the systematic error matrix, as:

$$b(e_p) = \sum_{i,j} \hat{w}_{ij} \mu_{ij}$$

Similarly, the weighted mean random error (e_p) shall be calculated as the element-wise product of the normalized weighting matrix and the random error matrix, as:

$$\sigma(e_p) = \sum_{i,j} \hat{w}_{ij} \sigma_{ij}$$

NOTE : The use of the weighted mean error is intended as a metric for validating model results over the represented H_{m0} - T_e domain of the validation site data set.

B.1 Analysis 01: CCD-GTZ dataset

CCD-GTZ dataset has mainly consisted 3 hourly measured data of significant wave height (H_{m0}), zero crossing period (T_z), mean wave direction (Θ). The wave measurements are separated into sea and swell components, but in their report, there is no any clear indication of cut off frequency of the used spectrum. However, authors have recommended to calculate nearshore overall wave parameters using following equations.

$$H_{m0,overall} = \sqrt{H_{m0,swell}^2 + H_{m0,sea}^2}$$

$$T_{z,overall} = \frac{H_{m0,overall}}{\sqrt{\frac{H_{m0,swell}^2}{T_{z,sea}^2} + \frac{H_{m0,sea}^2}{T_{z,swell}^2}}}$$

For the model validation, model outputs of significant wave height and zero crossing period were obtained for the given location and compared with the wave measured dataset. Here, the actual water depth of 70 m, mentioned under CCD-GTZ report has obtained with the model output location as well (71 m). Following described the results of Analysis 01.

Table B1: Summary of model validation details, Analysis 01

Location	Water depth	Period of analysis	No. of available wave records
5.914 °N 80.201 °E	71 m	05/1989 - 09/1992	7139

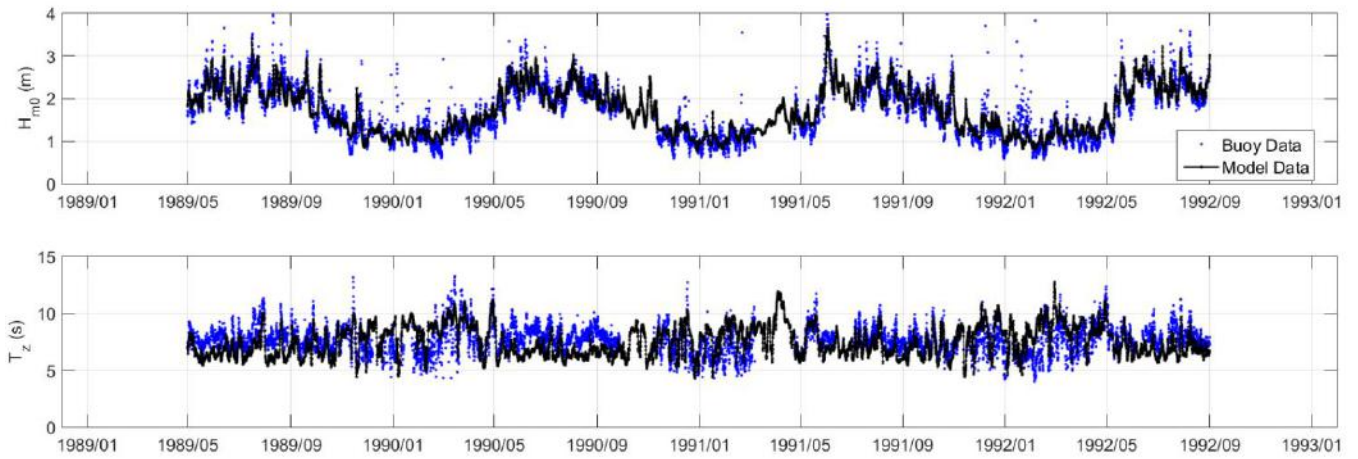


Figure B1: Significant wave height (H_{m0}) and zero crossing period (T_z) obtained from CCD-GTZ wave measurements and SWAN model

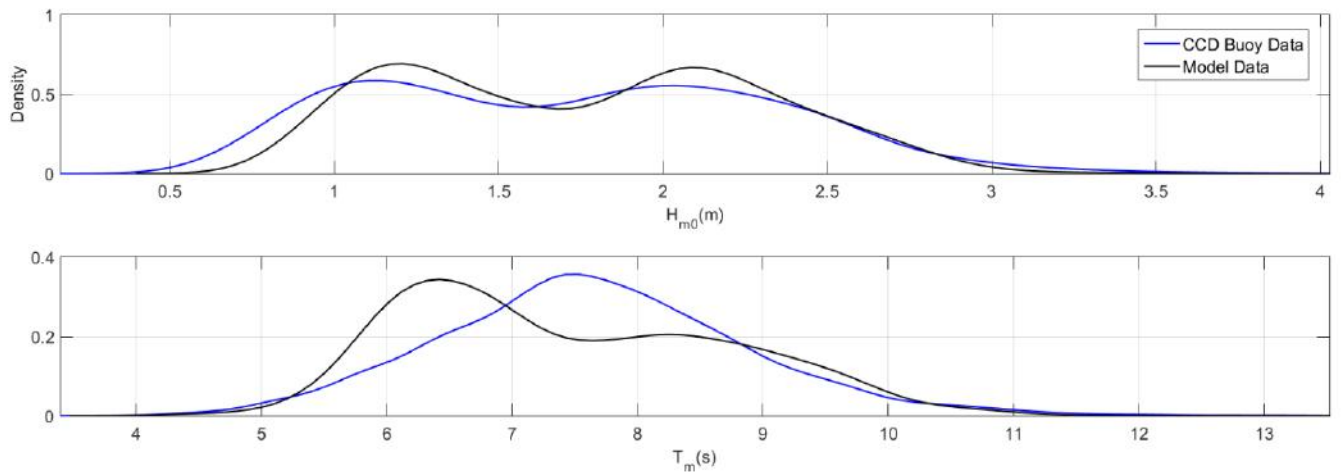


Figure B2: Probability density plots of H_{m0} and T_z of buoy and model data, Analysis 01

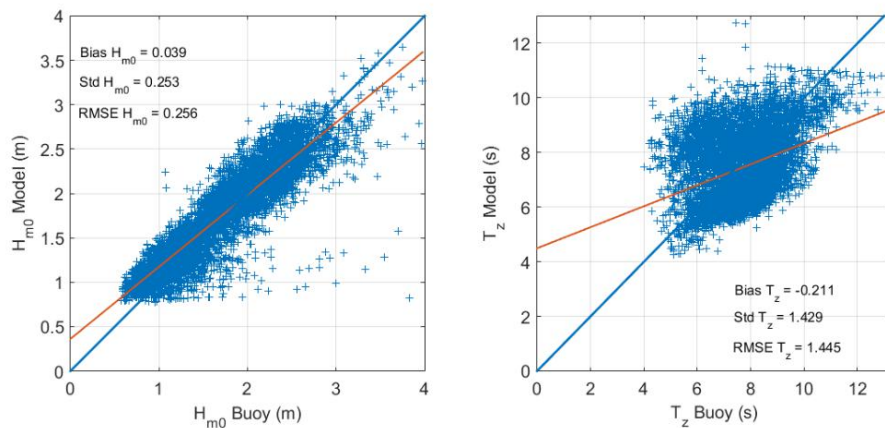


Figure B3: Scatter plots of H_{m0} and T_z of buoy and model data, Analysis 01

Table B2: Analysis of model outputs and CCD-GTZ buoy measurements w.r.t IEC-TS 62600-101 requirements

	Analysis of the model outputs	Minimum validation requirement (IEC-TS 62600-101)
Validation data coverage requirements		
Minimum number of validation data points to represent cell	3	3
Minimum coverage by validation data	95 %	90 %
Maximum acceptable weighted mean systematic error, $b(e_p)$		
Significant wave height, H_{m0}	2.2 %	10 %
Zero crossing period, T_z	- 6.7 %	10 %
Maximum acceptable weighted mean random error, $\sigma(e_p)$		
Significant wave height, H_{m0}	10.6 %	15 %
Zero crossing period, T_z	10.9 %	15 %

According to above analysis, model outputs at the CCD-GTZ buoy location have satisfied all the minimum validation requirements of the IEC-TS 62600-101. The uncertainty of H_{m0} and T_z can be occurred due to various reasons such as measurement uncertainty, device performance uncertainty, temporal and spatial extrapolation uncertainty. However, the analysis implies that the model is performing effectively well at the offshore location, specially near to the 70 m water depth which is close to the recommended range for reliable Wave Energy Convertor (WEC) deployments.

B.2 Analysis 02: SCSIO Buoy 01

The SCSIO Buoy 01 dataset was selected as Analysis 02 of the validation procedure which includes significant wave height, maximum wave height, 1/10th wave height and mean wave period, hourly air pressure, and water level every 10 min at a water depth of 20 m. As per the consideration of Class 01 assessment of IEC-TS 62600-101, the model outputs of significant wave height (H_{m0}) and mean wave period (T_m) were obtained from the model and compared with the wave measured dataset.

Here, the buoy location was described as close distance (~200 m) to the coast and the used bathymetric data of the model has not indicated the exact location with the same water depth. Also model wasn't performed very accurate to such a close distance. This is mainly occurred due to the poor resolution of the bathymetry and other input datasets at the coastal regions. Due to these reasons, the location of the validation point was selected as the nearest distance to the actual buoy location with similar water depth. Following described the results of Analysis 02.

Table B3: Summary of model validation details, Analysis 02

Selected location	Water depth	Period of measurement	No. of available wave records
5.916 °N 80.557 °E	21.4 m	09/2013 - 02/2014	3717

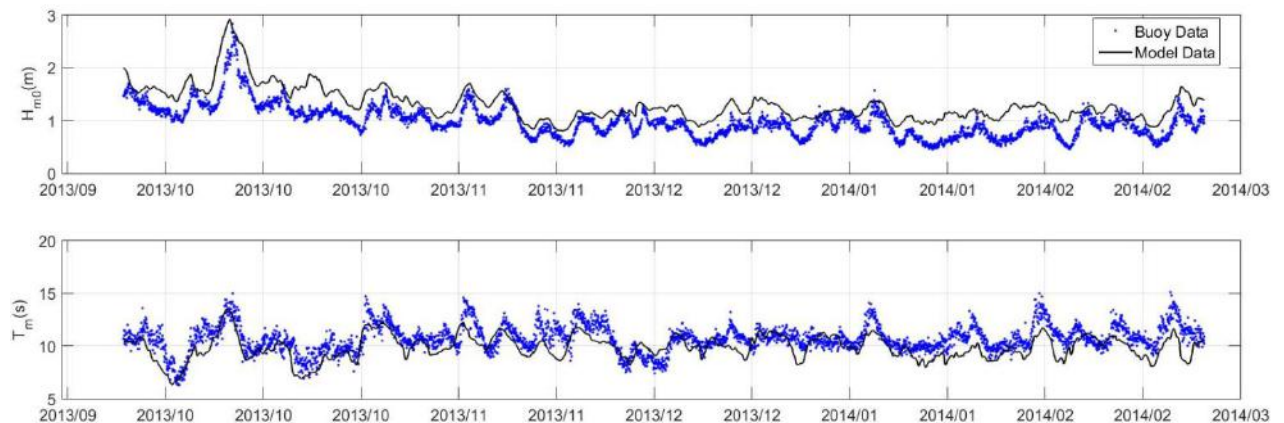


Figure B4: Significant wave height(H_{m0}) and mean absolute wave period (T_m) obtained from SCSIO buoy 01 wave measurements and SWAN model

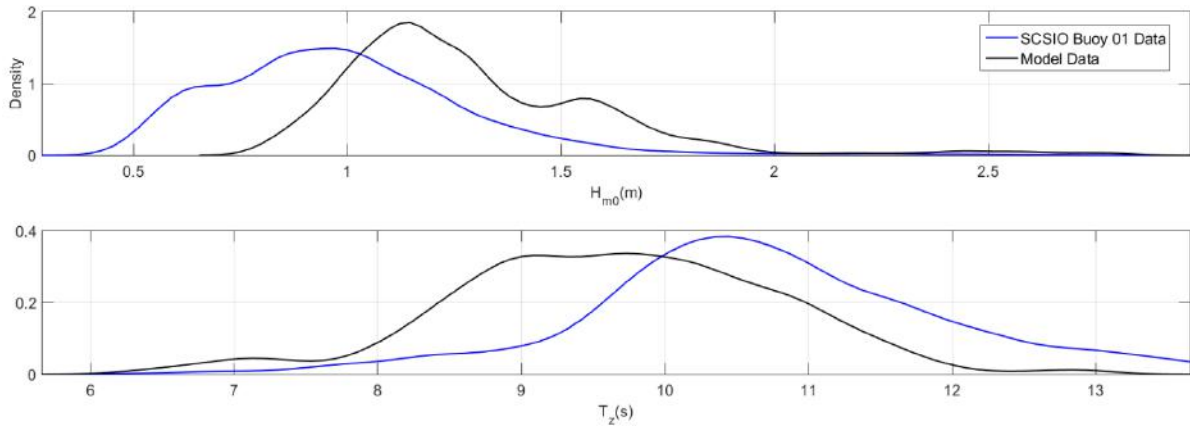


Figure B5: Probability density plots of H_{m0} and T_e of buoy and model data, Analysis 02

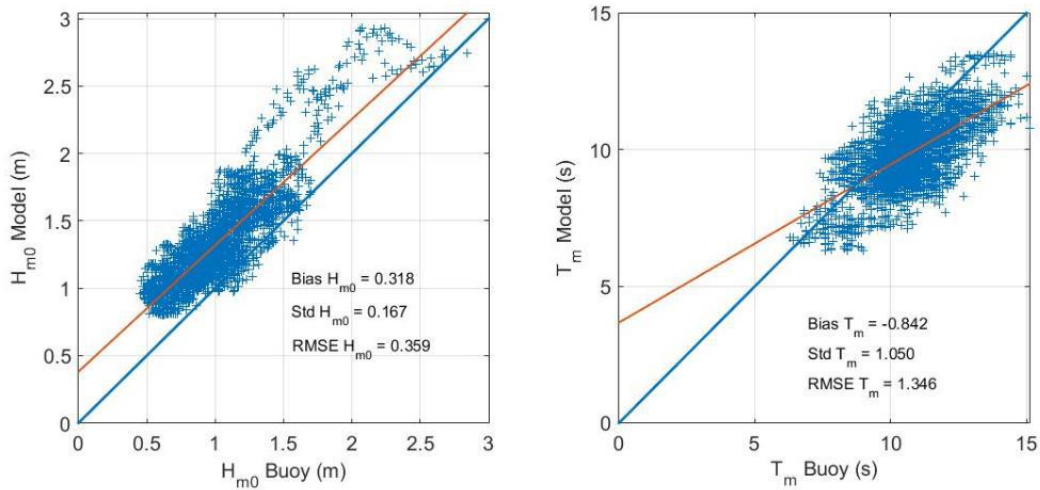


Figure B6: Scatter plots of H_{m0} and T_z of buoy and model data, Analysis 02

Table B4: Analysis of model outputs and SCSIO 20 m buoy measurements w.r.t IEC-TS 62600-101

	Analysis of the model outputs	Minimum validation requirement (IEC-TS 62600-101)
Validation data coverage requirements		
Minimum number of validation data points to represent cell	3	3
Minimum coverage by validation data	95 %	90 %
Max acceptable weighted mean systematic error, $b(e_p)$		
Significant wave height, H_{m0}	19.2 %	10 %

Mean absolute wave period, T_m	- 7.4 %	10 %
Max acceptable weighted mean random error, $\sigma(e_p)$		
Significant wave height, H_{m0}	16.7 %	15 %
Mean absolute wave period, T_m	7.9 %	15 %

According to above analysis, model outputs at the SCSIO buoy 01 location have marginally satisfied the minimum validation requirements of the IEC-TS 62600-101. Although the mean random error or standard deviation of H_{m0} and T_m variations have shown acceptable results, mean systematic error of H_{m0} has considerable difference. Again, this uncertainty of H_{m0} and T_z can be occurred due to various reasons such as measurement uncertainty, device performance uncertainty, temporal and spatial extrapolation uncertainty. This analysis implies that the model is over predicting the H_{m0} variations in considerable margin and under predicting the T_m variations with acceptable limits at the nearshore location.

B.3 Analysis 03: SCSIO Buoy 02

SCSIO Buoy 02 dataset includes hourly significant wave height, peak wave period, mean wave direction, and direction spectra at 10 m water depth. Again, as per the consideration of Class 01 assessment of IEC-TS 62600-101, the model outputs of significant wave height (H_{m0}) and peak period (T_p) were obtained from the model and compared with the wave measured dataset.

Table B5: Summary of model validation details, Analysis 03

Location	Water depth	Period of measurement	No. of available wave records
6.106 °N 80.080 °E	9.8 m	04/2013 - 04/2014	7777

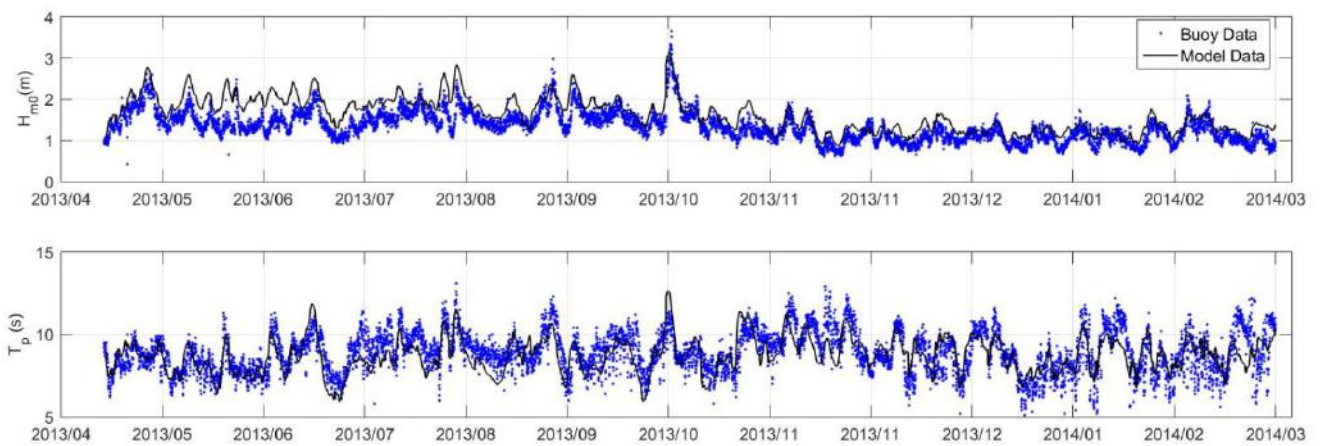


Figure B7: Significant wave height (H_{m0}) and peak period (T_p) obtained from SCSIO buoy 02 wave measurements and SWAN model

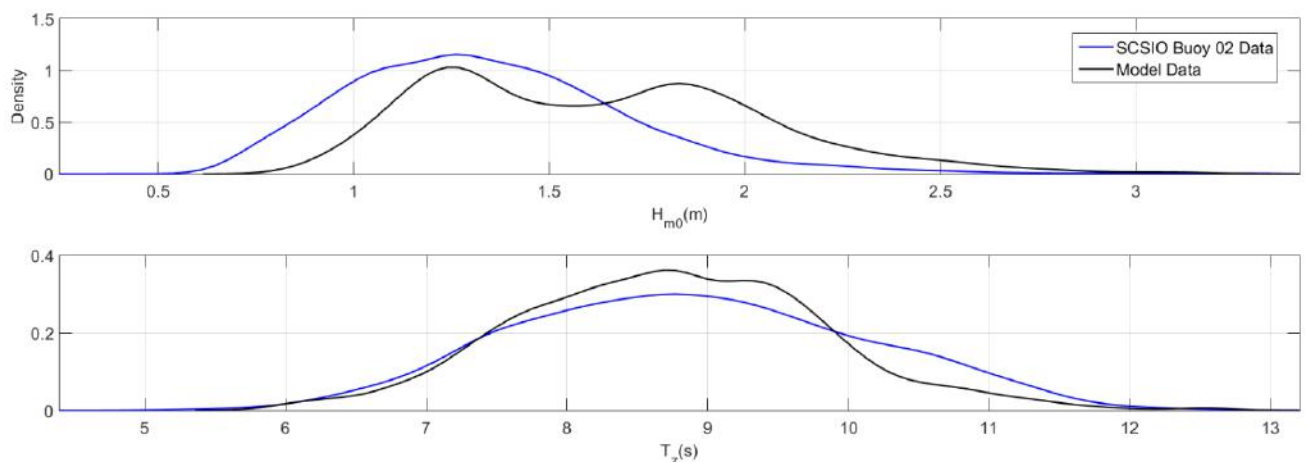


Figure B8: Probability density plots of H_{m0} and T_z of buoy and model data, Analysis 03

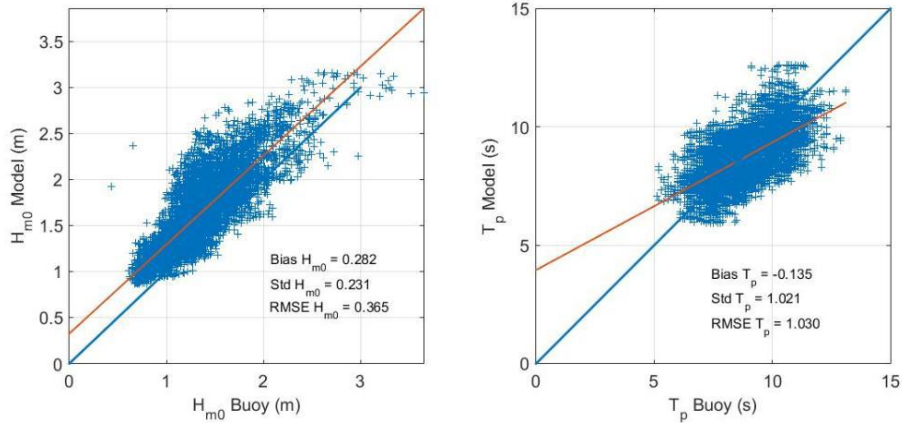


Figure B9: Scatter plots of H_{m0} and T_p of buoy and model data, Analysis 03

Table B6: Analysis of model outputs and SCSIO 10 m buoy measurements w.r.t IEC-TS 62600-101

	Validation requirement of the model	Minimum validation requirement (IEC-TS 62600-101)
Validation data coverage requirements		
Minimum number of validation data points to represent cell	3	3
Minimum coverage by validation data	95 %	90 %
Max acceptable weighted mean systematic error, $b(e_p)$		
Significant wave height, H_{m0}	8.1 %	10 %
Mean absolute wave period, T_m	-5.1 %	10 %
Max acceptable weighted mean random error, $\sigma(e_p)$		
Significant wave height, H_{m0}	13.8 %	15 %
Mean absolute wave period, T_m	10 %	15 %

Although buoy water depth is 10 m, the model outputs at the SCSIO buoy 02 location have satisfied the minimum validation requirements of the IEC-TS 62600-101. This is very important to conclude that the model outputs are working accurately for the nearshore locations.

B.4 Analysis of GOW2 spectral data

As described in Section 6.3, above validation datasets only cover the down south area of the model. Because of that, a global wave hindcast dataset had to use for further validation of other directions of the model. Here, four spectral data points were selected in all four directions considering the nearest distances to the coast. Other than the significant wave height and the mean wave period, GOW2 data consist of omni-directional wave power as well. As per the consideration of Class 01 assessment of IEC-TS 62600-101, the model outputs of significant wave height (H_{m0}), peak period (T_p) and Omni-directional wave power (J) were obtained from the model and compared with the particular GOW2 dataset. All four analysis have been conducted for five years (1995-1999) with 1 hour time intervals which consist of more than 40,000 data records.

B.4.1. Analysis 04: GOW2 data point: South Direction

Table B7: Summary of model validation details, Analysis 04

Location	Water depth	Period of measurement	No. of available wave records
5.5 °N 81.5 °E	3794 m	01/1995 - 12/1999	43562

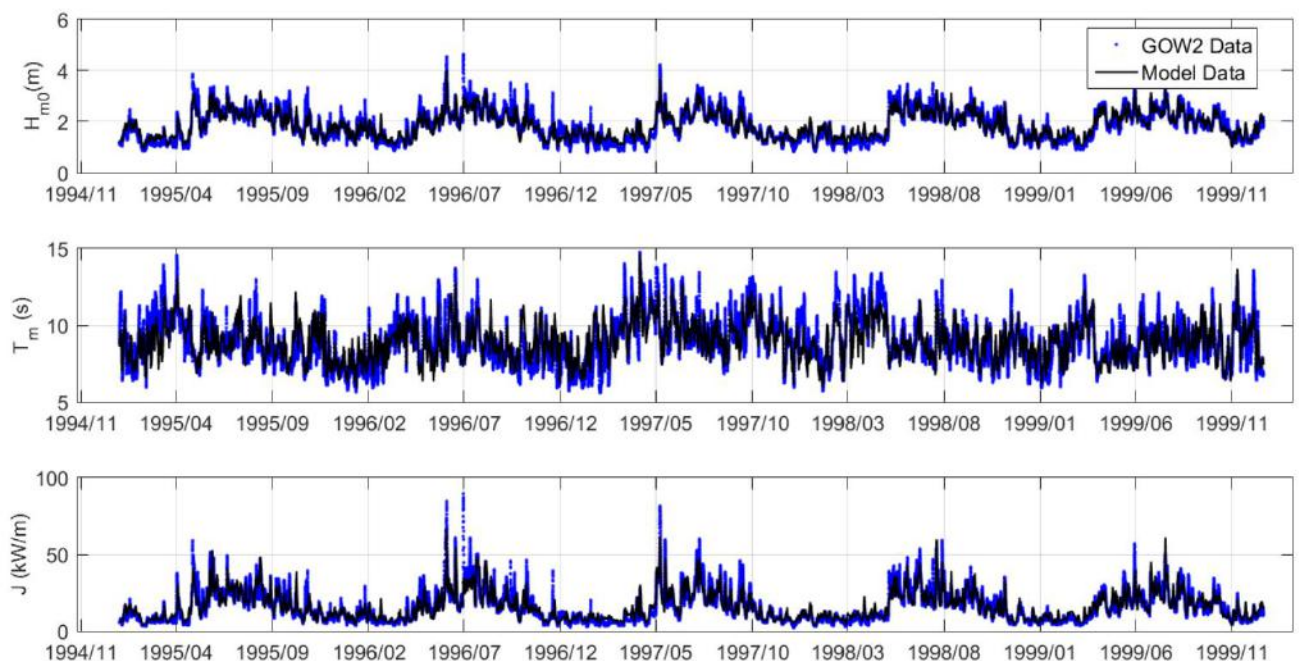


Figure B10: Significant wave height(H_{m0}) , mean absolute wave period (T_m) and Omni-directional wave power (J) obtained from GOW2 South direction point and SWAN model

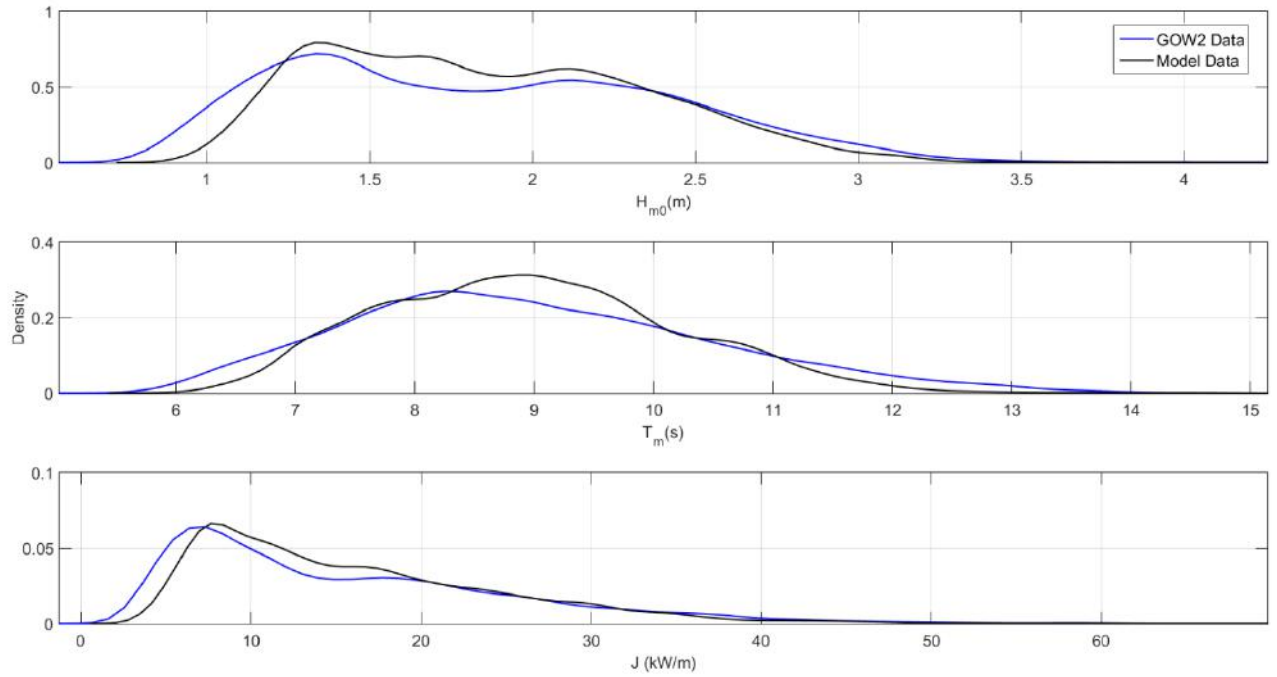


Figure B11: Probability density plots of H_{m0} , T_p and J of GOW2 South direction point and model data, Analysis 04

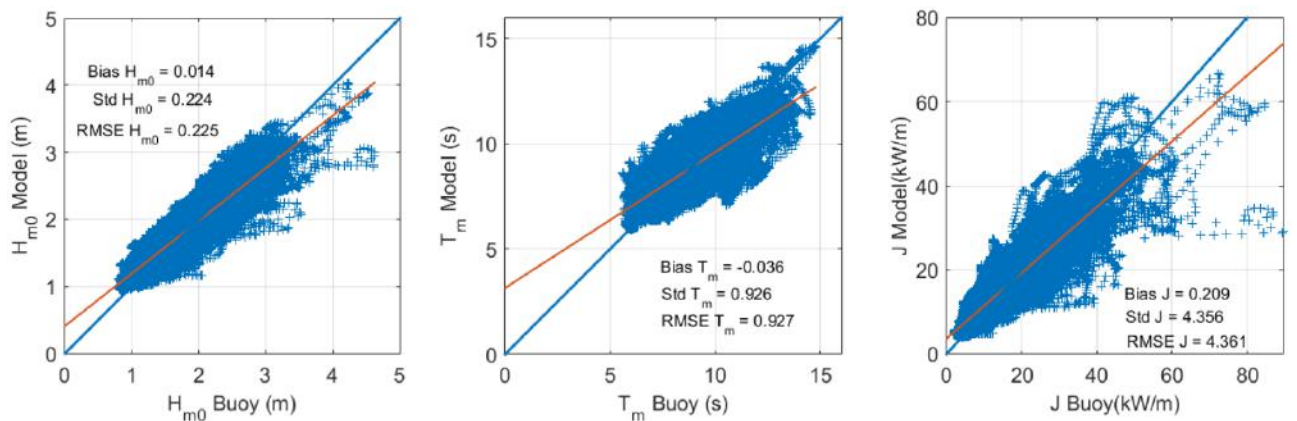


Figure B12: Scatter plots of H_{m0} , T_p and J of GOW2 South direction point and model data, Analysis 04

Table B8: Analysis of model outputs and GOW2 South direction point w.r.t IEC-TS 62600-101

	Validation requirement of the model	Minimum validation requirement (IEC-TS 62600-101)
Validation data coverage requirements		
Minimum number of validation data points to represent cell	3	3
Minimum coverage by validation data	98 %	90 %
Max acceptable weighted mean systematic error, $b(e_p)$		
Significant wave height, H_{m0}	- 0.5 %	10 %
Mean absolute wave period, T_m	- 0.5 %	10 %
Omni-directional wave power, J	1.8 %	25 %
Max acceptable weighted mean random error, $\sigma(e_p)$		
Significant wave height, H_{m0}	8.8 %	15 %
Mean absolute wave period, T_m	7.6 %	15 %
Omni-directional wave power, J	19.2 %	35%

B.4.2. Analysis 05: GOW2 data point: West Direction

Table B9: Summary of model validation details, Analysis 05

Location	Water depth	Period of measurement	No. of available wave records
7.0 °N 79.5 °E	1145 m	01/1995 - 12/1999	43562

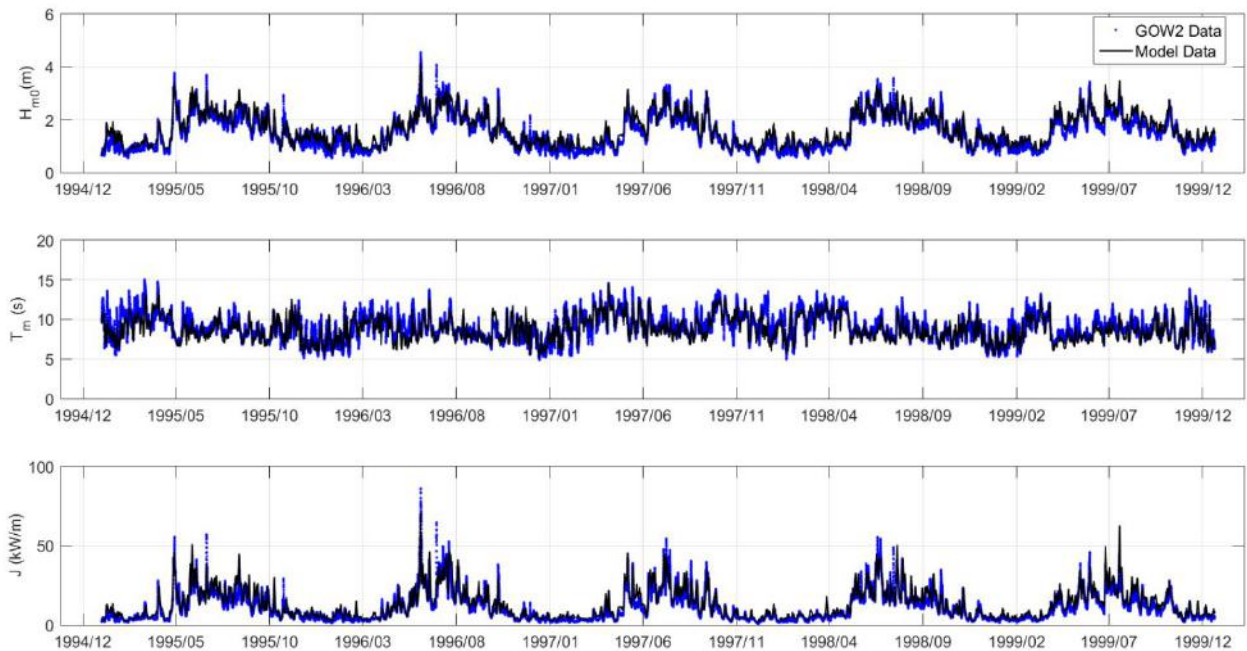


Figure B13: Significant wave height (H_{m0}), mean absolute wave period (T_m) and Omni-directional wave power (J) obtained from GOW2 West direction point and SWAN model

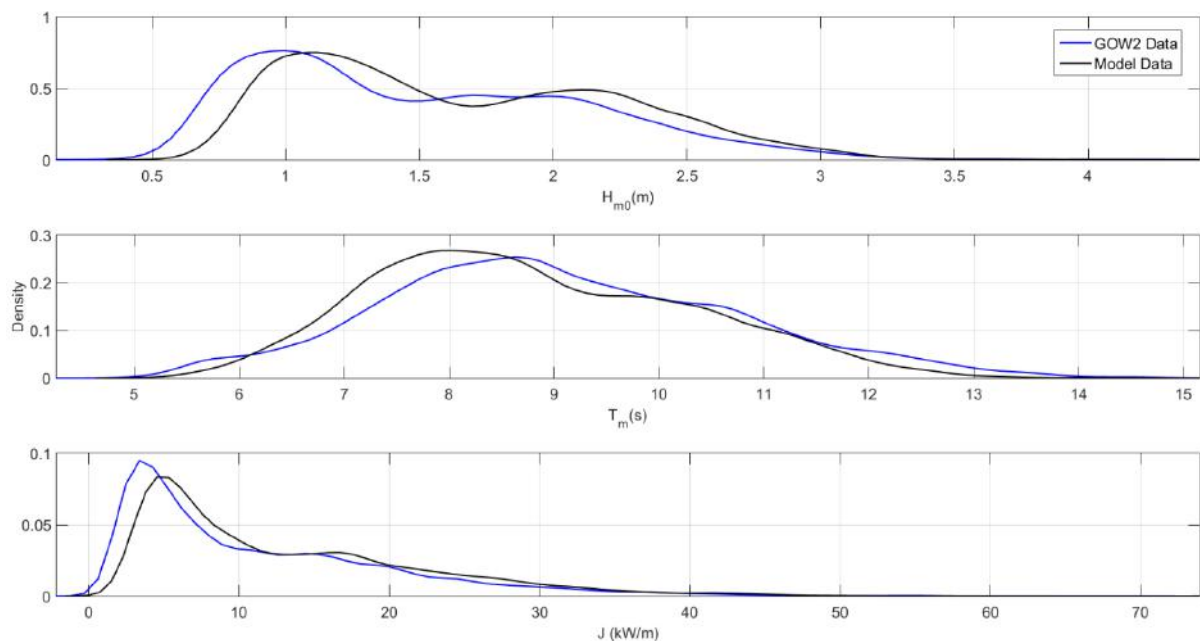


Figure B14: Probability density plot of H_{m0} , T_p and J of GOW2 West direction point and model data, Analysis 05

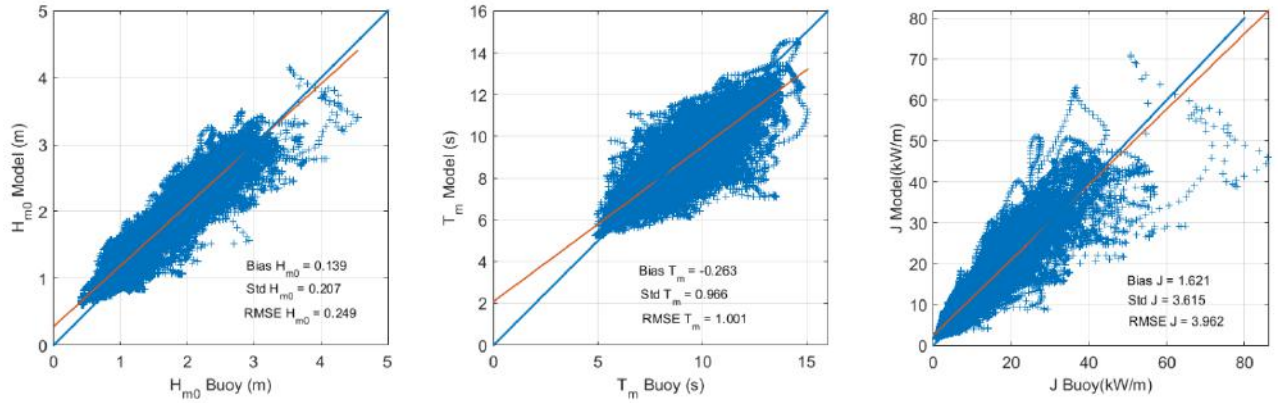


Figure B15: Scatter plot of H_{m0} , T_p and J of GOW2 West direction point and model data, Analysis 05

Table B10: Analysis of model outputs and GOW2 West direction point w.r.t IEC-TS 62600-101

	Validation requirement of the model	Minimum validation requirement (IEC-TS 62600-101)
Validation data coverage requirements		
Minimum number of validation data points to represent cell	3	3
Minimum coverage by validation data	98 %	90 %
Max acceptable weighted mean systematic error, $b(e_p)$		
Significant wave height, H_{m0}	7.3 %	10 %
Mean absolute wave period, T_m	- 3.6 %	10 %
Omni-directional wave power, J	14.9 %	25 %
Max acceptable weighted mean random error, $\sigma(e_p)$		
Significant wave height, H_{m0}	10.7 %	15 %
Mean absolute wave period, T_m	7.3 %	15 %
Omni-directional wave power, J	23.4 %	35 %

B.4.3. Analysis 06: GOW2 data point: East Direction

Table B11: Summary of model validation details, Analysis 06

Location	Water depth	Period of measurement	No. of available wave records
7.0 °N 82.5 °E	3949 m	01/1995 - 12/1999	43562

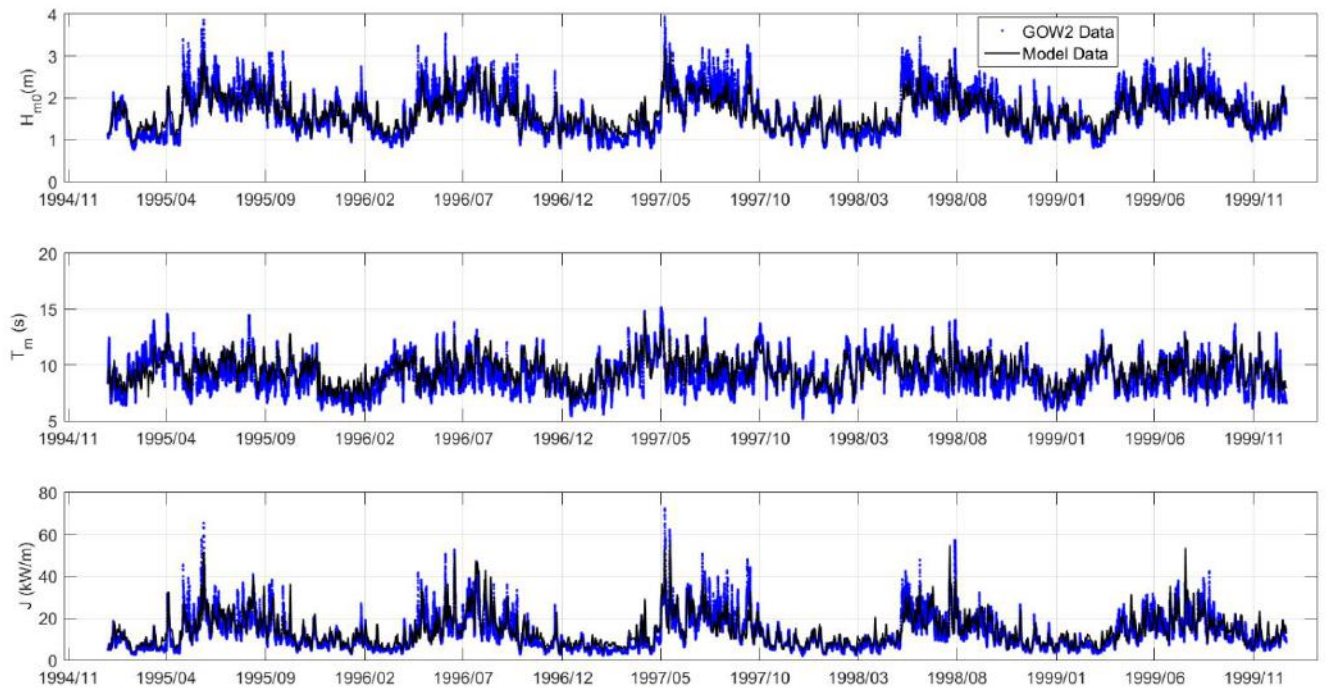


Figure B16: Significant wave height (H_{m0}), mean absolute wave period (T_m) and Omni-directional wave power (J) obtained from GOW2 East direction point and SWAN model

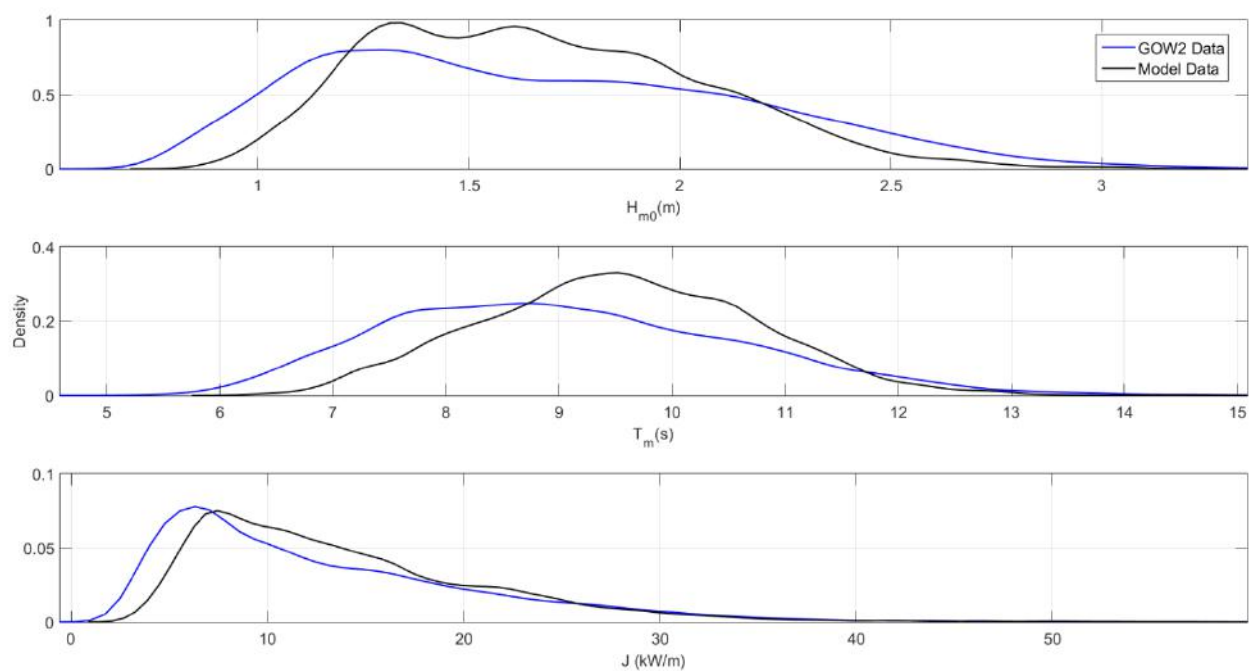


Figure B17: Probability density plots of H_{m0} , T_p and J of GOW2 East direction point and model data, Analysis 06

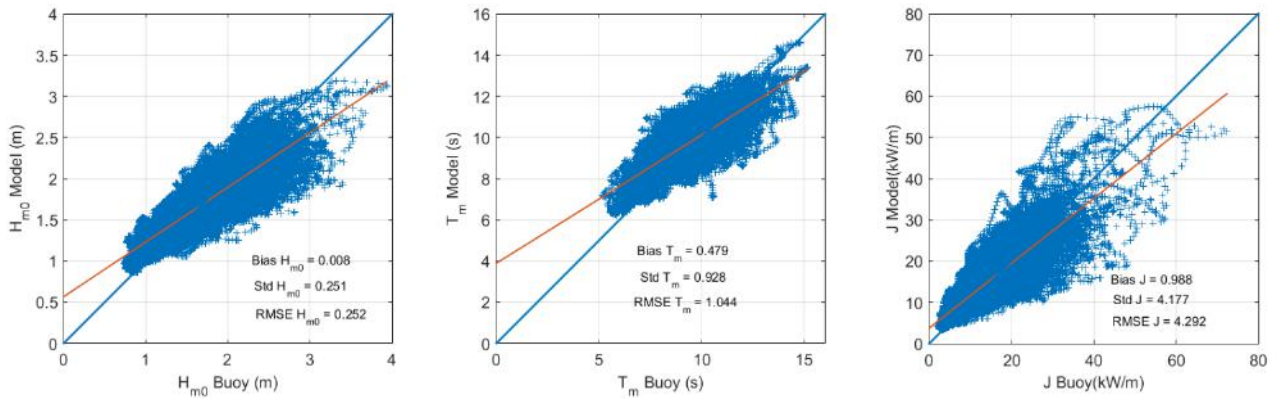


Figure B18: Scatter plots of H_{m0} , T_p and J of GOW2 East direction point and model data, Analysis 06

Table B12: Analysis of model outputs and GOW2 East direction point w.r.t IEC-TS 62600-101

	Validation requirement of the model	Minimum validation requirement (IEC-TS 62600-101)
Validation data coverage requirements		
Minimum number of validation data points to represent cell	3	3
Minimum coverage by validation data	98 %	90 %
Max acceptable weighted mean systematic error, $b(e_p)$		
Significant wave height, H_{m0}	- 1.1 %	10 %
Mean absolute wave period, T_m	7.0 %	10 %
Omni-directional wave power, J	8.3 %	25 %
Max acceptable weighted mean random error, $\sigma(e_p)$		
Significant wave height, H_{m0}	9.5 %	15 %
Mean absolute wave period, T_m	7.3 %	15 %
Omni-directional wave power, J	16.5 %	35%

B.4.4. Analysis 07: GOW2 data point: North Direction

Table B13: Summary of model validation details, Analysis 07

Location	Water depth	Period of measurement	No. of available wave records
10 °N 80.5 °E	426.3 m	01/1995 - 12/1999	43562

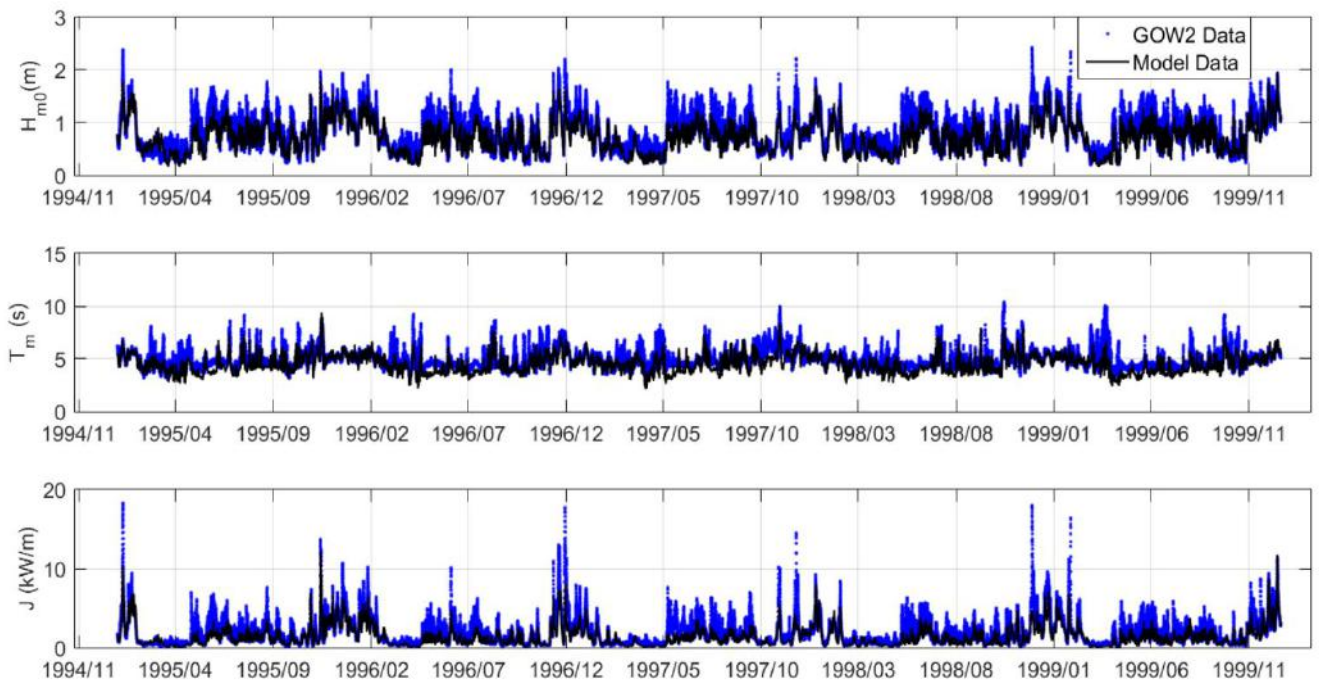


Figure B19: Significant wave height (H_{m0}), mean absolute wave period (T_m) and Omni-directional wave power (J) obtained from GOW2 North direction point and SWAN model

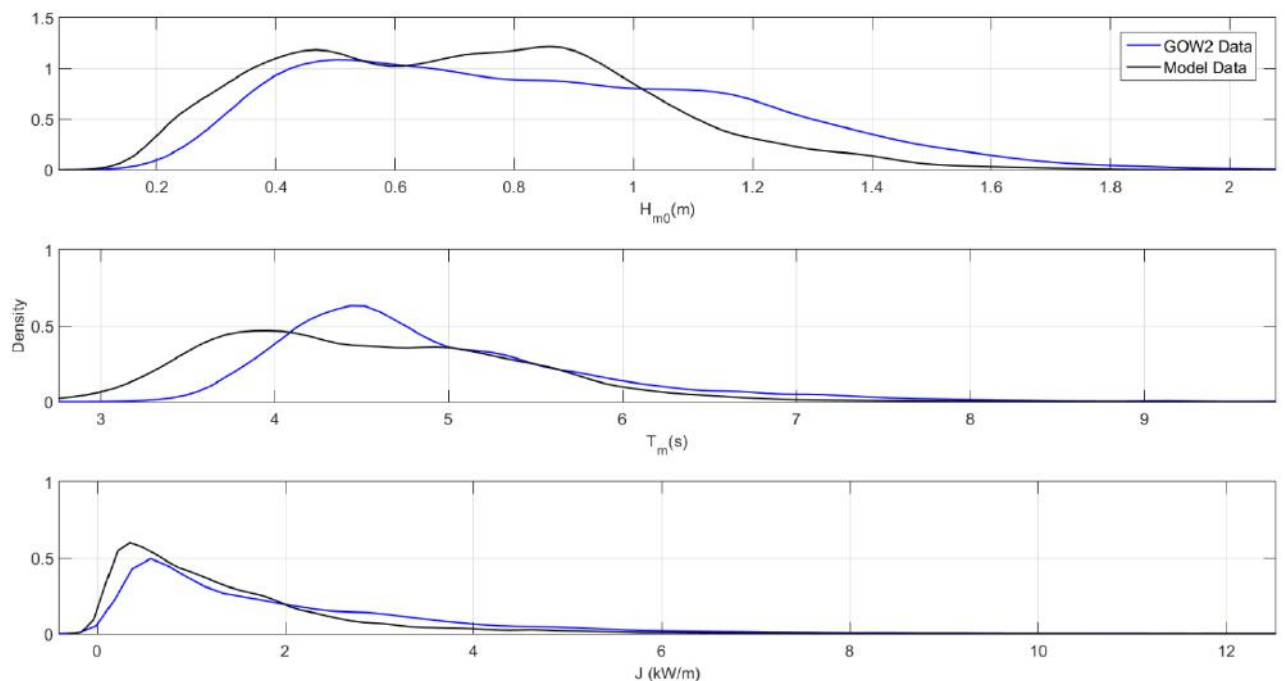


Figure B20: Probability density plots of H_{m0} , T_p and J of GOW2 North direction point and model data, Analysis 07

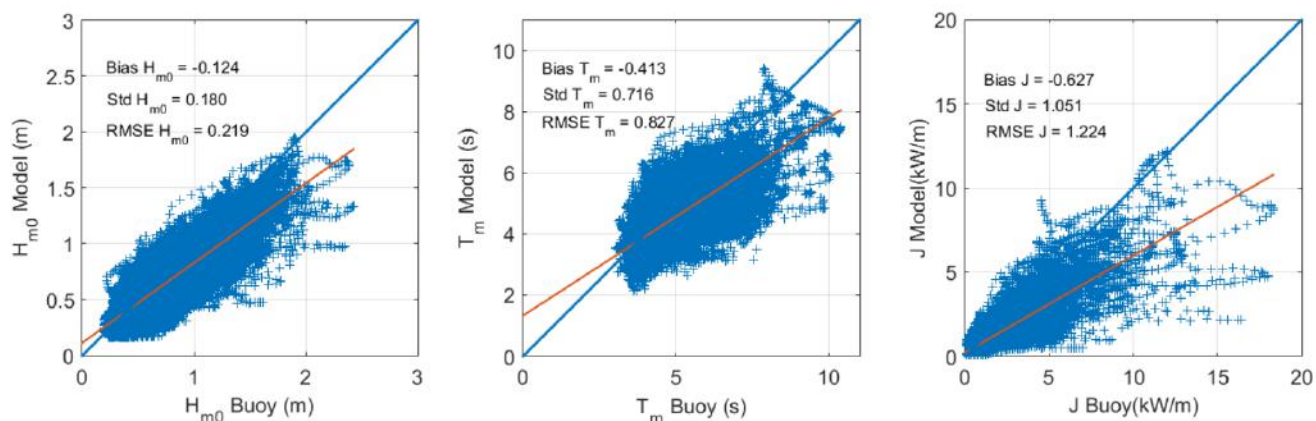


Figure B21: Scatter plot of H_{m0} , T_p and J of GOW2 North direction point and model data, Analysis 07

Table B14: Analysis of model outputs and GOW2 North direction point w.r.t IEC-TS 62600-101

	Validation requirement of the model	Minimum validation requirement (IEC-TS 62600-101)
Validation data coverage requirements		
Minimum number of validation data points to represent cell	3	3
Minimum coverage by validation data	98 %	90 %
Max acceptable weighted mean systematic error, $b(e_p)$		
Significant wave height, H_{m0}	- 9.1 %	10 %
Mean absolute wave period, T_m	- 7.5 %	10 %
Omni-directional wave power, J	- 15.2%	25 %
Max acceptable weighted mean random error, $\sigma(e_p)$		
Significant wave height, H_{m0}	10.1 %	15 %
Mean absolute wave period, T_m	10.8 %	15 %
Omni-directional wave power, J	18.5%	35 %

According to the above analysis, all four GOW2 datasets have satisfied all the minimum validation requirements of the IEC-TS 62600-101 es. Although H_{m0} and T_m model values have slight deviations at all four directions, mean random errors of wave power in all directions mostly deviate in a somewhat higher range, but within the minimum validation requirements. The overall performance of the model outputs is accurate at the GOW2 validation data points considering the minimum validation requirements of the IEC-TS 62600-101.

Annex C

Data Analysis Procedure

From IEC TS 62600-101:2015: Clause 9: Data analysis

9.1 Introductory remarks

The data analysis uses sea state data to produce characteristic parameters that are relevant to the performance of wave energy converters. The methods specified in 9.2.1 to 9.2.5 (used in IEC TS 62600-101) shall also be used to calculate characteristic parameters from non-directional wave spectra. If no directional information is available then the directionally resolved power and associated parameters may be omitted from the wave resource assessment.

Of primary importance is an estimate of the mean omni-directional energy flux per unit width, or wave power. In addition, the parameters for characterizing an individual sea state shall include:

- characteristic wave height,
- characteristic wave period,
- spectral width,
- direction of maximum directionally resolved wave power, and
- directionality coefficient.

9.2 Characterization using two-dimensional wave spectra

9.2.1 Overview

The sea state shall be characterised using the directional wave spectrum obtained at each grid point in time and space. For any given directional wave spectra, the variance density over the i^{th} discrete frequency and j^{th} discrete direction is S_{ij} .

Directionally unresolved characteristic quantities are more conveniently calculated by first transforming the two-dimensional frequency-directional variance densities to one-dimensional frequency variance densities according to the following equation:

$$S_i = \sum_j S_{ij} \Delta\theta_j$$

Spectral moments are used to calculate many characteristic sea state parameters. Spectral moments of the n^{th} order shall be calculated from the frequency variance density according to the equation:

$$m_n = \sum_i f_i^n S_i \Delta f_i$$

The following parameters shall be calculated at all the grid points.

9.2.2 Omni-directional wave power

The omni-directional, or directionally unresolved, wave power is the time averaged energy flux through an envisioned vertical cylinder of unit diameter, integrated from the sea floor to the surface. The omni-directional wave power is calculated as:

$$J = \rho g \sum_{i,j} c_{g,i} S_{ij} \Delta f_i \Delta \theta_j$$

$$c_{g,i} = \frac{\pi f_i}{k_i} \left(1 + \frac{2k_i h}{\sinh 2k_i h} \right)$$

The wave number associated with a given frequency and depth is implicitly defined through the dispersion relation:

$$(2\pi f_i)^2 = g k_i \tanh k_i h$$

9.2.3 Characteristic wave height

A spectrally derived estimate of the significant wave height shall be used to characterize the wave heights of a given sea state. It is calculated using the zeroth spectral moment according to the equation:

$$H_{m0} = 4 \sqrt{m_0}$$

NOTE: H_{m0} is not equal to the significant wave height defined as the mean of the highest third of waves, which is typically identified using the subscript s or $1/3$

9.2.4 Characteristic wave period

The preferred characteristic wave period is the energy period. The energy period is the variance-weighted mean period of the one-dimensional period variance density spectrum (i.e. variance spectral density as a function of period). The energy period shall be calculated using moments of the wave spectrum, according to the following equation:

$$T_e \equiv T_{-10} = \frac{m_{-1}}{m_0}$$

Additional characteristic periods may also be calculated. The peak period is the inverse of the frequency associated with the maximum value of the wave spectrum:

$$T_p = 1/f_p$$

NOTE: The peak period is very sensitive to spectral shape and it is not recommended that this period is used for defining the wave energy resource

The average period of zero-crossing waves can be spectrally estimated according to the following formula:

$$T_z \equiv T_{02} = \sqrt{\frac{m_0}{m_2}}$$

9.2.6 Directionally resolved wave power

Resolving the omni-directional wave power to a direction θ yields the time averaged energy flux through an envisioned vertical plane of unit width, extending from sea floor to surface, and with its normal vector parallel with θ . This directionally resolved wave power is the sum of the contributions of each component with a positive component in direction θ , and is calculated according to the equation:

$$J_\theta = \rho g \sum_{i,j} c_{g,i} S_{ij} \Delta f_i \Delta \theta_j \cos(\theta - \theta_j) \delta \begin{cases} \delta = 1, \cos(\theta - \theta_j) \geq 0 \\ \delta = 0, \cos(\theta - \theta_j) < 0 \end{cases}$$

The maximum value of J_θ is denoted as $J_{\theta_{max}}$ and represents the maximum time averaged wave power propagating in a single direction

9.2.6.2 Direction of maximum directionally resolved wave power

The direction corresponding to the maximum value of J_θ should be taken as the direction of maximum directionally resolved wave power, $\theta_{J_{max}}$.

9.2.6.3 Directionality coefficient

A characteristic measure of the directional spreading of wave power is the directionality coefficient, which is the ratio of the maximum directionally resolved wave power to the omnidirectional wave power. The directionality coefficient is calculated according to the following equation:

$$d = \frac{J_{\theta Jmax}}{J_{\theta}}$$

Annex D

Extent of Validation

1.1 Overview

Validation of numerical models is generally conducted by using a single validation point while assuming the similar parameter uncertainty for the locations around the validation point. However, this assumption has often produced difficulties to estimate the available wave power at the locations around the validation point. This may result into reduction of wave energy exploitation and expected economic outcome of wave energy sites. This phenomena of uncertainty propagation around the validation point can be described by estimating extent of validation of numerical models. According to IEC TS 62600-101 standards, the extent of validation is defined as the successful validation of mean annual wave power surrounding the areas of the validation point under the certain limitations. Although it describes a clear explanation on extent of validation, a particular method has not been stated on the specification. It further describes that better methods of generating estimates of extent of validation will be identified in future updates. However, the IEC TS 62600-101 recommends to use the methods describes in ASME 20-2009 to estimate extent of validation, but scope of that standard focuses on uncertainty quantification of specified validation variables at specified validation point in which the conditions of the actual experiment are simulated [ASME 20-2009]. It further clarifies that the consideration of solution accuracy at points within a domain other than the validation points is beyond the scope of the standard.

A non-exhaustive literature search has not identified a standard technique for determining how this uncertainty quantification may change with locations around the validation point. Thus, a methodology to estimate the extent of validation is an essential requirement, not only for a successful wave energy resource assessment, but also to achieve the optimistic power gain from wave energy convertors. So that any developed methodology of estimating the extent of validation should be focused on estimating the wave power uncertainty propagation of the locations away from the validation point.

1.2 Proposed method: overview

In this proposed method, uncertainty of bias and random error at the remote locations are calculated and analysed since they are considered as basic statistical measures of the uncertainty quantification. The purpose of the proposed method is to provide an estimate of

uncertainty propagation of the model is at locations away from the validation point. It may be expected that locations very close to the validation point will have a similar parameter bias and random error as the validation point, but that the parameter bias and random error will differ as the distance to the validation point increases. Following method was proposed as a potential method and this document will discuss the applicability of each step of the proposed methodology. This method can be applied for any of model output parameters such as significant wave height, wave period, wave power...etc.

Step 01

The best model is tuned and/or calibrated for the validation point and, biases at each seastate are calculated for this point. This validated model provides the “true” dataset.

Biases at each seastate are calculated by obtaining the difference between validated model and measured data values at each timestep. The validated model provides the ‘true’ dataset means that the validated dataset will be used as the basis for further analysis to estimate the uncertainties at locations away from the validated point. This is because there aren’t any measured datasets at the remote locations to make the estimates as it is held at the validation point.

Step 02

A set of Monte-Carlo simulations are used to generate estimates for the analysis of uncertainty propagation at locations around the validation point.

- a. The Monte-Carlo simulations involve using the probability distributions of the input parameters*
- b. Errors of the seastates (differences from the truth) of the generated MC datasets at the validation point and the remote locations are calculated relative to the values from the validated model.*
- c. A sub-set of the sea-states can be used to reduce the computational burden, but they should be an unbiased sub-set of sea-states*

Monte Carlo (MC) simulations are generally used to model the probability of different outcomes in a process that cannot easily be predicted due to the intervention of random variables. Also MC methods are said to be standard approach for uncertainty analysis where there are many dependent variables for the final outcome of the system [Rijkwaterstaat 2008].

So this would be an appropriate technique to generate estimates for the analysis of uncertainty propagation at locations around the validation point. This is achieved by using the probability distributions of the input parameters of the model.

These parameter values of the probability distributions can be defined by a range (using minimum and maximum values for each parameter) or setting a mean and a standard deviation or using some other methods. Obviously, the model parameter values which are selected for the validated model can be used as the mean values for each parameter while defining the min/max range or selecting a standard deviation. This selection can be referred to previous references or user experience where the defined parameter values have significant impact on the final results when there are smaller number of MC datasets.

Then seastate errors at validation point and remote locations of the generated MC datasets are calculated relative to the values from the validated model since it is used as the true dataset at the step 01. These error values represent the deviation of each seastate from the true dataset which can be used as a solid basis for the uncertainty estimation around the validation point.

Step 03

The offset values of the errors of Monte Carlo estimates are obtained between validation point and remote locations.

The offset is the difference between the error of the validation point and remote locations. Here, the offset implies how much divergence of the seastate errors at the remote locations with respect to the seastate errors at the validation point. This means that the calculated values or differences are clear indications of uncertainty propagation of each MC estimation at the remote location. By taking the appropriate number of MC estimates (this can be achieved by a convergence test), number of possible outcomes of can be achieved at the remote location.

Step 04

The average and standard deviation of the offsets for the locations around the validation point are calculated.

The basic estimates of average and standard deviation represents the clear indications of uncertainty propagation at each timestep at the remote location. The final step would be the analysis of the statistics of the average and standard deviation of offset errors for the locations around the validation point. Then the estimated bias in the model at the remote location will be

the bias of the validated model (at the validation point) plus the average offset, with a random error given by standard deviation of the offset.

Following numeric example shows the procedure of estimating uncertainty propagation for a single seastate.

	Validation point	Example remote location	
	Error (d)	Error (r)	Offset
dataset 01	d1	r1	d1 - r1
dataset 02	d2	r2	d2 - r2
dataset 03	d3	r3	d3 - r3
dataset 04	d4	r4	d4 - r4
.	.	.	.
.	.	.	.
dataset n	dn	rn	dn - rn
		Average offset of a single seastate (D₁)	$\frac{1}{n} \sum_{i=1}^n (d_i - r_i)$
		Standard deviation of the offset of a single seastate (SD₁)	$\sqrt{\frac{1}{n} \sum_{i=1}^n (D_1 - (d_i - r_i))^2}$

Offset at remote location for a single seastate, $B_1 = D_1 \pm SD_1$

Then the model error and uncertainty is given for a single time-step as

$$E_j = e_j + D_j \pm SD_j$$

This procedure can be extended to calculate the average and standard deviation of the offsets for all seastates as follows.

$$E = \text{mean}(e_j + D_j) \pm \text{mean}(SD_j)$$

n = Number of MC datasets

N = Number of timesteps

d_i = Error at the validation point of i^{th} MC dataset ($i = 1,2,3 \dots n$)

r_i = Error at the remote location of i^{th} MC dataset ($i = 1,2,3 \dots n$)

e_j = Error at the validation point relative to the measured data

D_j = Average offset of j^{th} timestep ($j = 1,2,3 \dots N$)

SD_j = Standard deviation of offset of j^{th} timestep ($j = 1,2,3 \dots N$)

E_j = Model error and uncertainty j^{th} timestep ($j = 1,2,3 \dots N$)

Application of the proposed methodology to estimate the extent of validation for the study points

The above methodology is applied for the selected study points by using 50 Monte Carlo simulation datasets. Here, the estimates are made for the significant wave height values since energy period or wave power is not available with the buoy dataset.

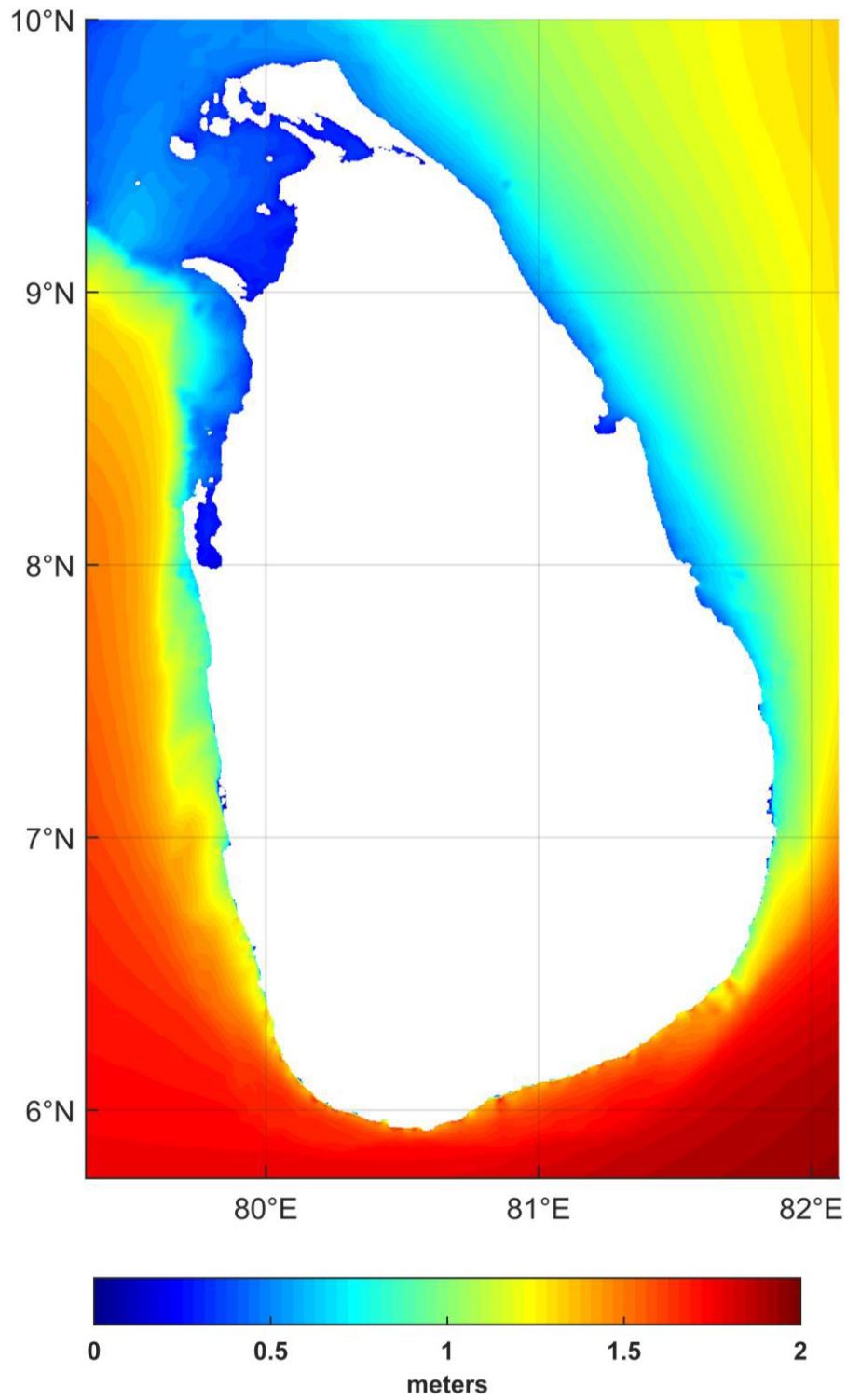
Study Point	$mean(e_j + D_j)$	$mean(SD_j)$
P1	-0.03	0.20
P2	0.15	0.21
P3	0.20	0.18
P4	0.18	0.18
P5	0.09	0.18
P6	0.13	0.17
P7	0.16	0.19
P8	0.04	0.25
P9	-0.14	0.25
P10	-0.04	0.17
Average	0.07	0.20

Modelling uncertainty for significant wave height = **0.07 ± 0.2 m**

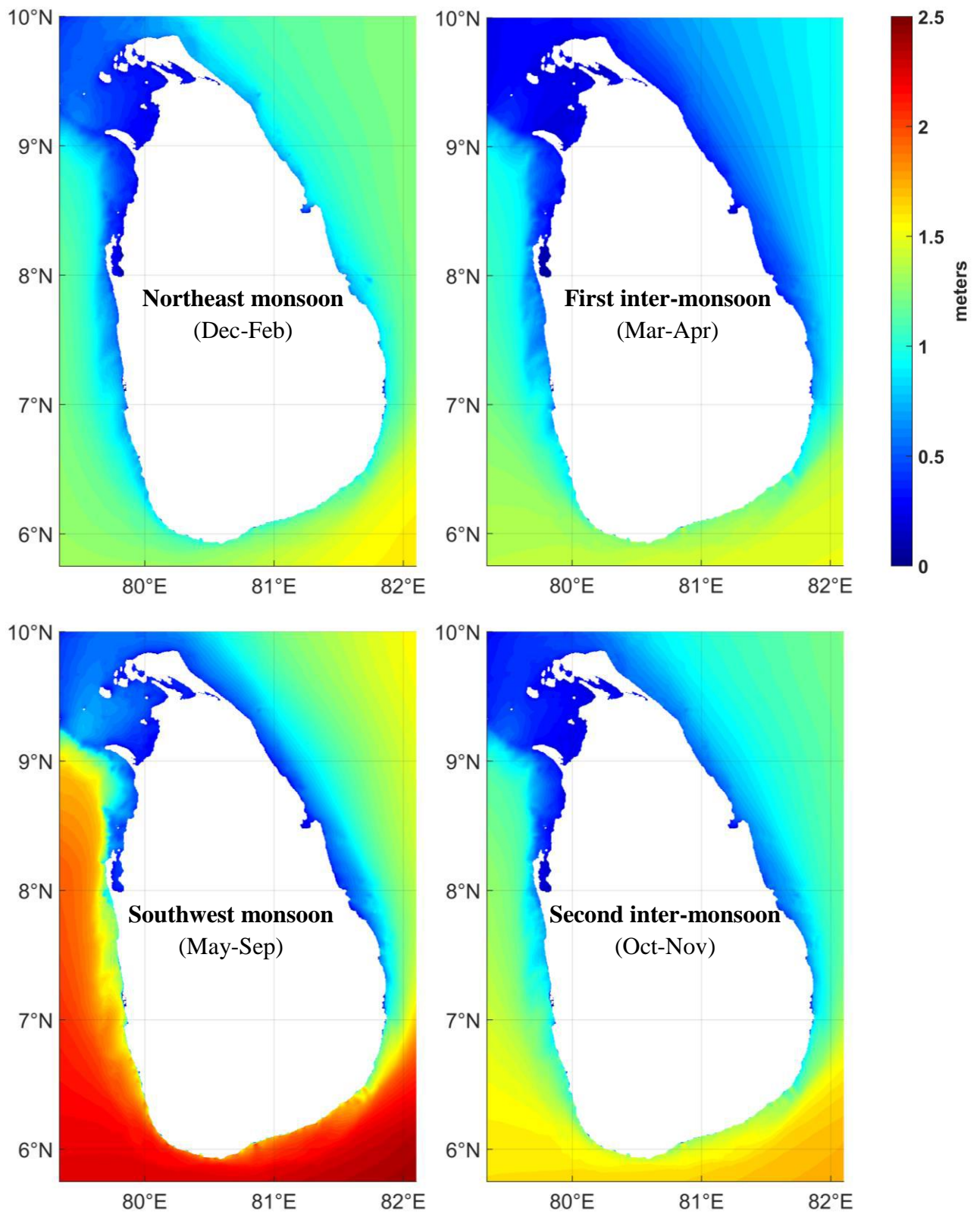
Annex E

Presentation of Regional Information

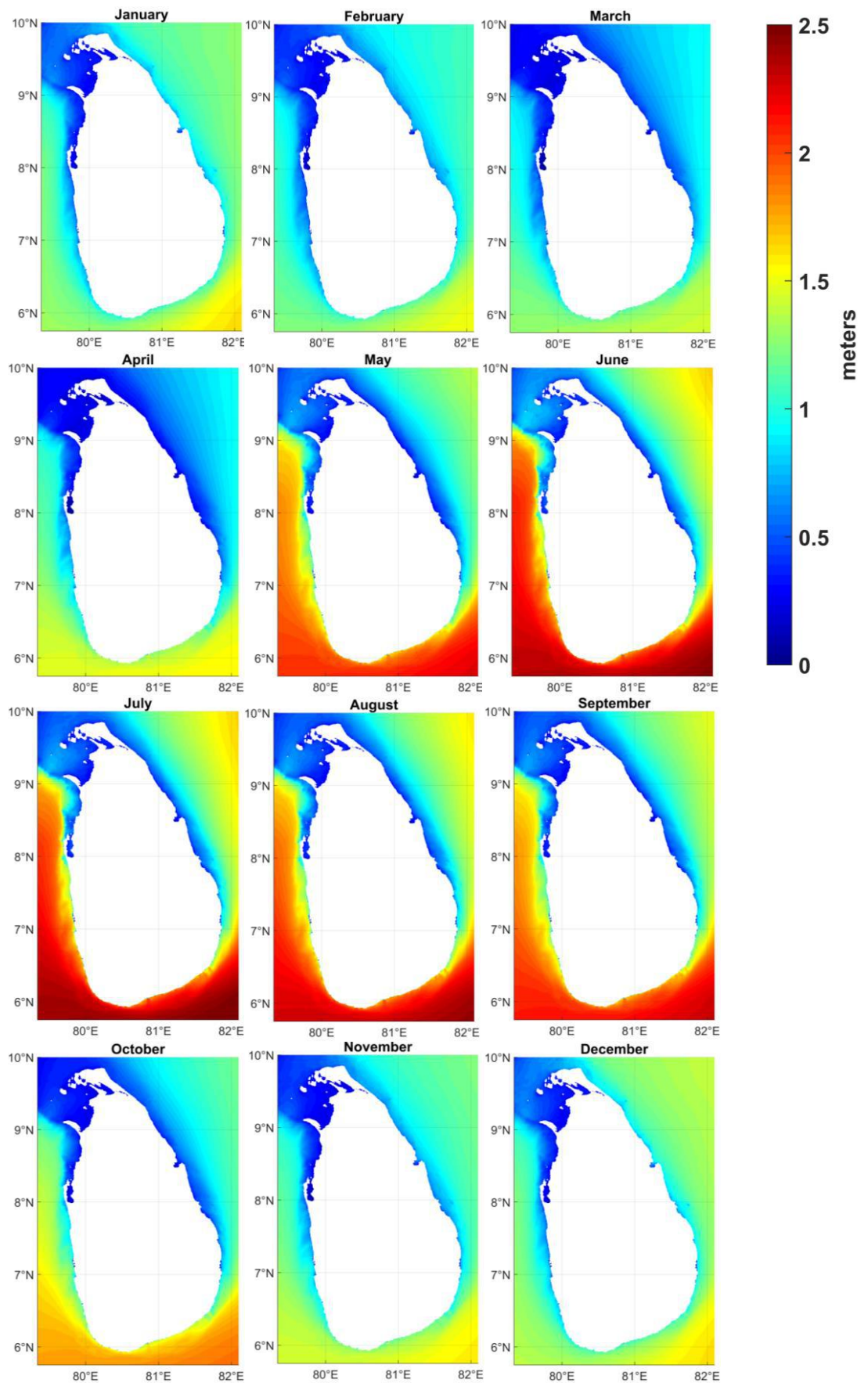
E.1 Mean annual significant wave height (2001-2018)



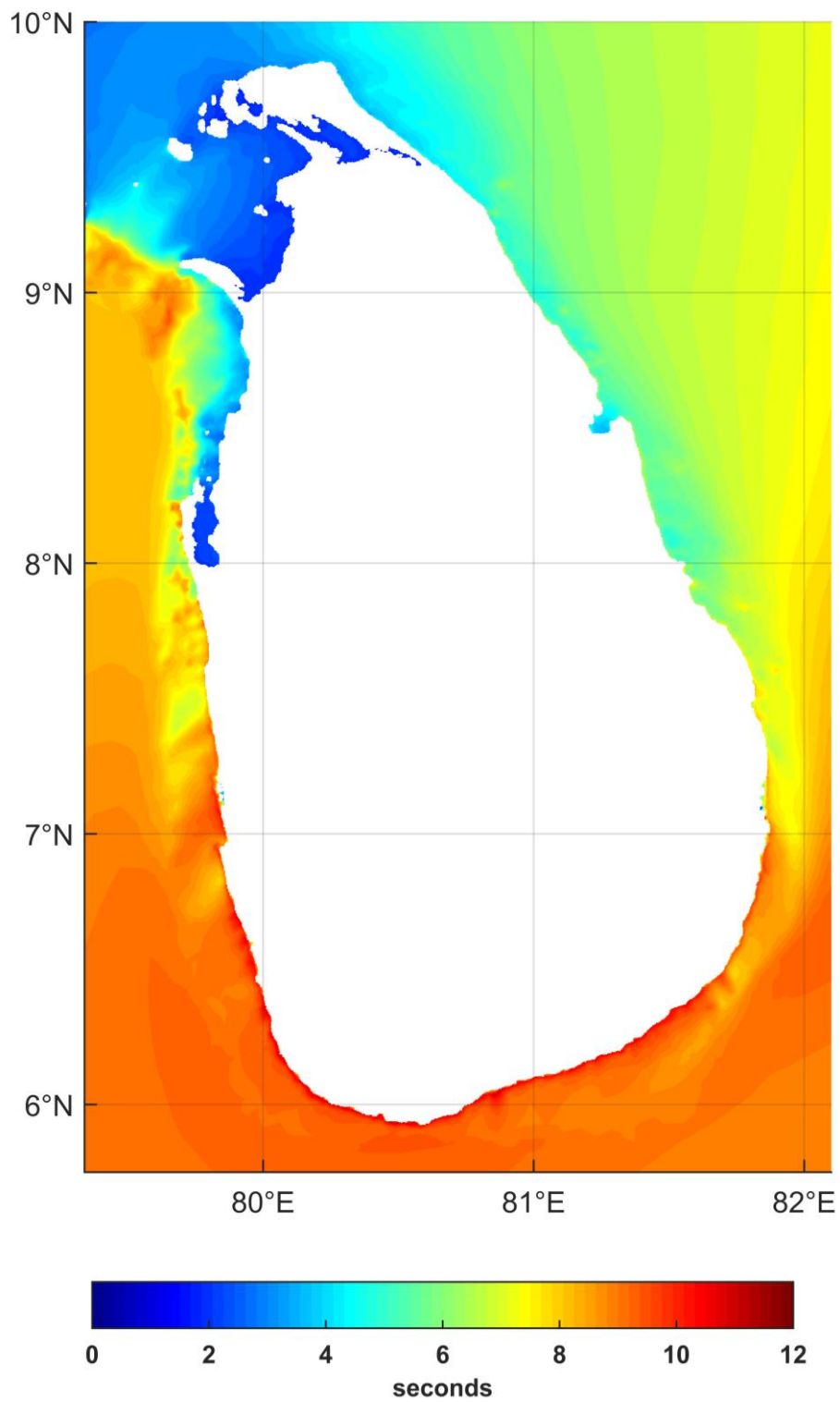
E.2 Mean seasonal significant wave height (2001-2018)



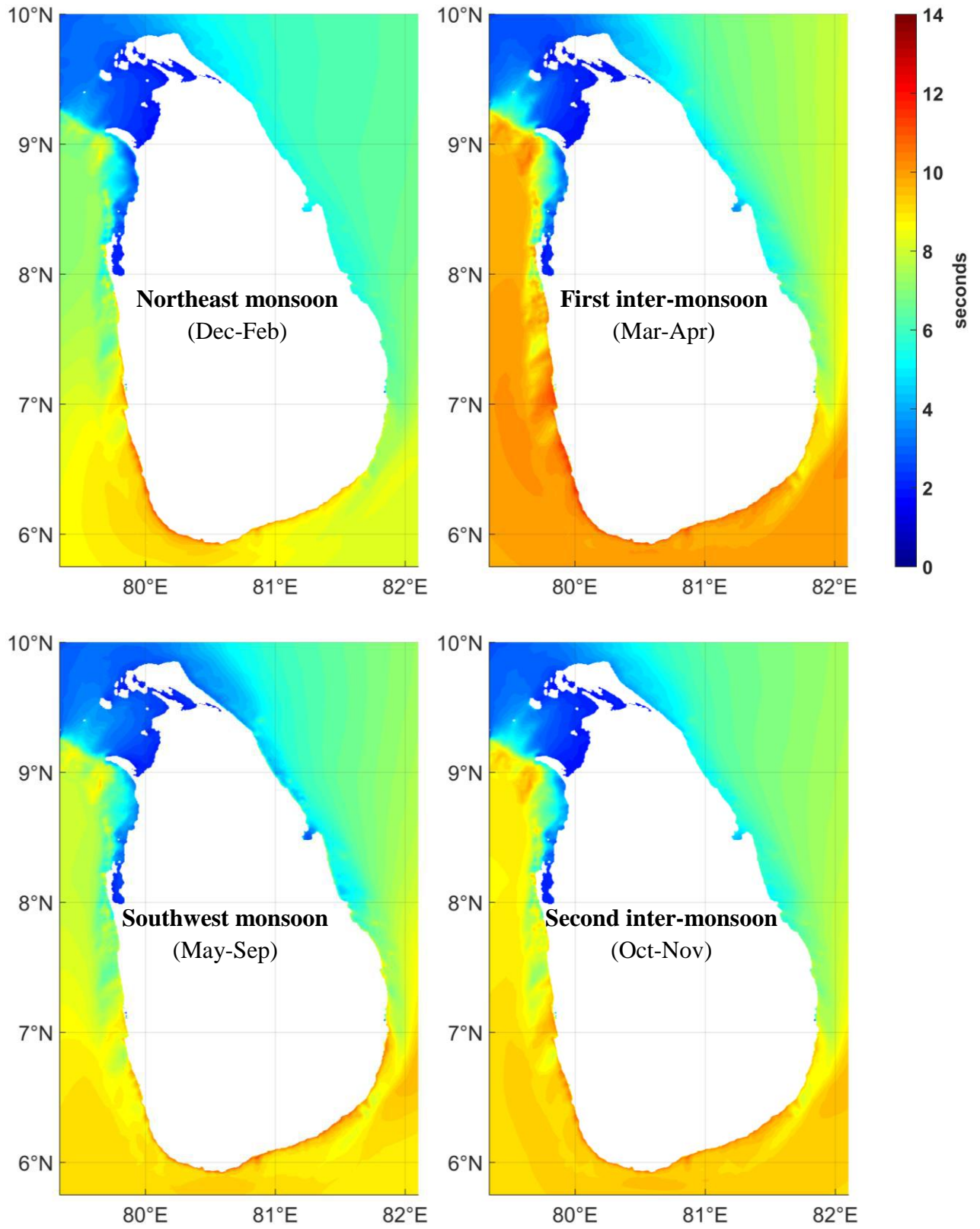
E.3 Monthly mean significant wave height



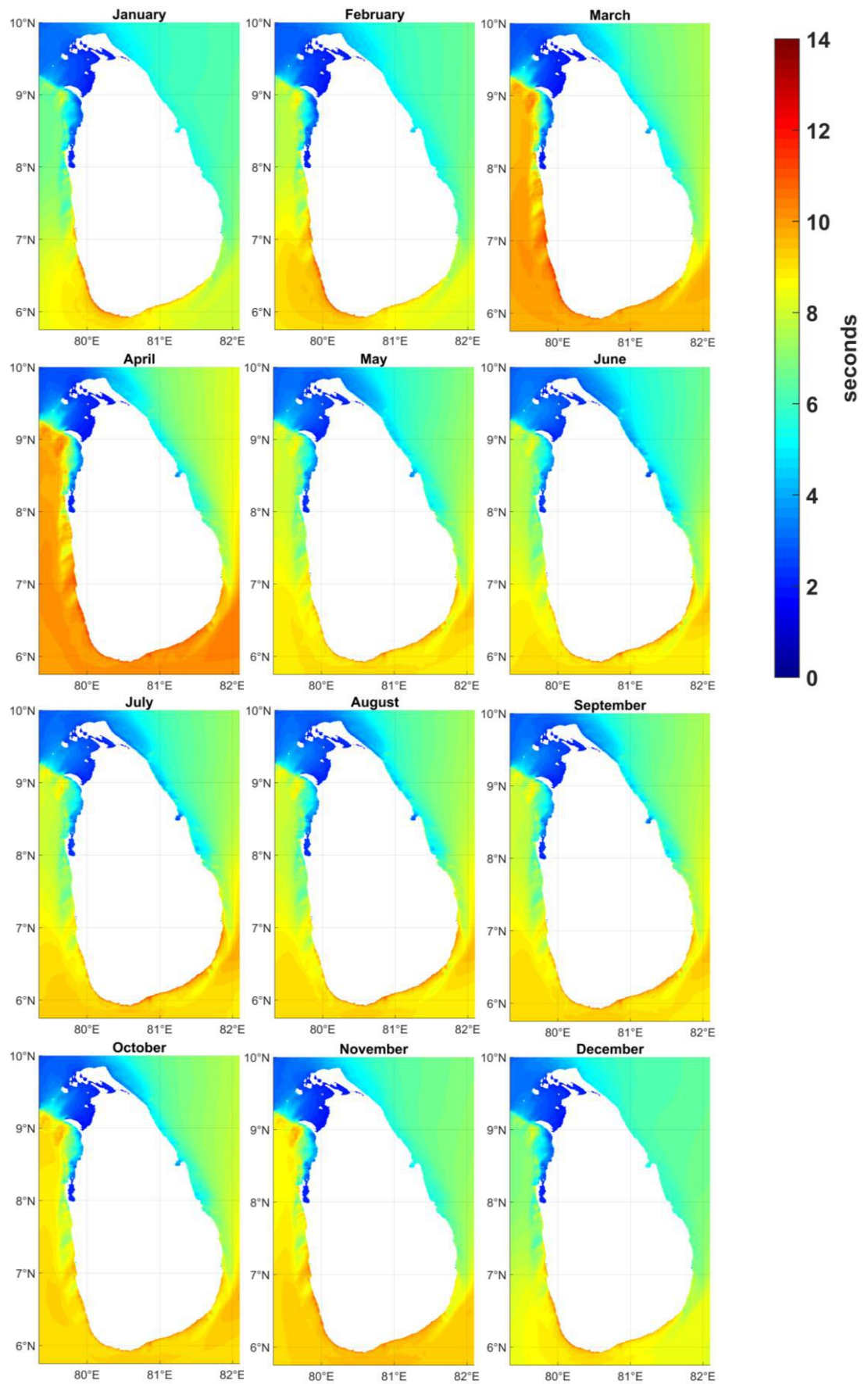
E.4 Mean annual wave period (2001-2018)



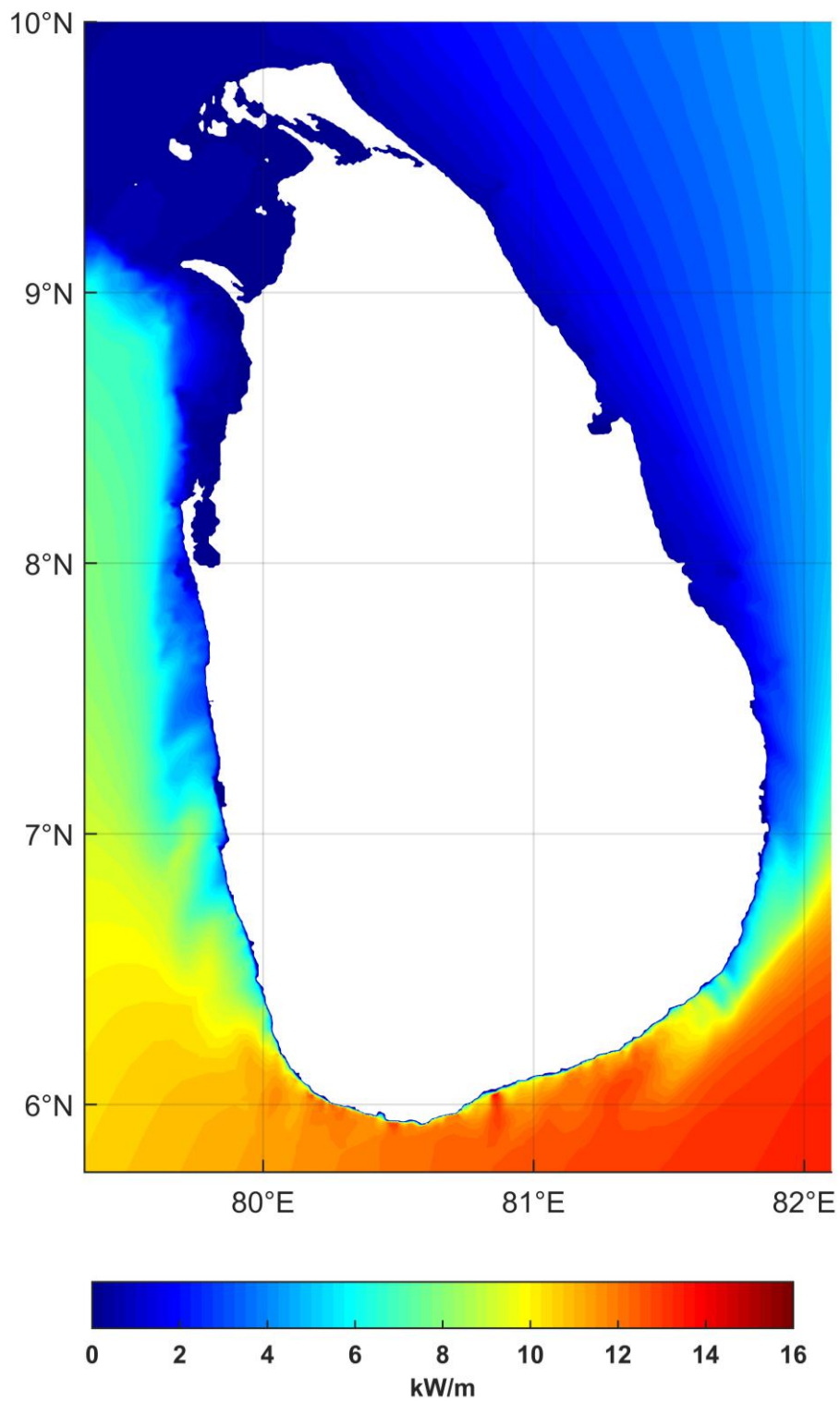
E.5 Mean seasonal wave period (2001-2018)



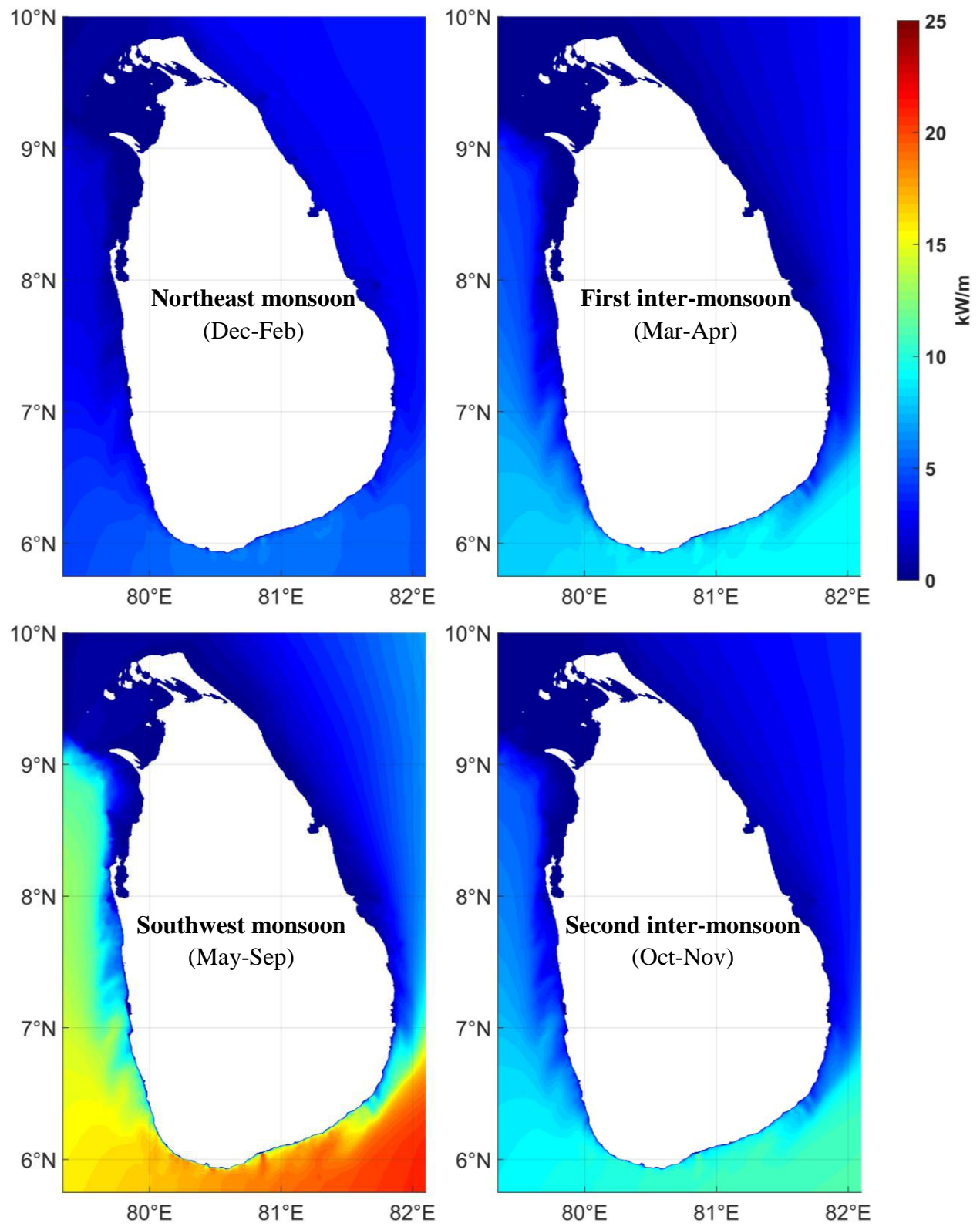
E.6 Monthly mean wave period



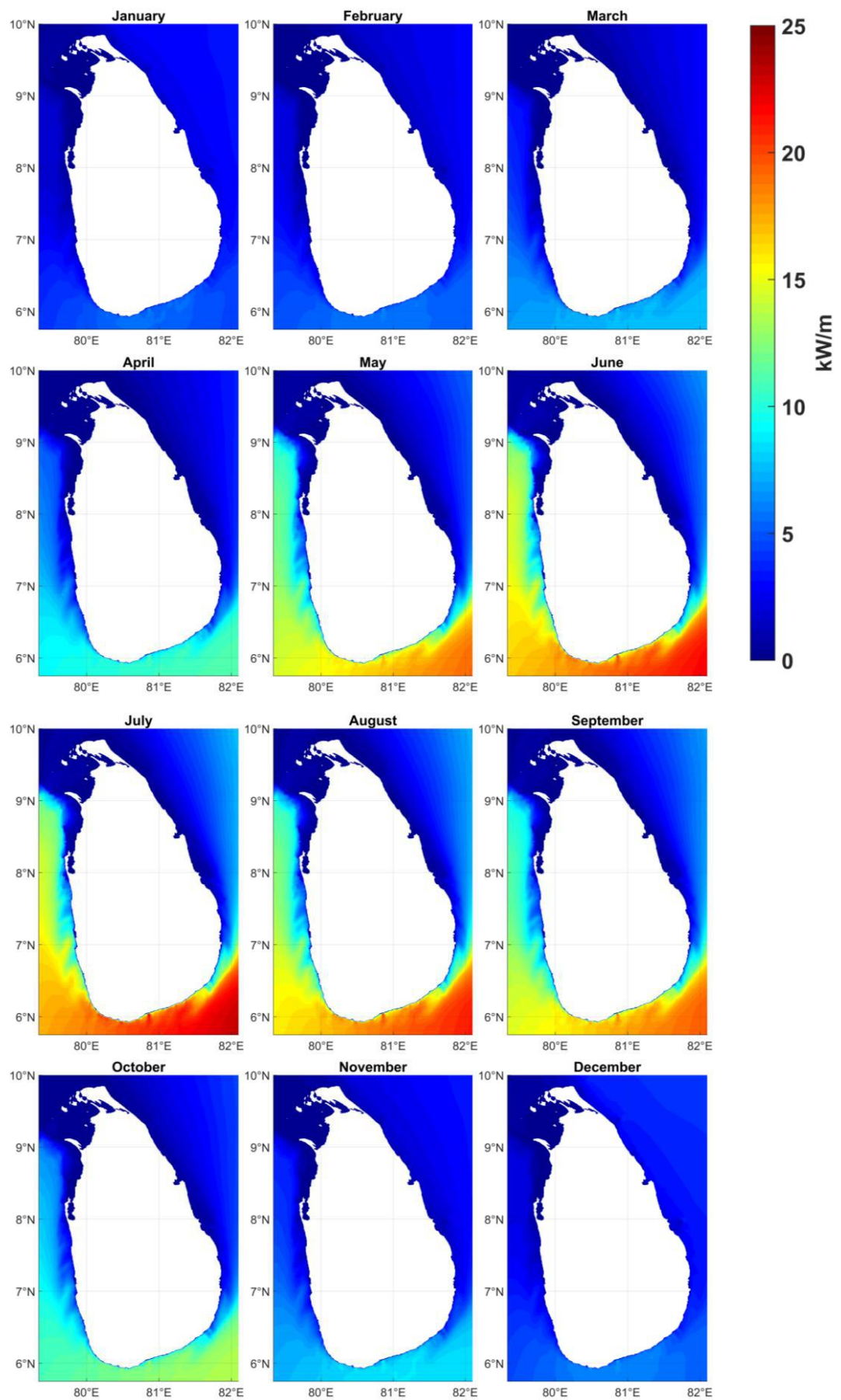
E.7 Mean annual omni-directional wave power (2001-2018)



E.8 Mean seasonal omni-directional wave power (2001-2018)



E.9 Monthly mean omni-directional wave power



Annex F

Analysis of Study Points

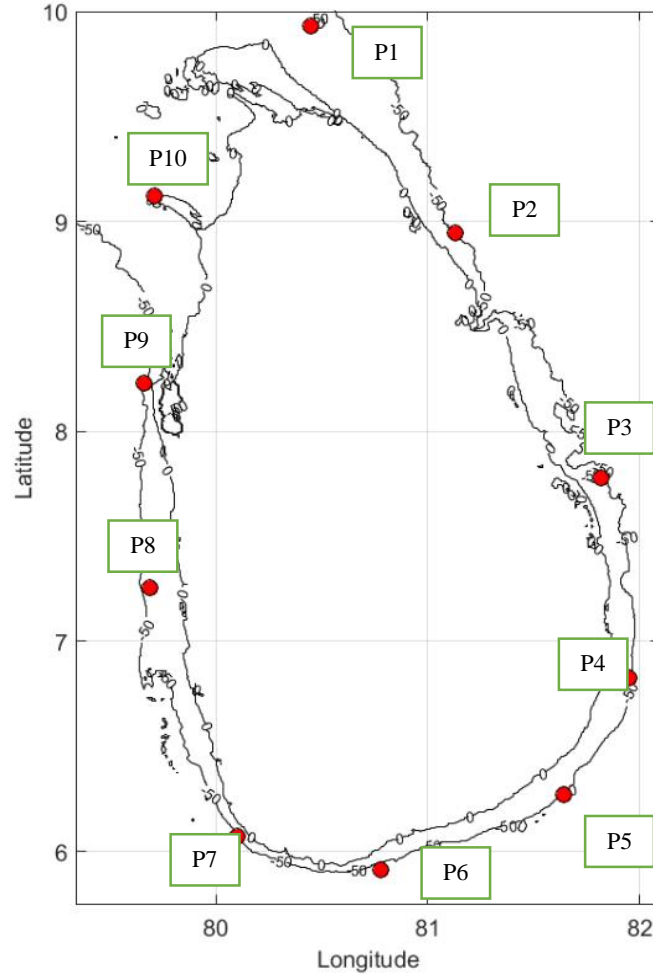


Figure F.1: Locations of study points along 50 m bathymetric contour

Study Point	Location
P1	9.929 ⁰ N , 80.45 ⁰ E
P2	8.946 ⁰ N , 81.13 ⁰ E
P3	7.779 ⁰ N , 81.82 ⁰ E
P4	6.829 ⁰ N , 81.95 ⁰ E
P5	6.271 ⁰ N , 81.64 ⁰ E
P6	5.913 ⁰ N , 80.78 ⁰ E
P7	6.071 ⁰ N , 80.10 ⁰ E
P8	7.254 ⁰ N , 79.69 ⁰ E
P9	8.229 ⁰ N , 79.66 ⁰ E
P10	9.121 ⁰ N , 79.71 ⁰ E

Note: The θ_{Jmax} is measured anticlockwise starting from east direction

Analysis: Study Point P1

Table F1.1 : Scatter table for P1 (2001-2018)

P1		Te (s)													Total
		0-3	3-4	4-5	5-6	6-7	7-8	8-9	9-10	10-11	11-12	12-13	13-14	14-15	
H _{ms} (m)	0.0 - 0.5	0.00	23.71	20.57	10.65	2.13	0.54	0.13	0.03	0.00	0.00	0.00	0.00	0.00	57.77
	0.5 - 1.0	0.00	1.87	6.12	9.36	0.99	0.27	0.07	0.00	0.00	0.00	0.00	0.00	0.00	18.69
	1.0 - 1.5	0.00	0.00	0.01	1.19	0.67	0.06	0.04	0.02	0.00	0.00	0.00	0.00	0.00	1.98
	1.5 - 2.0	0.00	0.00	0.00	0.01	0.14	0.04	0.03	0.01	0.00	0.00	0.00	0.00	0.00	0.22
	2.0 - 2.5	0.00	0.00	0.00	0.00	0.01	0.03	0.01	0.00	0.00	0.00	0.00	0.00	0.00	0.05
	2.5 - 3.0	0.00	0.00	0.00	0.00	0.00	0.00	0.00	0.00	0.00	0.00	0.00	0.00	0.00	0.00
	3.0 - 3.5	0.00	0.00	0.00	0.00	0.00	0.00	0.00	0.00	0.00	0.00	0.00	0.00	0.00	0.00
	3.5-4.0	0.00	0.00	0.00	0.00	0.00	0.00	0.00	0.00	0.00	0.00	0.00	0.00	0.00	0.00
	4-4.5	0.00	0.00	0.00	0.00	0.00	0.00	0.00	0.00	0.00	0.00	0.00	0.00	0.00	0.00
	Total	0.00	25.58	26.70	21.21	3.94	0.94	0.28	0.06	0.00	0.00	0.00	0.00	0.00	100.0

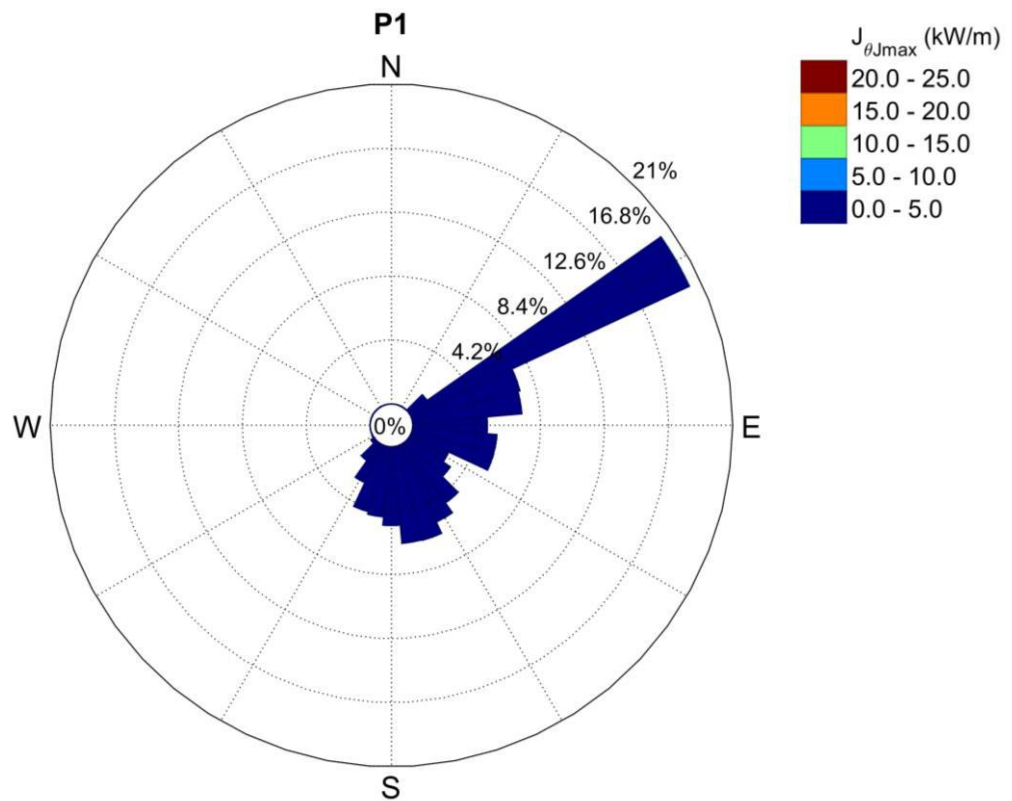


Figure F1.1: Wave power rose of $J_{\theta} J_{max}$ and θ_{Jmax}

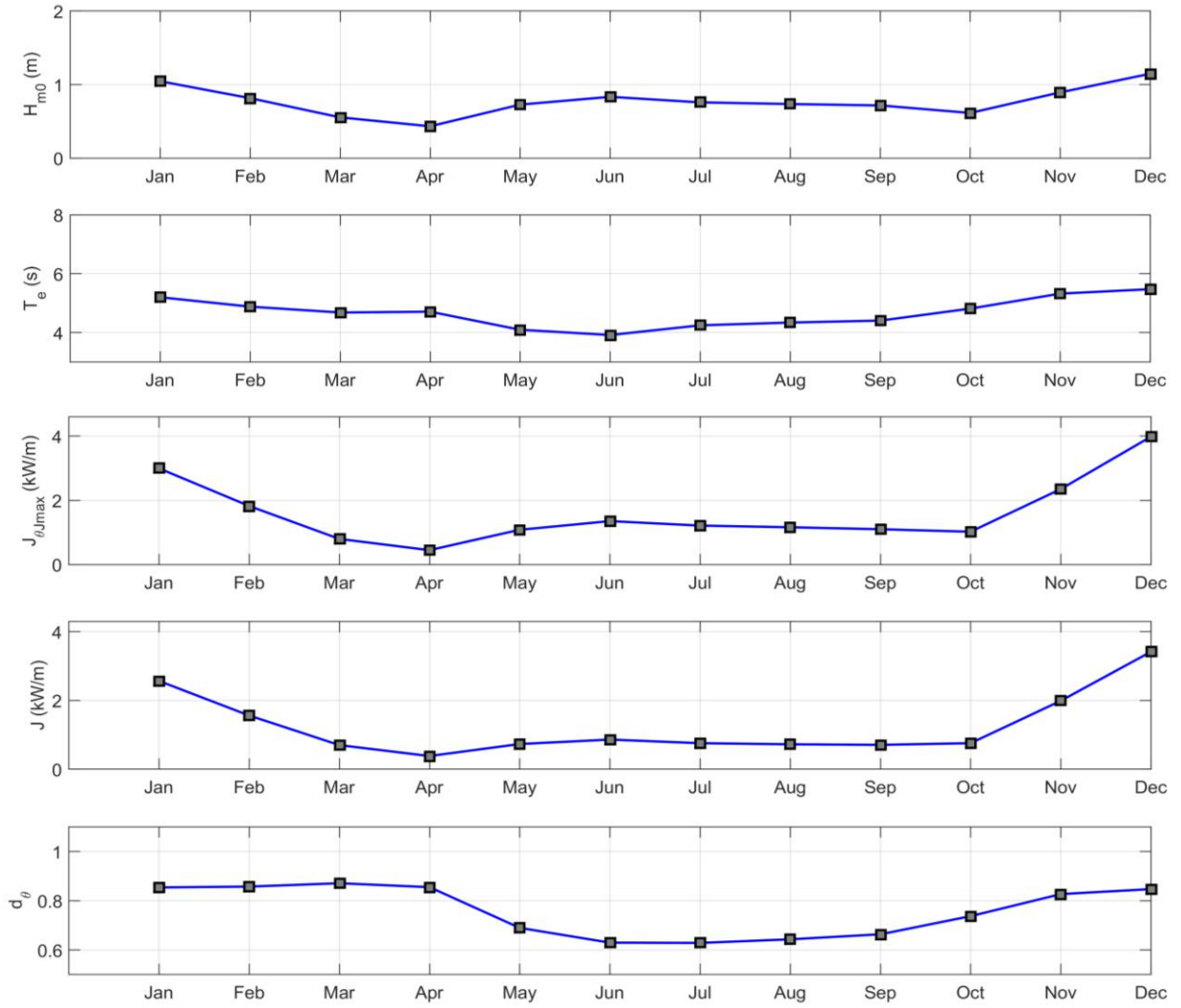


Figure F1.2: Monthly mean variation of H_{m0} , T_e , $J_{\theta_{max}}$, J and d_{θ} for P1

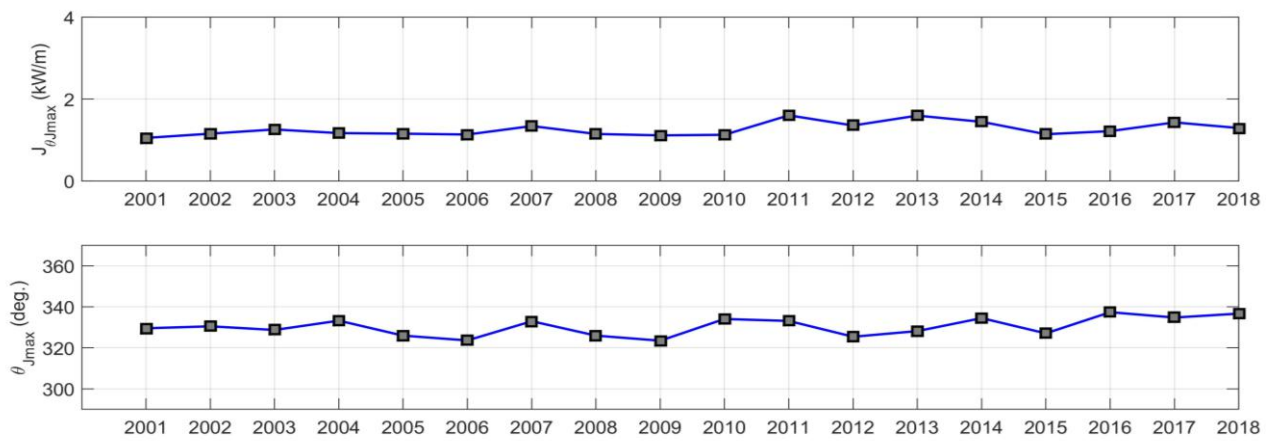


Figure F1.3 : Annual mean variation of $J_{\theta_{max}}$ and $\theta_{J_{max}}$ for P1

Analysis: Study Point P2

Table F2.1: Annual scatter table for P2 (2001-2018)

P2		Te (s)													
		0-3	3-4	4-5	5-6	6-7	7-8	8-9	9-10	10-11	11-12	12-13	13-14	14-15	Total
H _{m0} (m)	0.0 - 0.5	0.01	2.90	13.79	30.01	11.44	3.45	0.70	0.10	0.02	0.00	0.00	0.00	0.00	62.43
	0.5 - 1.0	0.00	0.00	0.02	3.83	5.58	0.55	0.12	0.01	0.00	0.00	0.00	0.00	0.00	10.10
	1.0 - 1.5	0.00	0.00	0.00	0.00	0.29	0.11	0.09	0.03	0.01	0.00	0.00	0.00	0.00	0.51
	1.5 - 2.0	0.00	0.00	0.00	0.00	0.01	0.03	0.03	0.03	0.00	0.00	0.00	0.00	0.00	0.10
	2.0 - 2.5	0.00	0.00	0.00	0.00	0.00	0.00	0.00	0.00	0.00	0.00	0.00	0.00	0.00	0.00
	2.5 - 3.0	0.00	0.00	0.00	0.00	0.00	0.00	0.00	0.00	0.00	0.00	0.00	0.00	0.00	0.00
	3.0 - 3.5	0.00	0.00	0.00	0.00	0.00	0.00	0.00	0.00	0.00	0.00	0.00	0.00	0.00	0.00
	3.5-4.0	0.00	0.00	0.00	0.00	0.00	0.00	0.00	0.00	0.00	0.00	0.00	0.00	0.00	0.00
	4-4.5	0.00	0.00	0.00	0.00	0.00	0.00	0.00	0.00	0.00	0.00	0.00	0.00	0.00	0.00
	Total	0.01	2.90	13.81	33.84	17.32	4.14	0.94	0.17	0.02	0.00	0.00	0.00	0.00	100.0

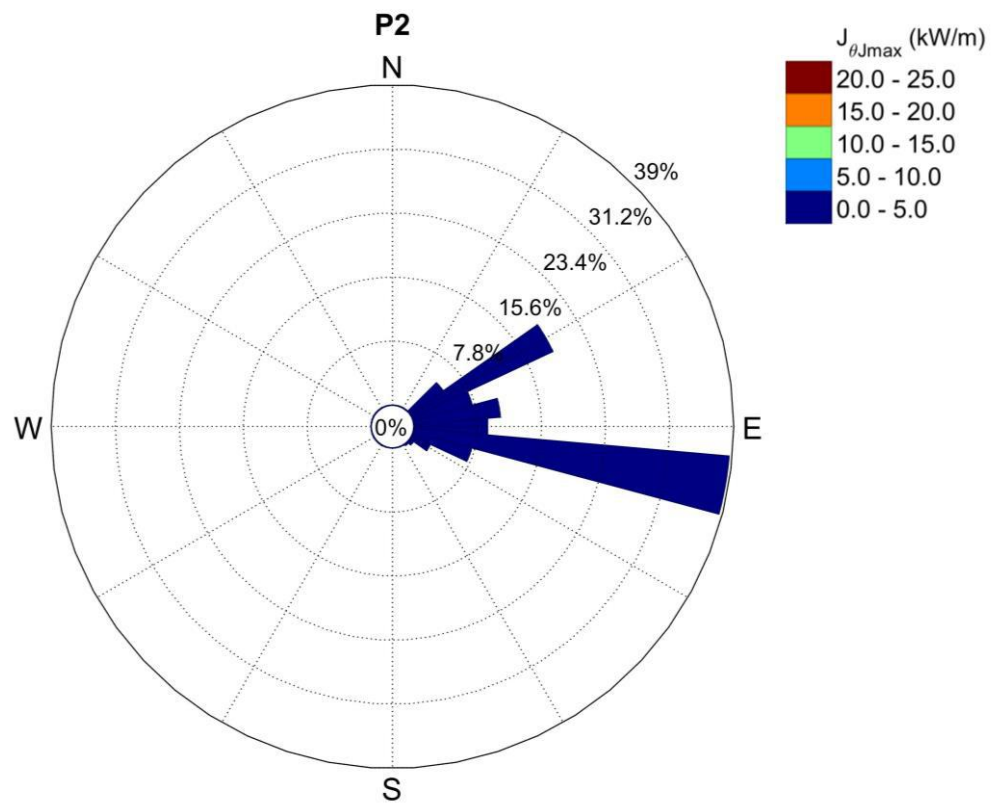


Figure F2.1: Wave power rose of $J_{\theta_{Jmax}}$ and θ_{Jmax}

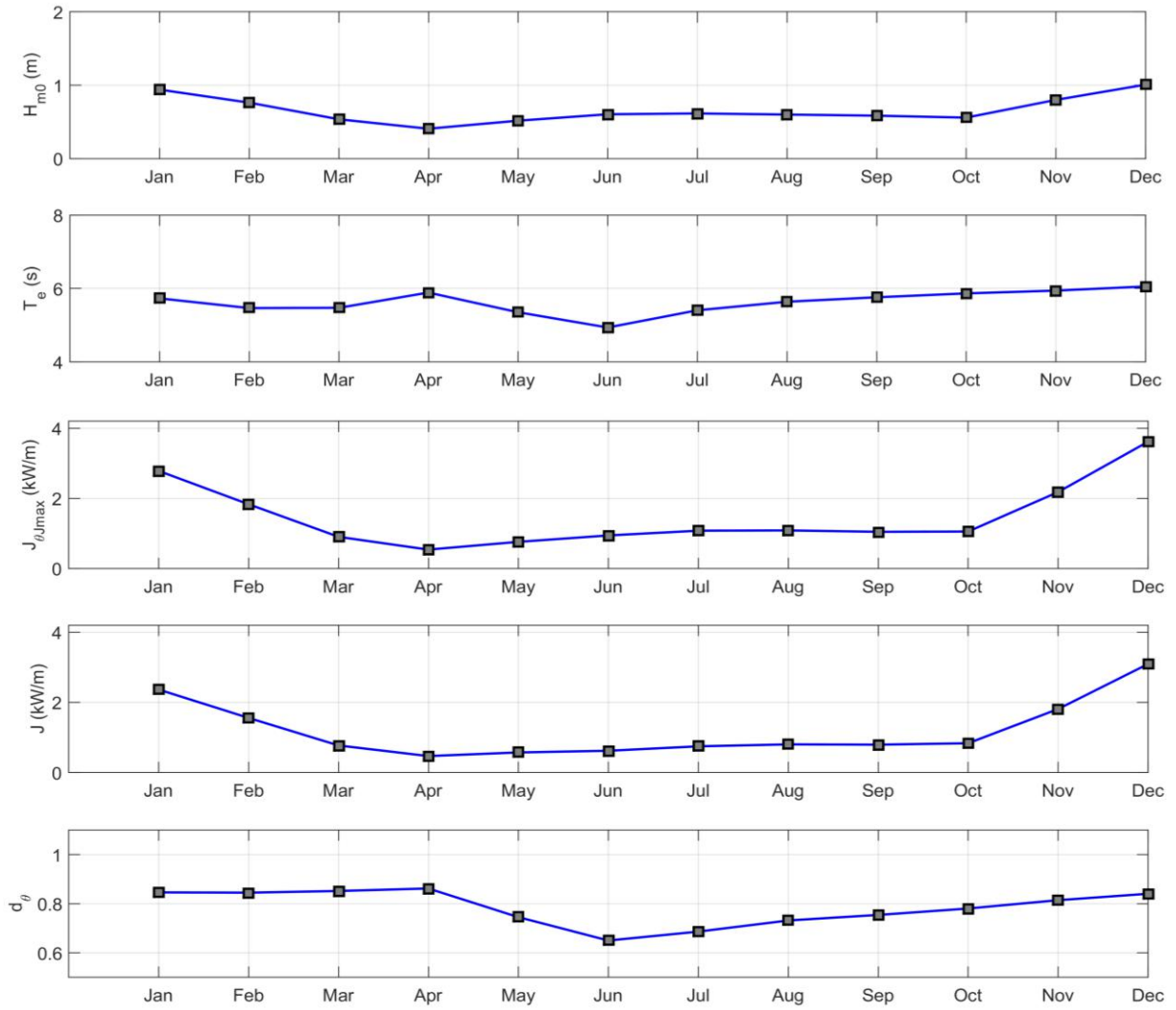


Figure F2.2: Monthly mean values of H_{m0} , T_e , $J_{\theta_{jmax}}$, J and d_{θ} for P2

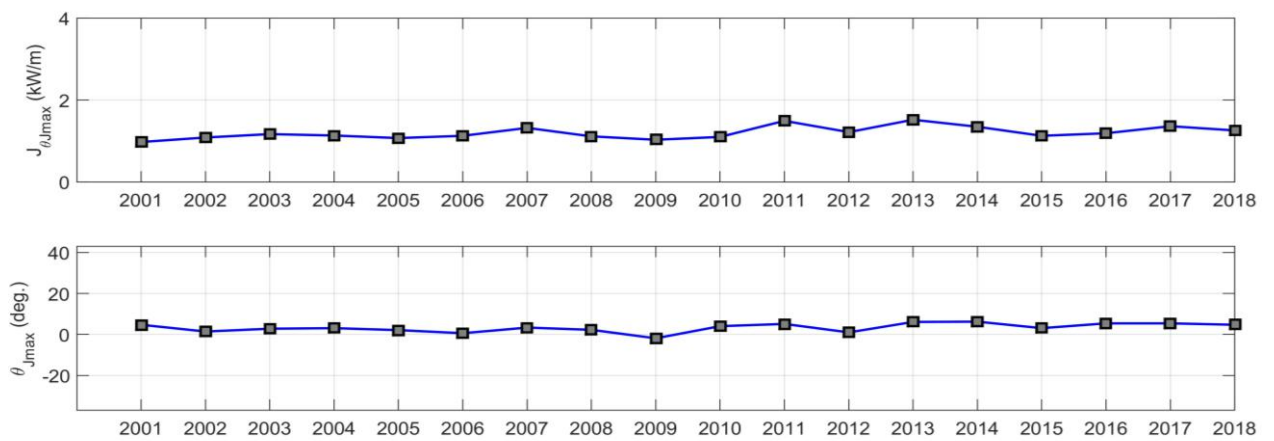


Figure F2.2 : Annual mean variation of $J_{\theta_{jmax}}$ and θ_{jmax} for P2

Analysis: Study Point P3

Table F3.1: Annual scatter table for P3 (2001-2018)

P3		Te (s)													Total
		0-3	3-4	4-5	5-6	6-7	7-8	8-9	9-10	10-11	11-12	12-13	13-14	14-15	
H _{m0} (m)	0.0 - 0.5	0.00	0.00	0.95	15.50	28.48	19.20	7.97	1.76	0.15	0.00	0.00	0.00	0.00	74.02
	0.5 - 1.0	0.00	0.00	0.03	3.54	11.88	3.78	1.59	0.47	0.15	0.03	0.00	0.00	0.00	21.48
	1.0 - 1.5	0.00	0.00	0.00	0.00	0.52	0.35	0.09	0.06	0.00	0.00	0.00	0.00	0.00	1.03
	1.5 - 2.0	0.00	0.00	0.00	0.00	0.01	0.01	0.02	0.02	0.00	0.00	0.00	0.00	0.00	0.06
	2.0 - 2.5	0.00	0.00	0.00	0.00	0.00	0.00	0.00	0.00	0.00	0.00	0.00	0.00	0.00	0.00
	2.5 - 3.0	0.00	0.00	0.00	0.00	0.00	0.00	0.00	0.00	0.00	0.00	0.00	0.00	0.00	0.00
	3.0 - 3.5	0.00	0.00	0.00	0.00	0.00	0.00	0.00	0.00	0.00	0.00	0.00	0.00	0.00	0.00
	3.5-4.0	0.00	0.00	0.00	0.00	0.00	0.00	0.00	0.00	0.00	0.00	0.00	0.00	0.00	0.00
	4-4.5	0.00	0.00	0.00	0.00	0.00	0.00	0.00	0.00	0.00	0.00	0.00	0.00	0.00	0.00
	Total	0.00	0.00	0.99	19.04	40.89	23.35	9.67	2.31	0.30	0.30	0.03	0.00	0.00	0.00

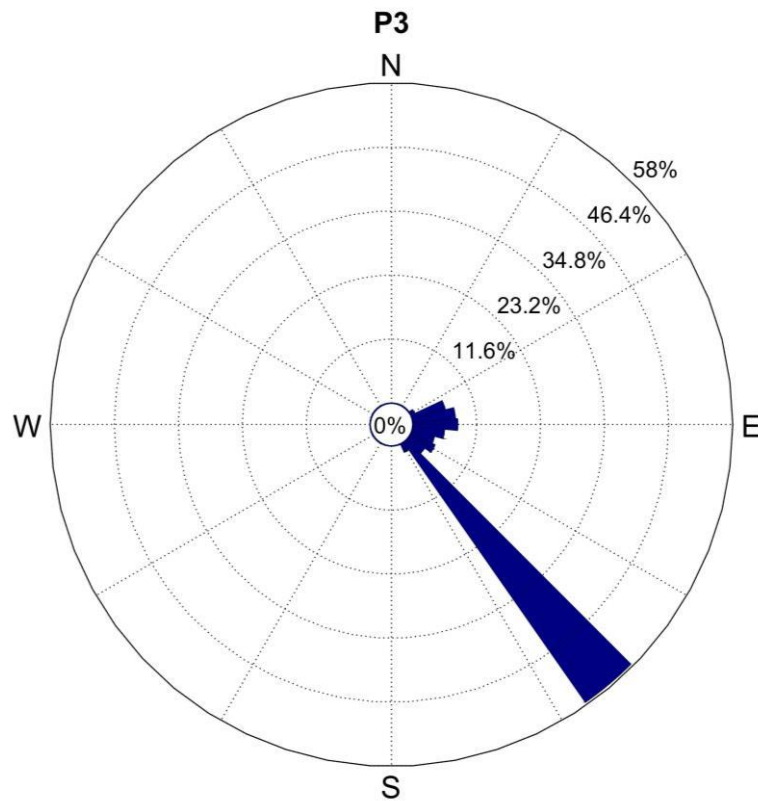


Figure F3.1: Wave power rose of $J_{\theta_{Jmax}}$ and θ_{Jmax} for P3

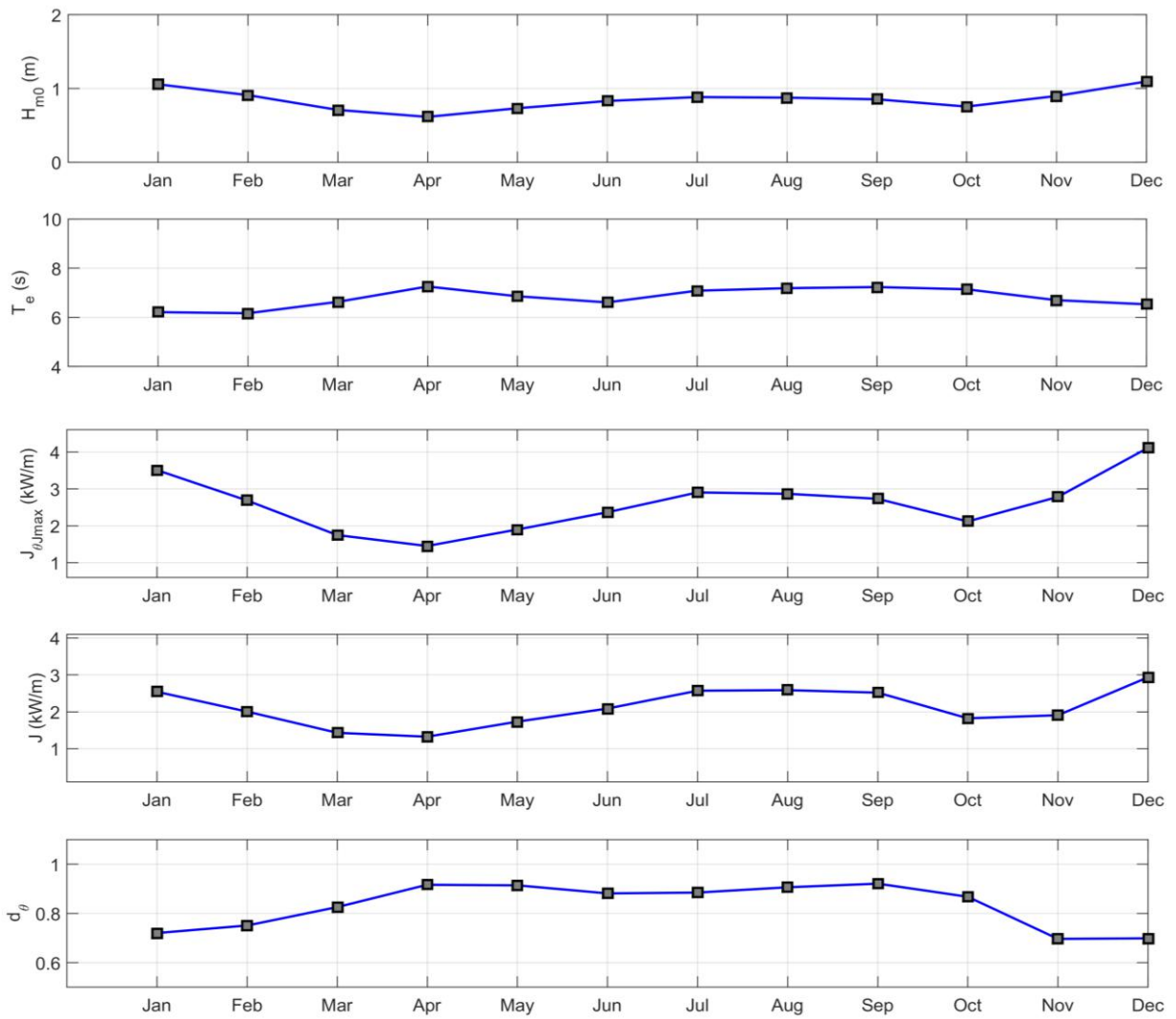


Figure F3.2: Monthly mean values of H_{m0} , T_e , $J_{\theta_{max}}$, J and d_{θ} for P3

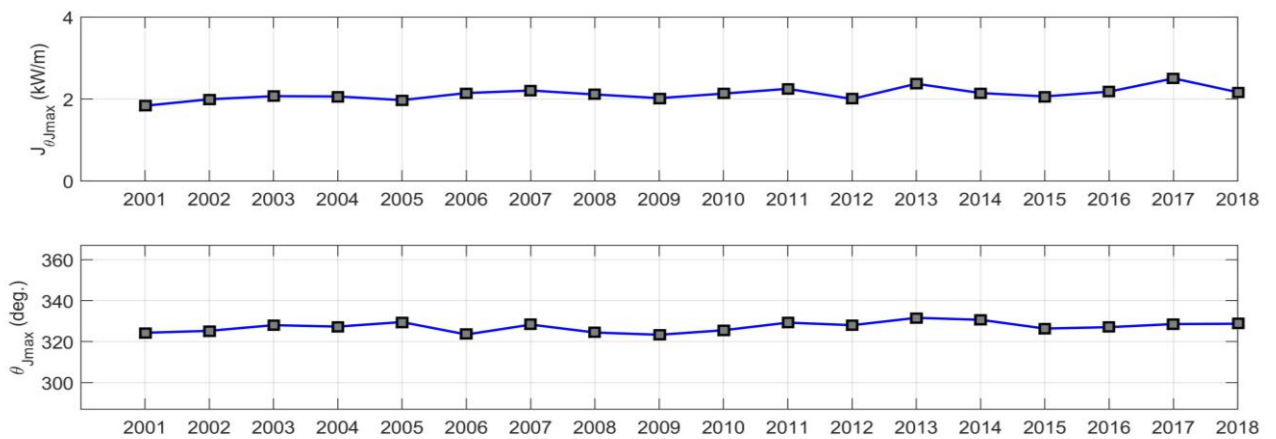


Figure F3.3 : Annual mean variation of $J_{\theta_{max}}$ and $\theta_{J_{max}}$ for P3

Analysis: Study Point P4

Table F4.1: Annual scatter table for P4 (2001-2018)

P4		Te (s)														
		0-3	3-4	4-5	5-6	6-7	7-8	8-9	9-10	10-11	11-12	12-13	13-14	14-15	Total	
H _{amb} (m)	0.0 - 0.5	0.00	0.00	0.00	0.00	0.00	0.00	0.00	0.00	0.00	0.00	0.00	0.00	0.00	0.00	0.00
	0.5 - 1.0	0.00	0.00	0.00	0.24	1.63	4.69	6.41	2.58	0.39	0.02	0.00	0.00	0.00	0.00	15.95
	1.0 - 1.5	0.00	0.00	0.00	0.29	8.94	22.40	19.59	10.33	2.52	0.41	0.08	0.01	0.00	0.00	64.59
	1.5 - 2.0	0.00	0.00	0.00	0.00	0.87	4.86	7.05	4.56	1.45	0.34	0.04	0.02	0.00	0.00	19.19
	2.0 - 2.5	0.00	0.00	0.00	0.00	0.00	0.01	0.05	0.09	0.07	0.03	0.01	0.00	0.00	0.00	0.26
	2.5 - 3.0	0.00	0.00	0.00	0.00	0.00	0.01	0.00	0.00	0.00	0.00	0.00	0.00	0.00	0.00	0.01
	3.0 - 3.5	0.00	0.00	0.00	0.00	0.00	0.00	0.00	0.00	0.00	0.00	0.00	0.00	0.00	0.00	0.00
	3.5-4.0	0.00	0.00	0.00	0.00	0.00	0.00	0.00	0.00	0.00	0.00	0.00	0.00	0.00	0.00	0.00
	4-4.5	0.00	0.00	0.00	0.00	0.00	0.00	0.00	0.00	0.00	0.00	0.00	0.00	0.00	0.00	0.00
	Total	0.00	0.00	0.00	0.53	11.44	31.97	33.10	17.56	4.44	0.80	0.13	0.03	0.00	0.00	100.0

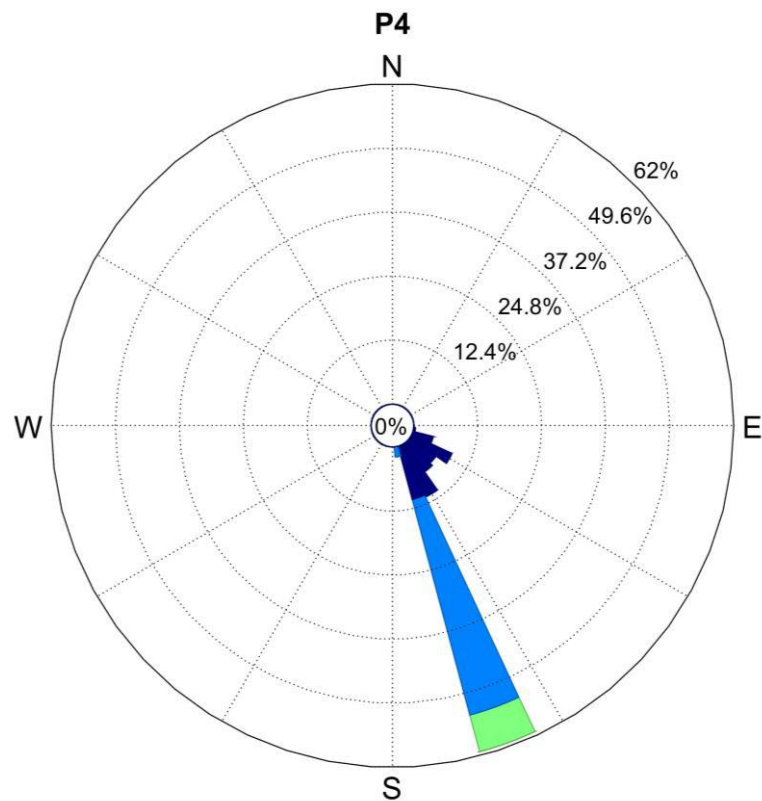


Figure F4.1: Wave power rose of $J_{\theta_{jmax}}$ and θ_{jmax} for P4

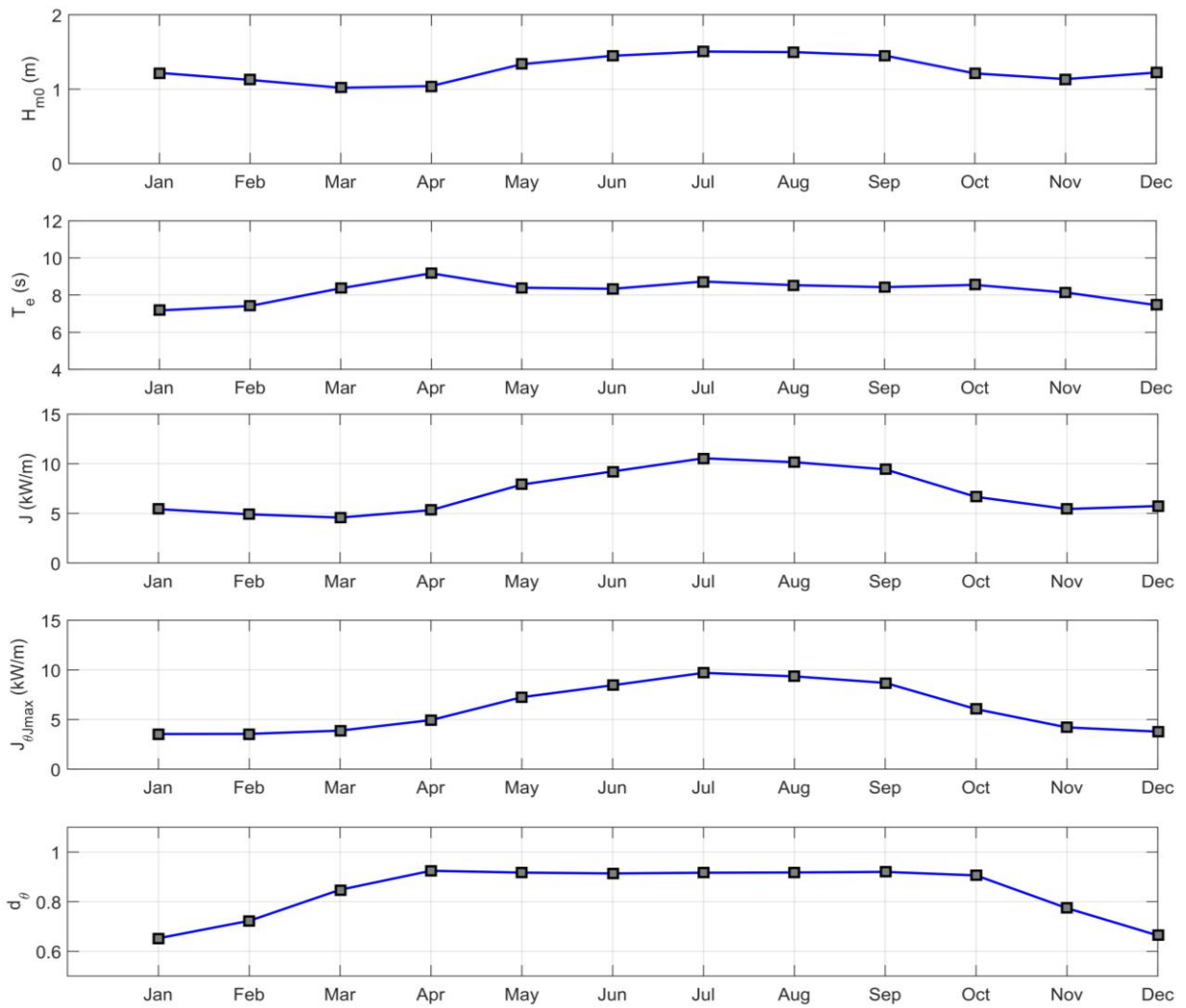


Figure F4.2: Monthly mean values of H_{m0} , T_e , $J_{\theta_{max}}$, J and d_{θ} for P3

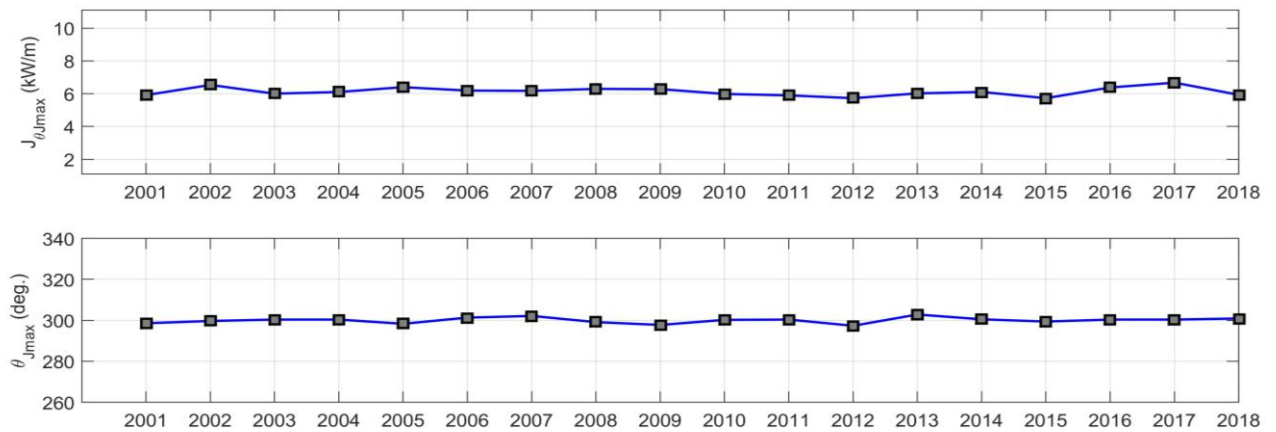


Figure F4.3: Annual mean variation of $J_{\theta_{max}}$ and $\theta_{J_{max}}$ for P1

Analysis: Study Point P5

Table F5.1: Annual scatter table for P5 (2001-2018)

P5		Te (s)													
		0-3	3-4	4-5	5-6	6-7	7-8	8-9	9-10	10-11	11-12	12-13	13-14	14-15	Total
H _{ms0} (m)	0.0 - 0.5	0.00	0.00	0.00	0.00	0.00	0.00	0.00	0.00	0.00	0.00	0.00	0.00	0.00	0.00
	0.5 - 1.0	0.00	0.00	0.00	0.08	0.32	0.98	2.33	0.96	0.16	0.00	0.00	0.00	0.00	4.84
	1.0 - 1.5	0.00	0.00	0.00	0.18	4.17	10.22	13.41	12.17	4.55	0.82	0.16	0.01	0.00	45.69
	1.5 - 2.0	0.00	0.00	0.00	0.03	2.64	12.76	11.10	5.20	1.83	0.74	0.24	0.03	0.00	34.57
	2.0 - 2.5	0.00	0.00	0.00	0.00	0.20	3.40	5.96	3.05	1.08	0.33	0.09	0.01	0.01	14.13
	2.5 - 3.0	0.00	0.00	0.00	0.00	0.00	0.05	0.21	0.23	0.16	0.07	0.02	0.02	0.00	0.76
	3.0 - 3.5	0.00	0.00	0.00	0.00	0.00	0.00	0.00	0.00	0.00	0.00	0.00	0.00	0.00	0.00
	3.5 - 4.0	0.00	0.00	0.00	0.00	0.00	0.00	0.00	0.00	0.00	0.00	0.00	0.00	0.00	0.00
	4-4.5	0.00	0.00	0.00	0.00	0.00	0.00	0.00	0.00	0.00	0.00	0.00	0.00	0.00	0.00
	Total	0.00	0.00	0.00	0.30	7.32	27.41	33.02	21.61	7.78	1.97	0.52	0.06	0.01	100.0

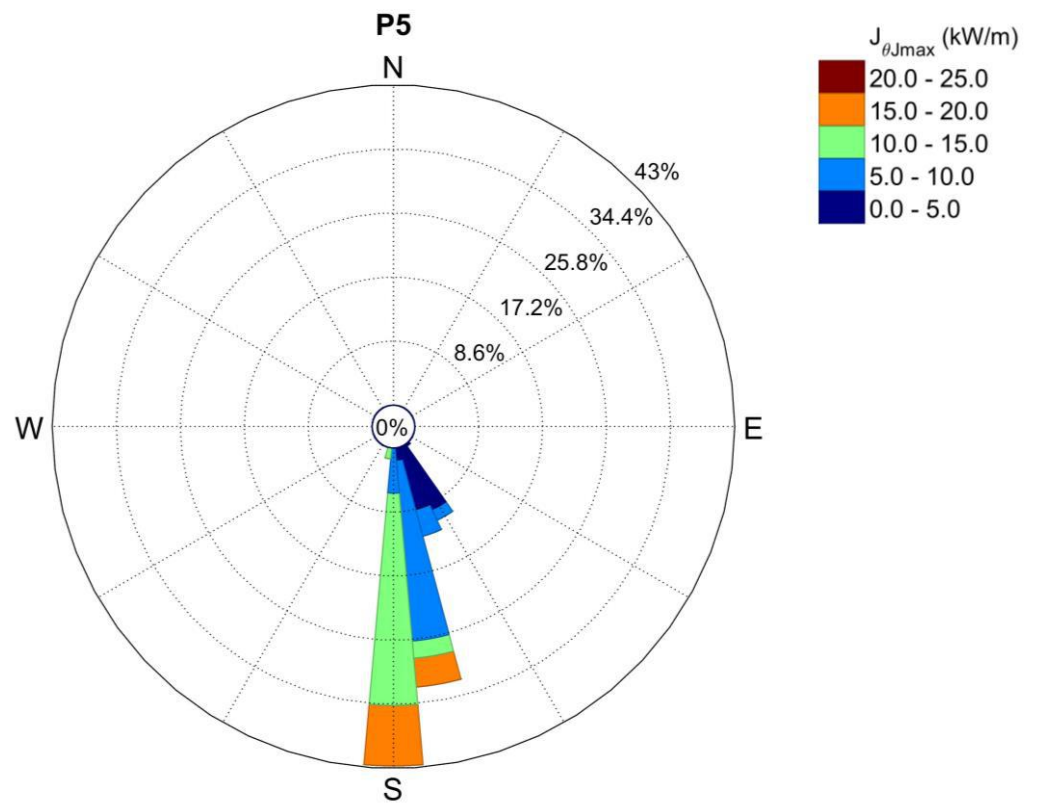


Figure F5.1: Wave power rose of $J_{\theta/J_{max}}$ and $\theta_{J_{max}}$ for P5

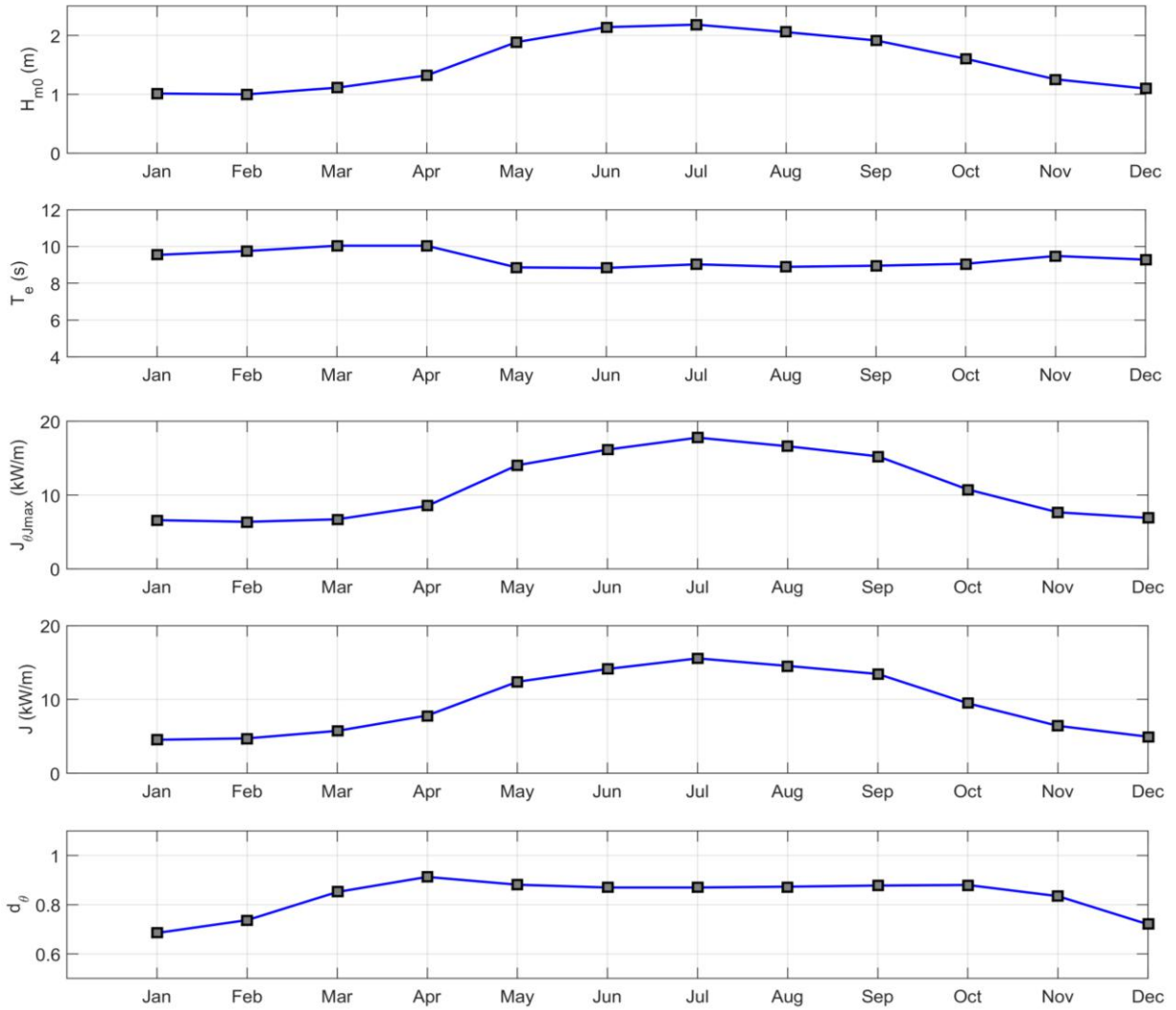


Figure F5.2: Monthly mean values of H_{m0} , T_e , $J_{\theta_{max}}$, J and d_{θ} for P5

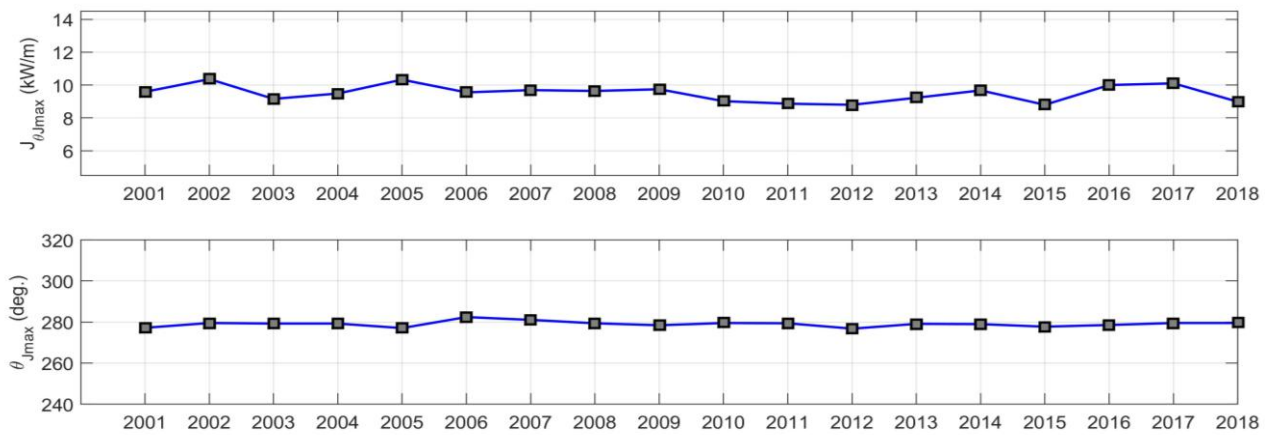


Figure F5.3: Annual mean variation of $J_{\theta_{max}}$ and $\theta_{J_{max}}$ for P5

Analysis: Study Point P6

Table F6.1: Annual scatter table for P6 (2001-2018)

P6		Te (s)														
		0-3	3-4	4-5	5-6	6-7	7-8	8-9	9-10	10-11	11-12	12-13	13-14	14-15	Total	
H _{m0} (m)	0.0 - 0.5	0.00	0.00	0.00	0.00	0.00	0.00	0.00	0.00	0.00	0.00	0.00	0.00	0.00	0.00	0.00
	0.5 - 1.0	0.00	0.00	0.00	0.00	0.10	0.57	1.66	1.45	0.20	0.00	0.00	0.00	0.00	0.00	3.98
	1.0 - 1.5	0.00	0.00	0.00	0.05	1.27	5.39	9.37	14.72	8.77	1.54	0.19	0.01	0.00	0.00	41.30
	1.5 - 2.0	0.00	0.00	0.00	0.02	0.95	6.21	9.67	7.36	4.51	2.13	0.65	0.12	0.01	0.00	31.62
	2.0 - 2.5	0.00	0.00	0.00	0.00	0.11	2.98	7.65	5.38	2.90	0.89	0.31	0.09	0.01	0.00	20.33
	2.5 - 3.0	0.00	0.00	0.00	0.00	0.00	0.14	0.53	0.89	0.56	0.30	0.20	0.05	0.02	0.00	2.68
	3.0 - 3.5	0.00	0.00	0.00	0.00	0.00	0.00	0.02	0.03	0.02	0.01	0.00	0.00	0.00	0.00	0.09
	3.5-4.0	0.00	0.00	0.00	0.00	0.00	0.00	0.00	0.00	0.00	0.00	0.00	0.00	0.00	0.00	0.00
	4-4.5	0.00	0.00	0.00	0.00	0.00	0.00	0.00	0.00	0.00	0.00	0.00	0.00	0.00	0.00	0.00
	Total	0.00	0.00	0.00	0.07	2.43	15.30	28.90	29.84	16.96	4.87	1.34	0.27	0.04	100.0	

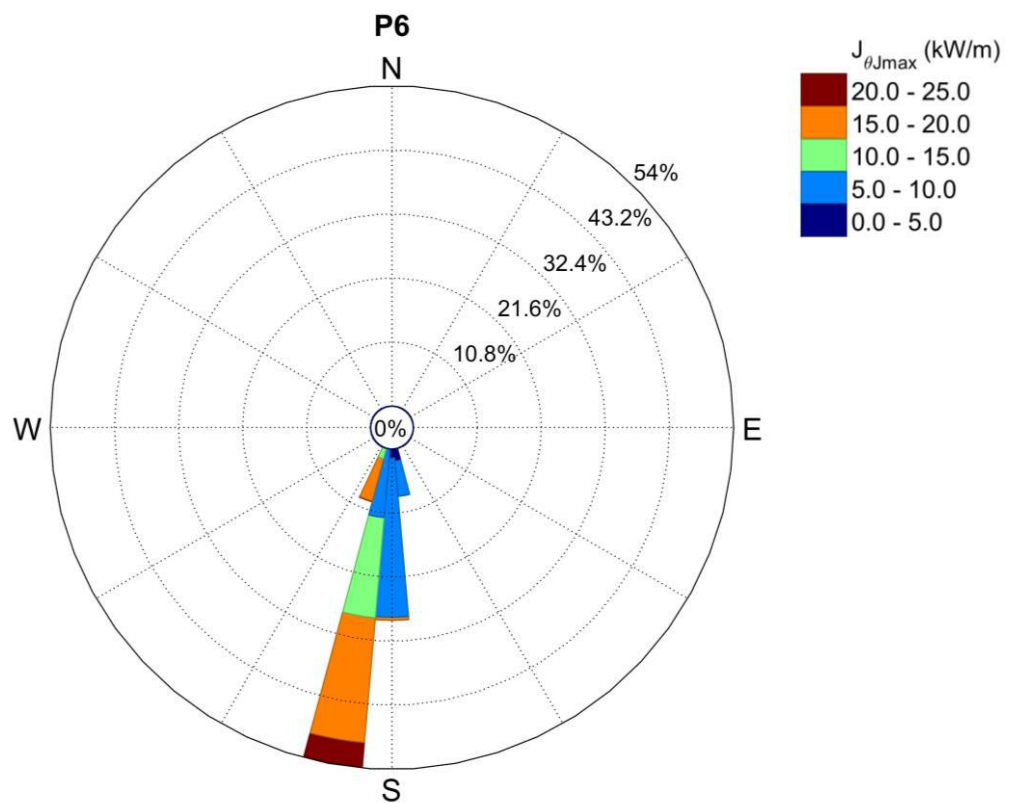


Figure F6.1: Wave power rose of $J_{\theta J_{max}}$ and $\theta_{J_{max}}$ for P6

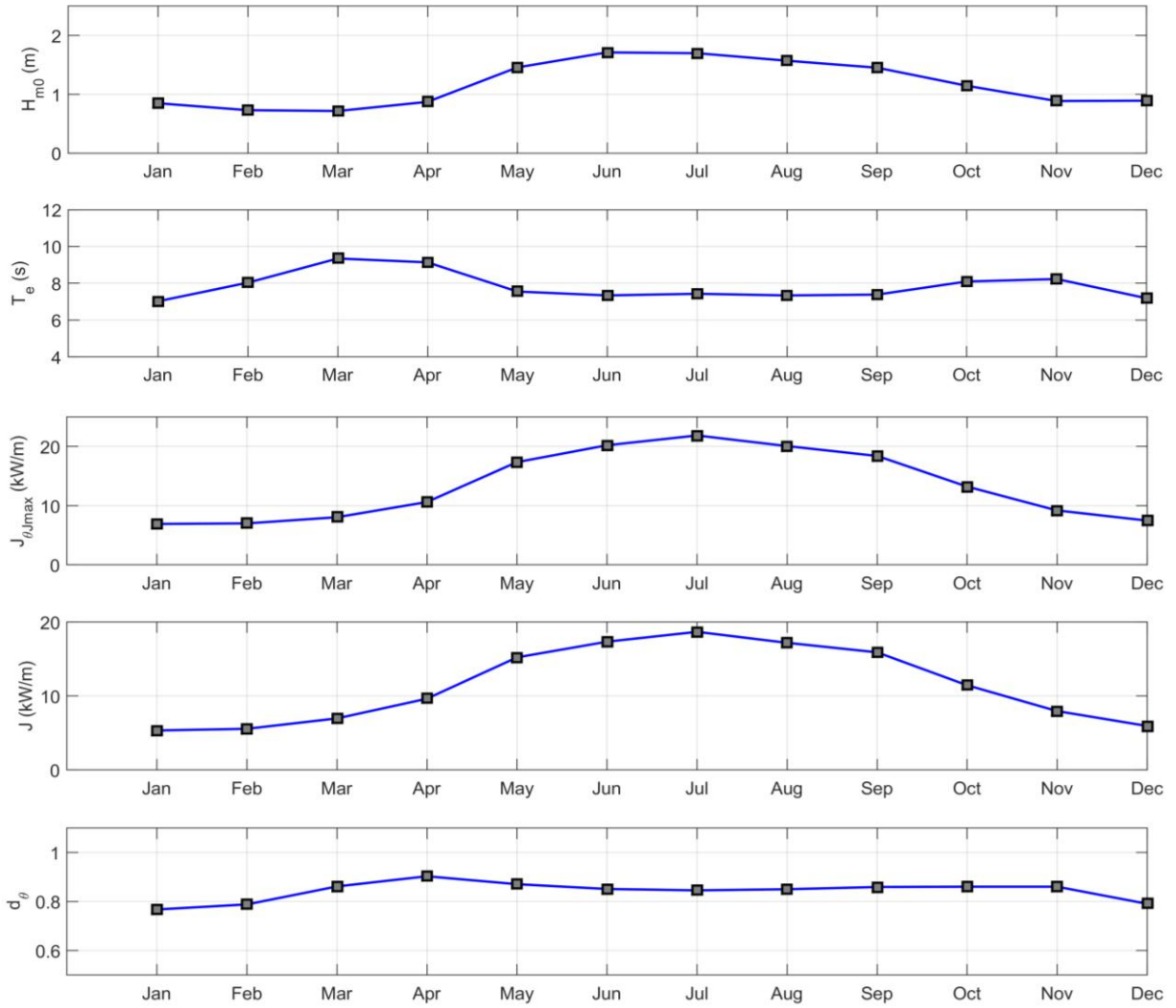


Figure F6.2: Monthly mean values of H_{m0} , T_e , $J_{\theta_{max}}$, J and d_{θ} for P6

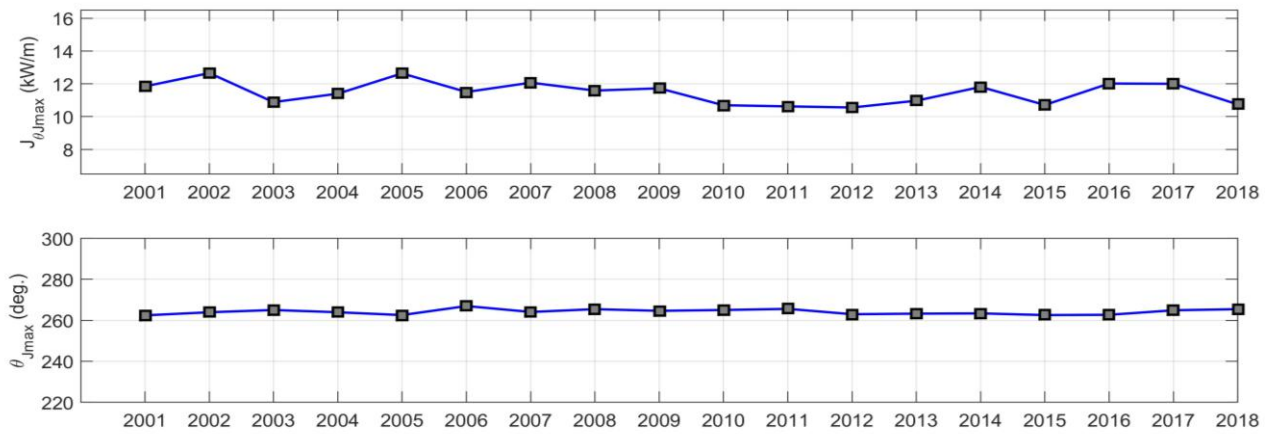


Figure F6.3: Annual mean variation of $J_{\theta_{max}}$ and $\theta_{J_{max}}$ for P6

Analysis: Study Point P7

Table A7.1: Annual scatter table for P7 (2001-2018)

P7		Te (s)													Total	
		0-3	3-4	4-5	5-6	6-7	7-8	8-9	9-10	10-11	11-12	12-13	13-14	14-15		
H _{max} (m)	0.0 - 0.5	0.00	0.00	0.00	0.00	0.00	0.00	0.00	0.00	0.00	0.00	0.00	0.00	0.00	0.00	0.00
	0.5 - 1.0	0.00	0.00	0.00	0.01	0.07	0.72	4.75	7.40	1.98	0.18	0.02	0.00	0.00	0.00	15.15
	1.0 - 1.5	0.00	0.00	0.00	0.02	0.42	1.94	5.20	12.48	12.15	3.42	0.72	0.11	0.01	0.00	36.46
	1.5 - 2.0	0.00	0.00	0.00	0.01	0.93	5.72	7.64	5.29	2.73	1.43	0.64	0.20	0.03	0.00	24.61
	2.0 - 2.5	0.00	0.00	0.00	0.00	0.18	4.28	7.67	4.61	1.95	0.67	0.21	0.10	0.02	0.00	19.68
	2.5 - 3.0	0.00	0.00	0.00	0.00	0.00	0.42	1.36	1.13	0.52	0.21	0.17	0.04	0.00	0.00	3.84
	3.0 - 3.5	0.00	0.00	0.00	0.00	0.00	0.01	0.07	0.05	0.05	0.06	0.01	0.00	0.00	0.00	0.25
	3.5 - 4.0	0.00	0.00	0.00	0.00	0.00	0.00	0.00	0.00	0.00	0.00	0.00	0.00	0.00	0.00	0.00
	4-4.5	0.00	0.00	0.00	0.00	0.00	0.00	0.00	0.00	0.00	0.00	0.00	0.00	0.00	0.00	0.00
	Total	0.00	0.00	0.00	0.05	1.60	13.09	26.69	30.97	19.38	5.97	1.77	0.43	0.06	0.00	100.0

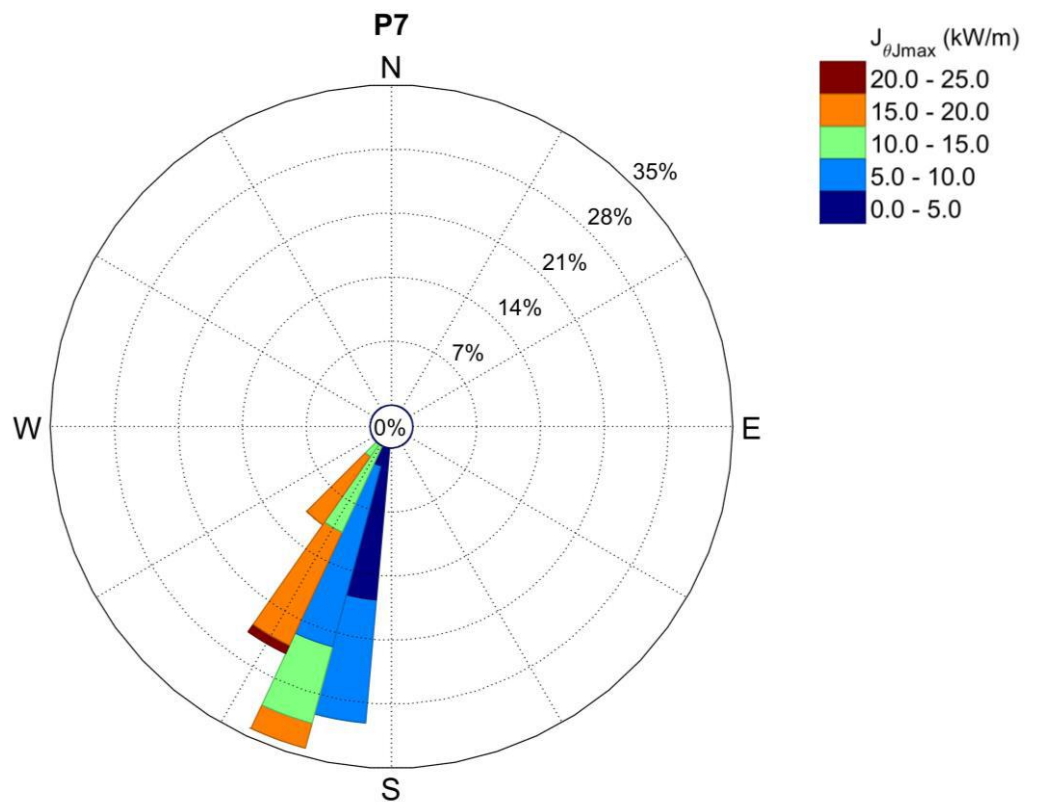


Figure F7.1: Wave power rose of $J_{\theta J_{max}}$ and $\theta_{J_{max}}$ for P7

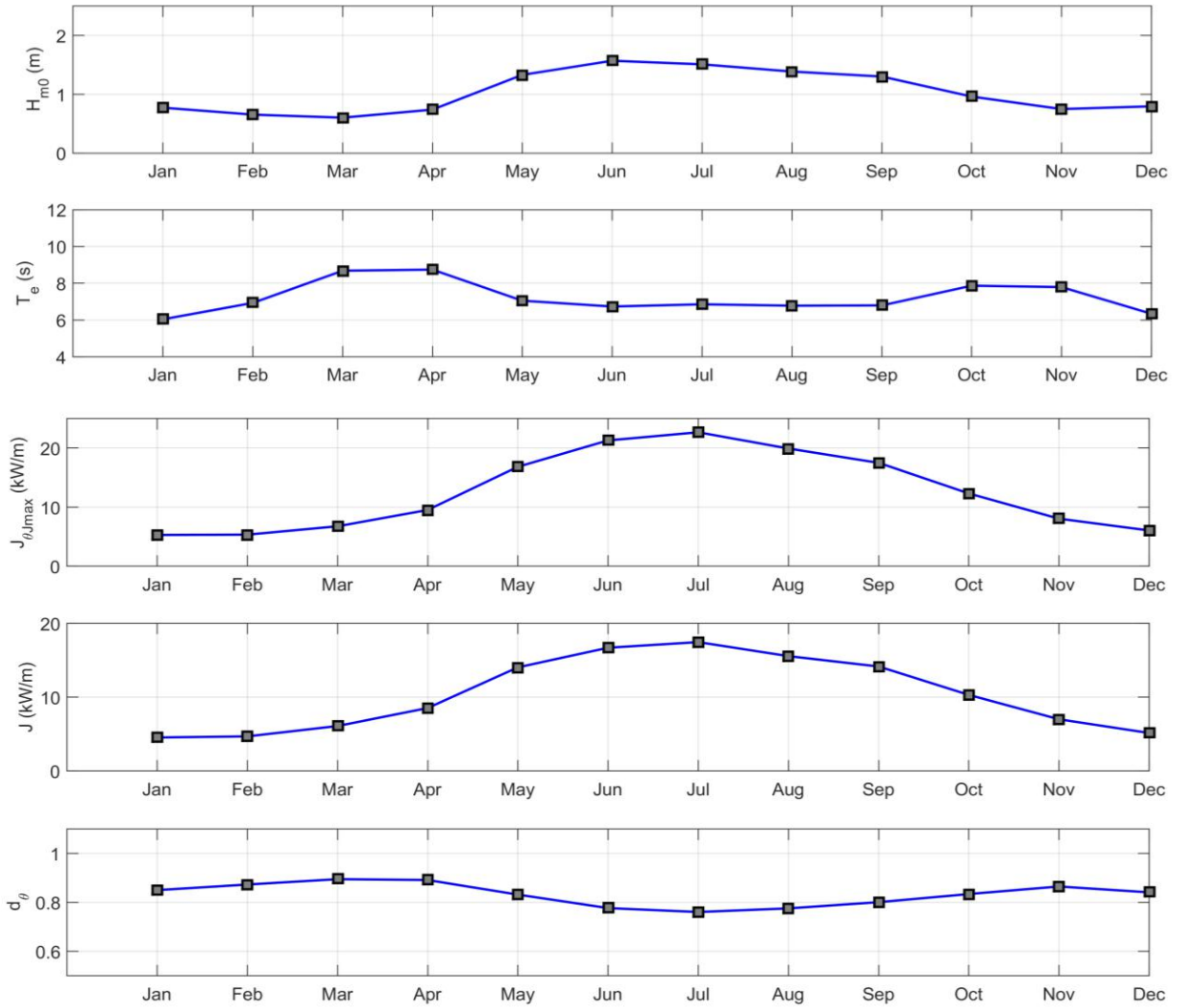


Figure F7.2: Monthly mean values of H_{m0} , T_e , $J_{\theta_{max}}$, J and d_{θ} for P7

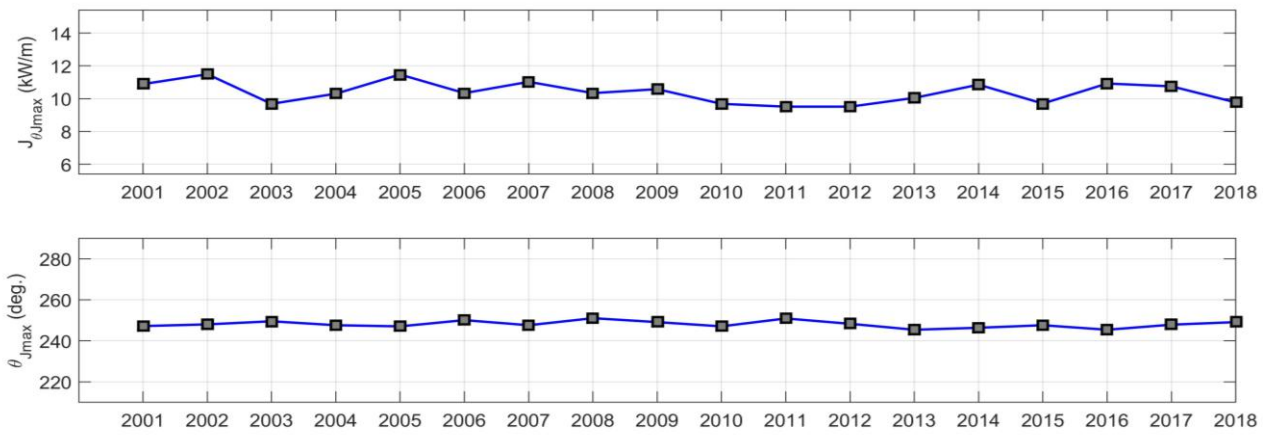


Figure F7.3: Annual mean variation of $J_{\theta_{max}}$ and $\theta_{J_{max}}$ for P7

Analysis: Study Point P8

Table F8.1: Annual scatter table for P8 (2001-2018)

P8		Te (s)													
		0-3	3-4	4-5	5-6	6-7	7-8	8-9	9-10	10-11	11-12	12-13	13-14	14-15	Total
H _{m0} (m)	0.0 - 0.5	0.00	0.00	0.00	0.00	0.05	0.14	0.29	0.39	0.17	0.03	0.01	0.00	0.00	1.09
	0.5 - 1.0	0.00	0.00	0.10	3.20	7.29	8.28	8.96	8.71	5.63	1.66	0.45	0.14	0.00	44.42
	1.0 - 1.5	0.00	0.00	0.05	2.11	9.46	9.07	4.19	1.42	0.67	0.38	0.22	0.07	0.00	27.65
	1.5 - 2.0	0.00	0.00	0.00	0.16	9.93	9.70	2.66	0.60	0.12	0.04	0.01	0.01	0.00	23.22
	2.0 - 2.5	0.00	0.00	0.00	0.00	0.70	2.01	0.61	0.17	0.03	0.00	0.00	0.00	0.00	3.52
	2.5 - 3.0	0.00	0.00	0.00	0.00	0.00	0.08	0.03	0.00	0.00	0.00	0.00	0.00	0.00	0.11
	3.0 - 3.5	0.00	0.00	0.00	0.00	0.00	0.00	0.00	0.00	0.00	0.00	0.00	0.00	0.00	0.00
	3.5-4.0	0.00	0.00	0.00	0.00	0.00	0.00	0.00	0.00	0.00	0.00	0.00	0.00	0.00	0.00
	4-4.5	0.00	0.00	0.00	0.00	0.00	0.00	0.00	0.00	0.00	0.00	0.00	0.00	0.00	0.00
	Total	0.00	0.00	0.15	5.47	27.44	29.28	16.74	11.28	6.61	2.12	0.69	0.22	0.00	100.0

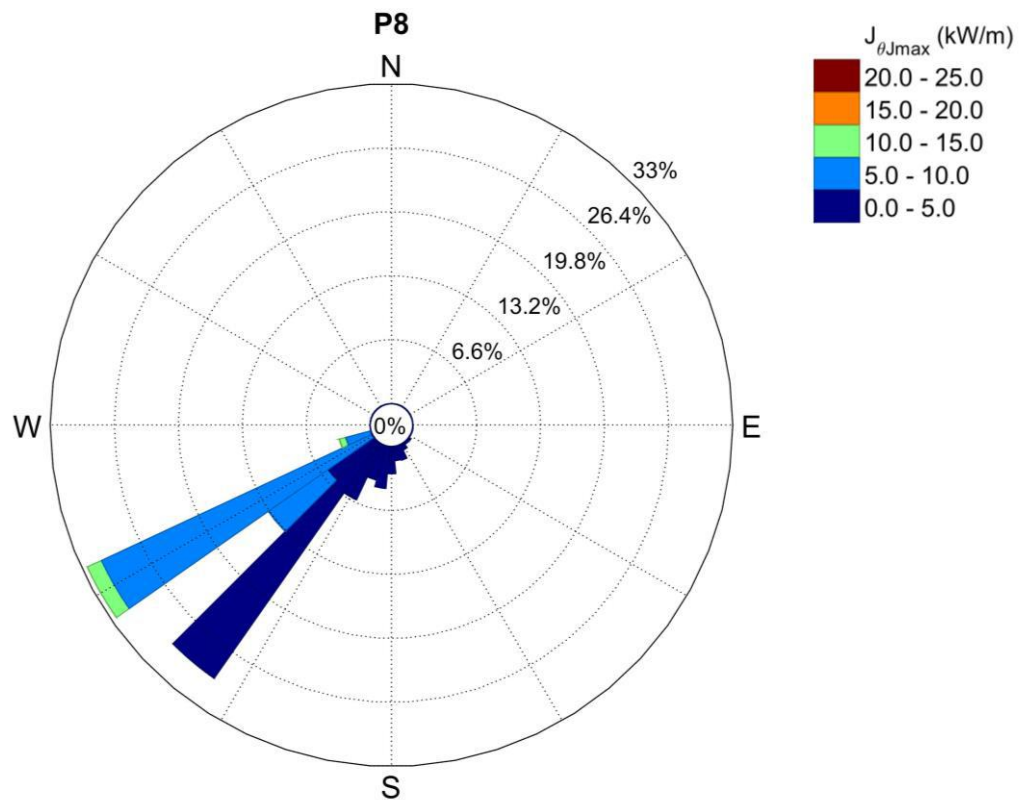


Figure F8.1: Wave power rose of $J_{\theta} J_{max}$ and θ_{Jmax} for P8

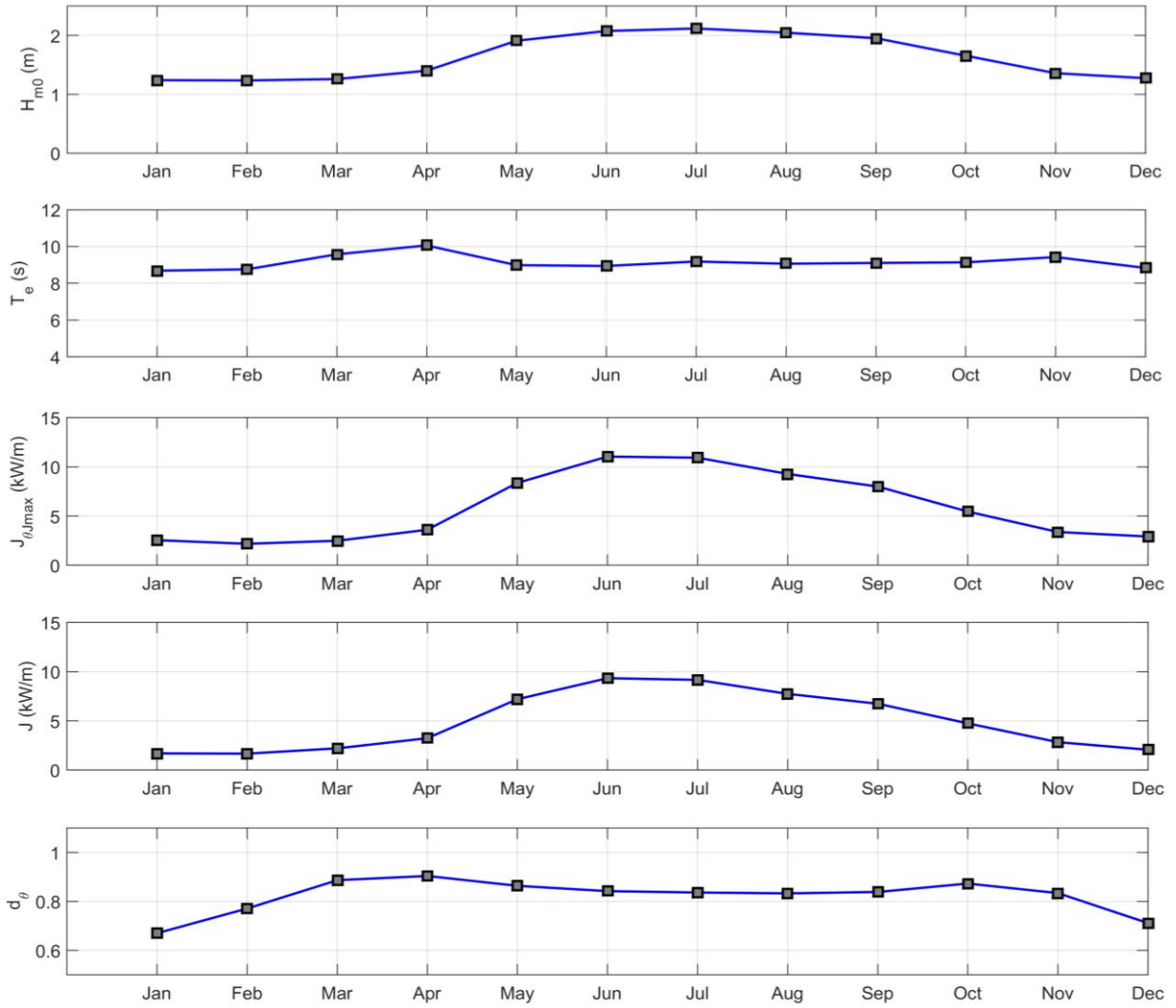


Figure F8.2: Monthly mean values of H_{m0} , T_e , $J_{\theta_{max}}$, J and d_{θ} for P8

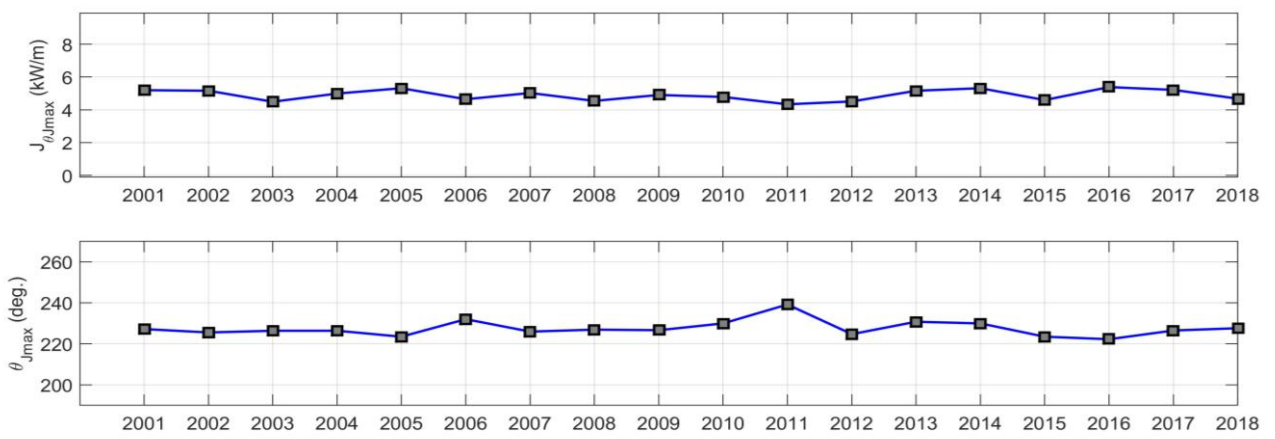


Figure F8.3: Annual mean variation of $J_{\theta_{max}}$ and $\theta_{j_{max}}$ for P8

Analysis: Study Point P9

Table A9.1: Annual scatter table for P9 (2001-2018)

P9		Te (s)													
		0-3	3-4	4-5	5-6	6-7	7-8	8-9	9-10	10-11	11-12	12-13	13-14	14-15	Total
H _{ms} (m)	0.0 - 0.5	0.00	0.00	0.05	0.26	0.70	1.42	1.81	1.32	0.46	0.04	0.02	0.00	0.00	47.77
	0.5 - 1.0	0.00	0.03	4.07	9.75	8.03	7.38	6.07	5.46	3.78	2.13	0.69	0.28	0.08	28.71
	1.0 - 1.5	0.00	0.00	0.38	8.05	12.92	4.58	1.63	0.50	0.32	0.13	0.13	0.05	0.01	16.37
	1.5 - 2.0	0.00	0.00	0.00	1.55	9.40	4.02	1.00	0.30	0.07	0.02	0.00	0.00	0.01	1.03
	2.0 - 2.5	0.00	0.00	0.00	0.00	0.44	0.39	0.16	0.04	0.00	0.00	0.00	0.00	0.00	0.02
	2.5 - 3.0	0.00	0.00	0.00	0.00	0.00	0.02	0.00	0.00	0.00	0.00	0.00	0.00	0.00	0.00
	3.0 - 3.5	0.00	0.00	0.00	0.00	0.00	0.00	0.00	0.00	0.00	0.00	0.00	0.00	0.00	0.00
	3.5-4.0	0.00	0.00	0.00	0.00	0.00	0.00	0.00	0.00	0.00	0.00	0.00	0.00	0.00	0.00
	4-4.5	0.00	0.00	0.00	0.00	0.00	0.00	0.00	0.00	0.00	0.00	0.00	0.00	0.00	0.00
	Total	0.00	0.03	4.51	19.61	31.50	17.81	10.68	7.62	4.64	2.33	0.85	0.34	0.09	100.0

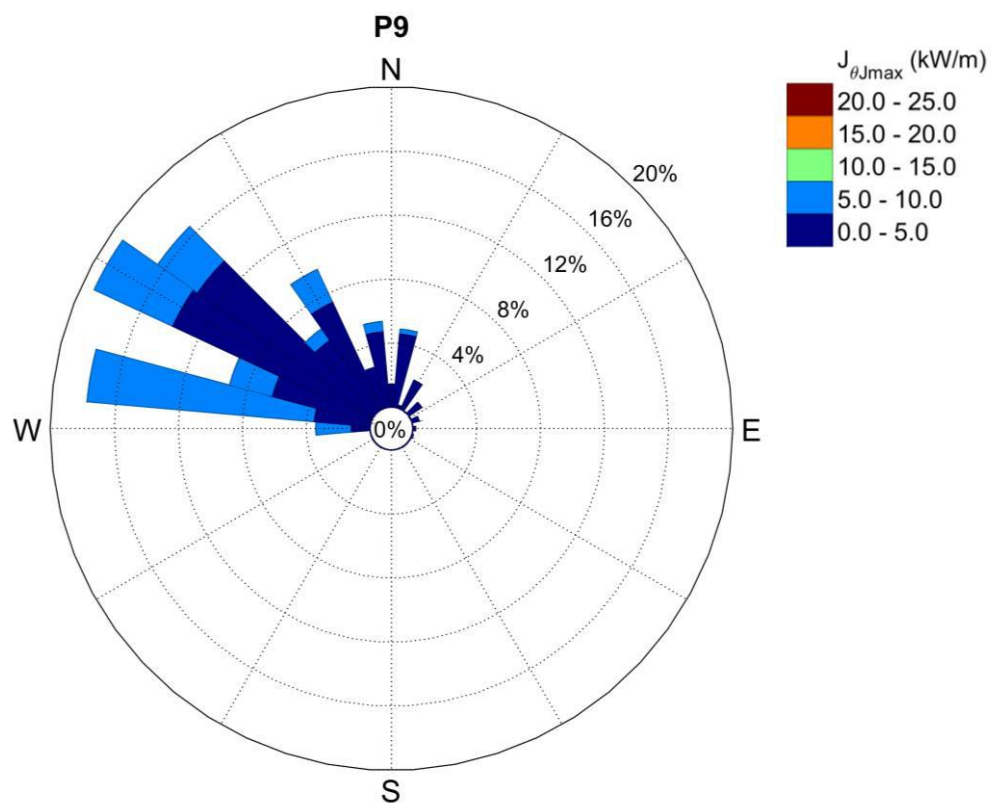


Figure F9.1: Wave power rose of $J_{\theta J_{max}}$ and $\theta_{J_{max}}$ for P9

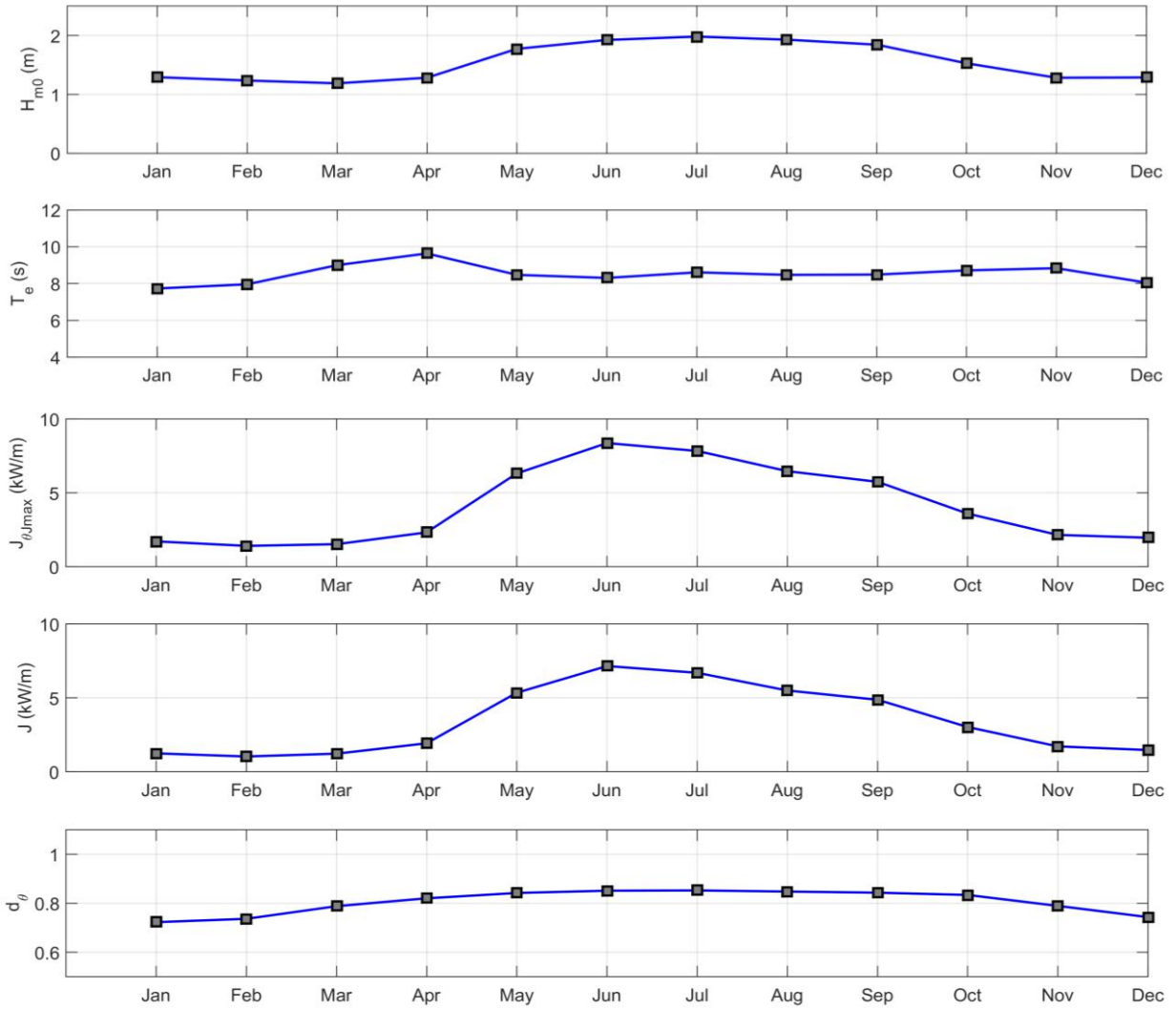


Figure F9.2: Monthly mean values of H_{m0} , T_e , $J_{\theta_{max}}$, J and d_{θ} for P9

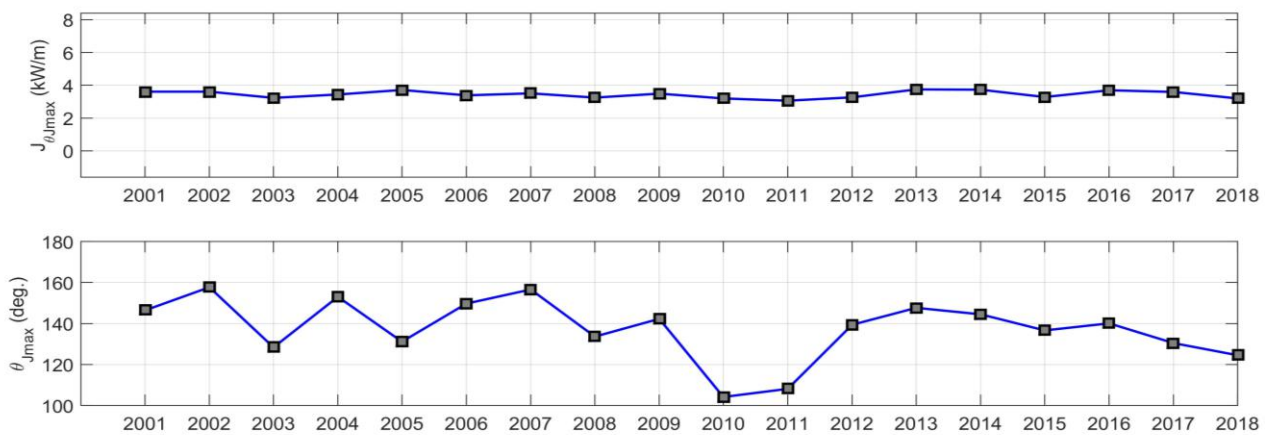


Figure F9.3: Annual mean variation of $J_{\theta_{max}}$ and $\theta_{J_{max}}$ for P9

Analysis: Study Point P10

Table A20.1: Annual scatter table for P10 (2001-2018)

P10		Te (s)													
		0-3	3-4	4-5	5-6	6-7	7-8	8-9	9-10	10-11	11-12	12-13	13-14	14-15	Total
H _{mo} (m)	0.0 - 0.5	46.54	33.71	6.49	2.01	0.46	0.05	0.00	0.00	0.00	0.00	0.00	0.00	0.00	89.28
	0.5 - 1.0	5.41	5.30	0.00	0.00	0.00	0.00	0.00	0.00	0.00	0.00	0.00	0.00	0.00	10.72
	1.0 - 1.5	0.00	0.01	0.00	0.00	0.00	0.00	0.00	0.00	0.00	0.00	0.00	0.00	0.00	0.01
	1.5 - 2.0	0.00	0.00	0.00	0.00	0.00	0.00	0.00	0.00	0.00	0.00	0.00	0.00	0.00	0.00
	2.0 - 2.5	0.00	0.00	0.00	0.00	0.00	0.00	0.00	0.00	0.00	0.00	0.00	0.00	0.00	0.00
	2.5 - 3.0	0.00	0.00	0.00	0.00	0.00	0.00	0.00	0.00	0.00	0.00	0.00	0.00	0.00	0.00
	3.0 - 3.5	0.00	0.00	0.00	0.00	0.00	0.00	0.00	0.00	0.00	0.00	0.00	0.00	0.00	0.00
	3.5-4.0	0.00	0.00	0.00	0.00	0.00	0.00	0.00	0.00	0.00	0.00	0.00	0.00	0.00	0.00
	4-4.5	0.00	0.00	0.00	0.00	0.00	0.00	0.00	0.00	0.00	0.00	0.00	0.00	0.00	0.00
	Total	51.96	39.02	6.49	2.01	0.46	0.05	0.00	0.00	0.00	0.00	0.00	0.00	0.00	100.0

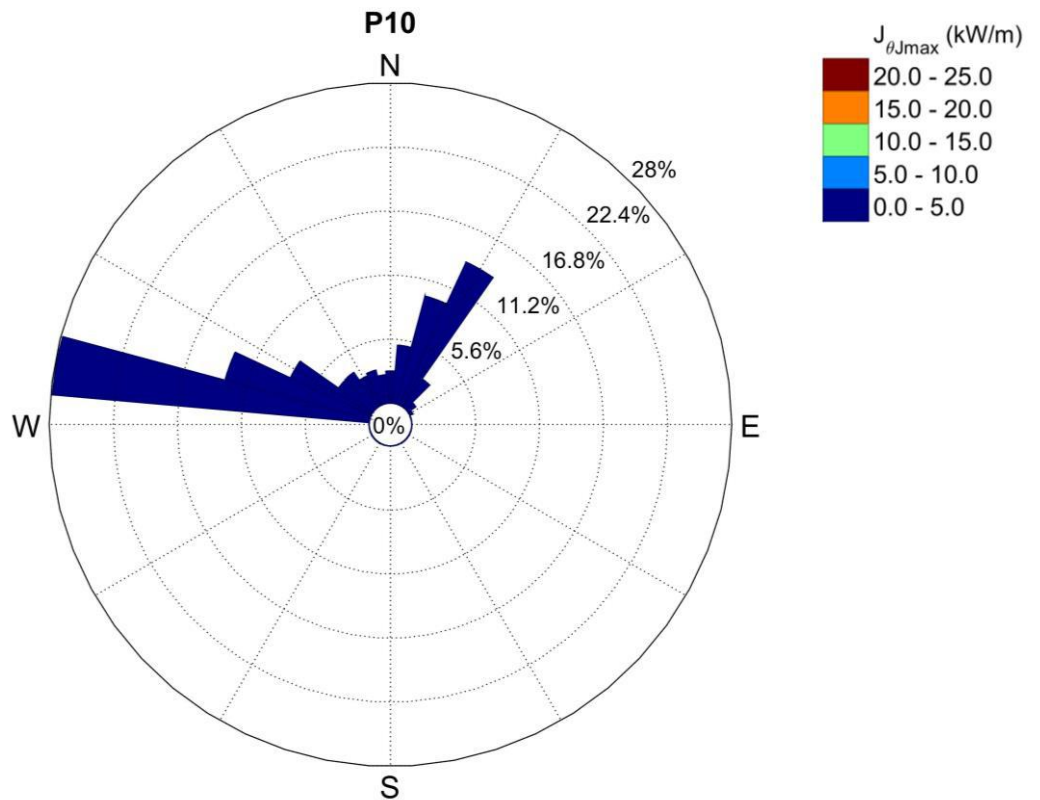


Figure F10.1: Wave power rose of $J_{\theta J_{max}}$ and $\theta_{J_{max}}$ for P10

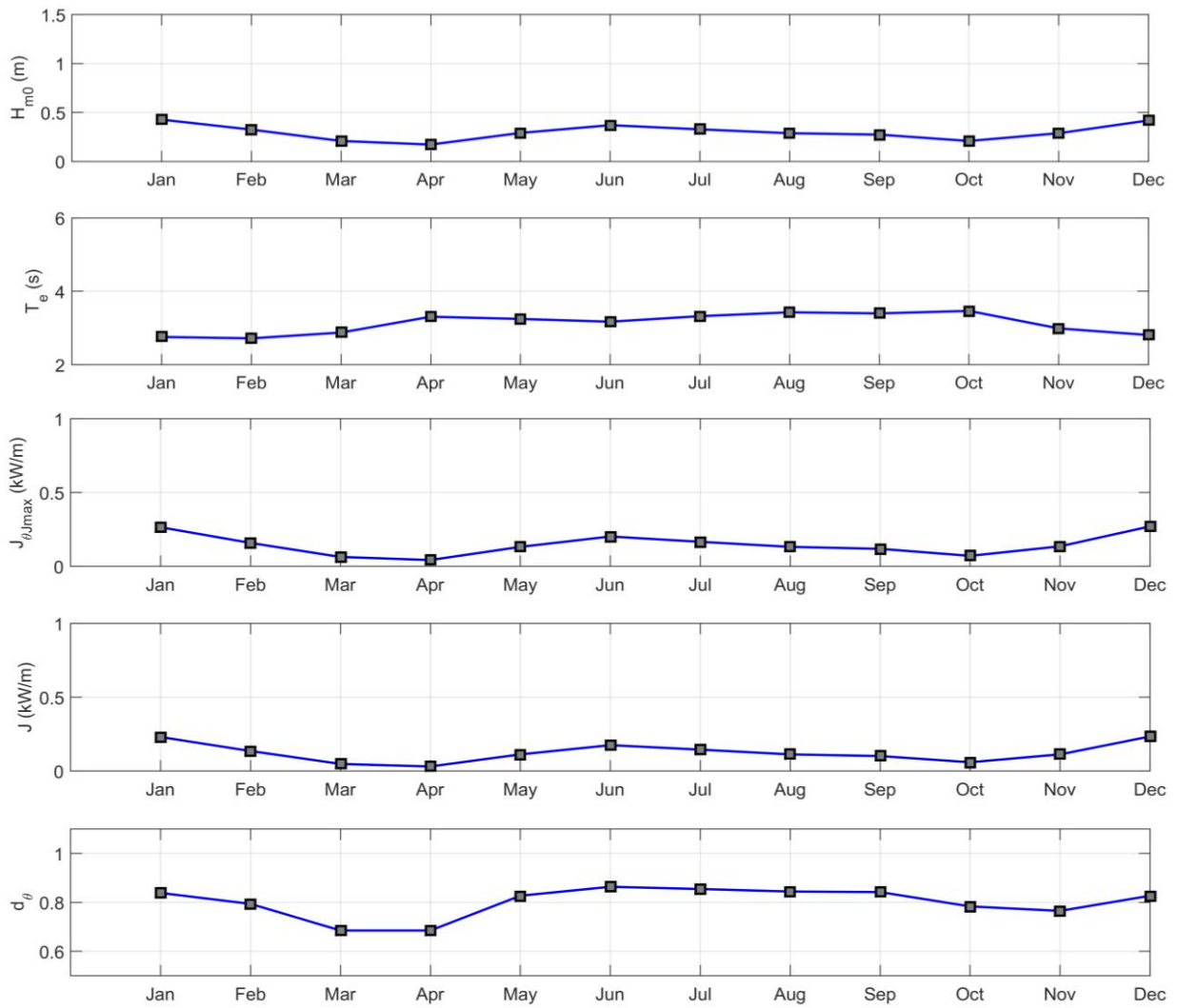


Figure F10.2: Monthly mean values of H_{m0} , T_e , $J_{\theta_{max}}$, J and d_{θ} for P10

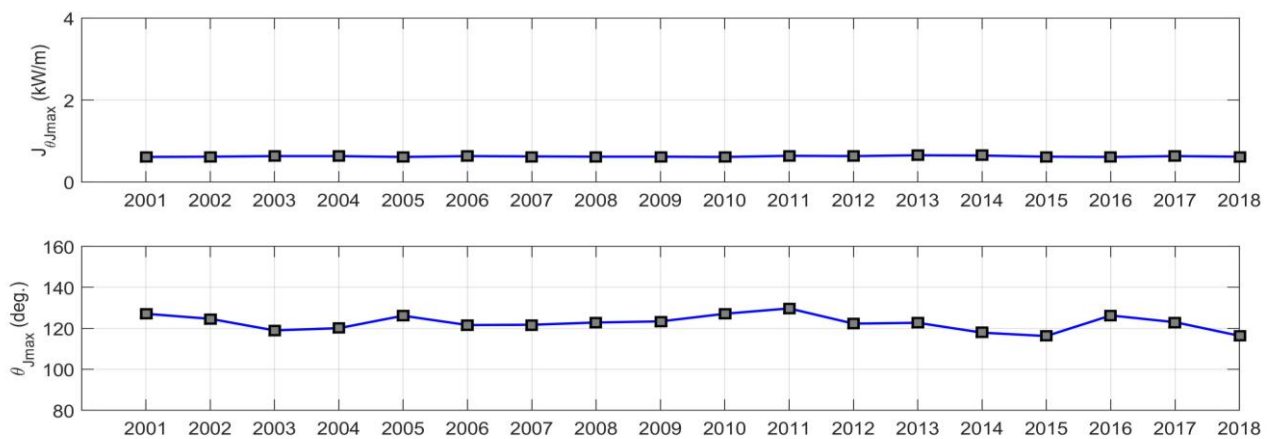


Figure F10.3: Annual mean variation of $J_{\theta_{max}}$ and $\theta_{J_{max}}$ for P10

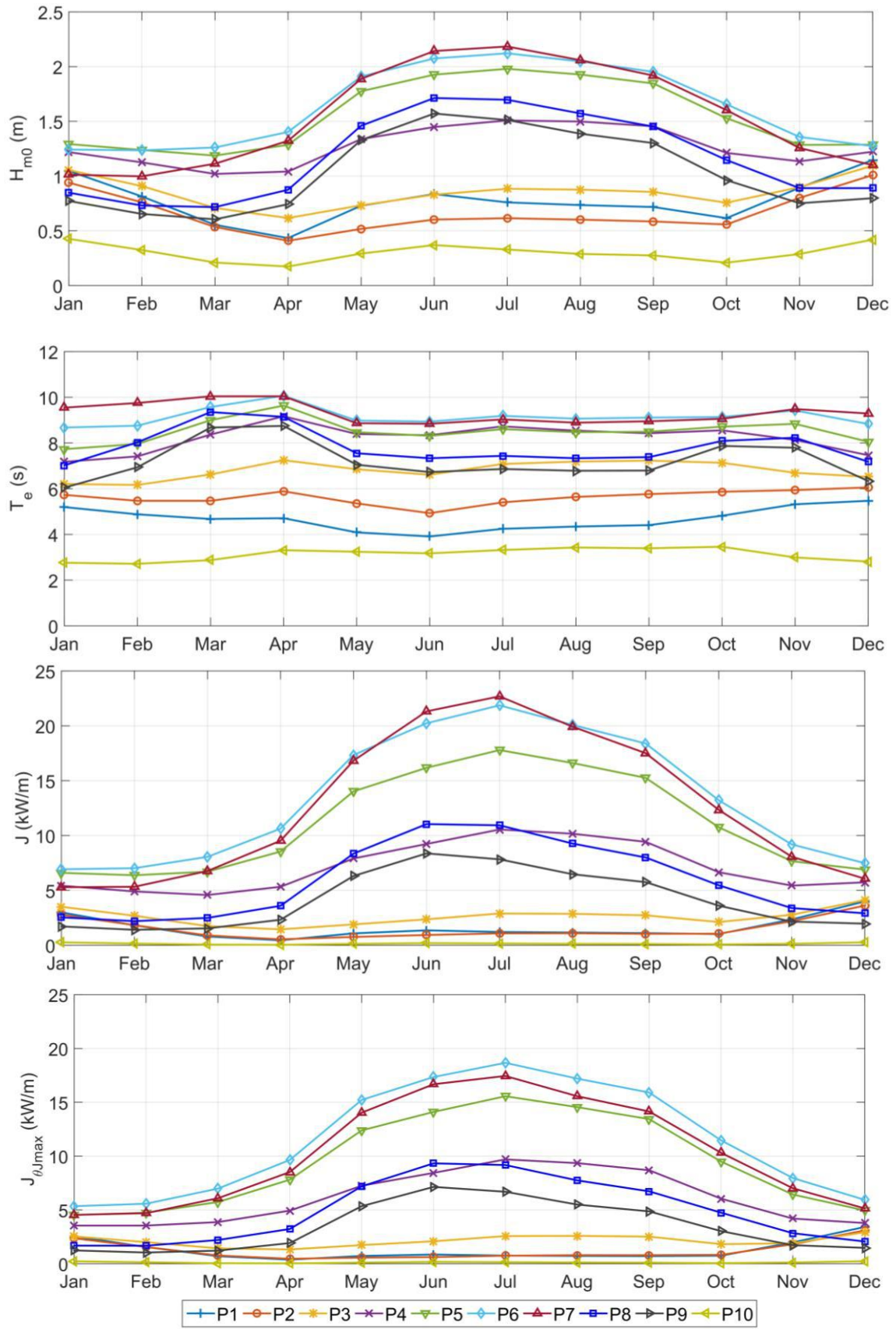


Figure F.1: Monthly mean values of H_{m0} , T_e , $J_{\theta_{max}}$, J and d_{θ} for all points

Annex G
Long-term uncertainty of the study points

Table G.1: Mean Average Error (MAE) and Maximum Error (ME) percentages of P1-P10 study points

Study Point	H_{m0} (%)		T_e (%)		J (%)	
	MAE	ME	MAE	ME	MAE	ME
P1	3.2	9.0	1.4	4.0	11.3	27.6
P2	3.2	8.9	1.7	4.7	10.9	25.1
P3	2.4	6.5	1.5	5.0	4.7	15.7
P4	1.4	3.5	1.0	2.4	3.2	8.5
P5	1.9	3.6	1.0	2.3	4.3	8.6
P6	2.1	4.0	1.2	2.5	5.0	10.0
P7	2.3	4.5	1.4	3.6	5.2	10.5
P8	2.7	4.8	1.7	4.7	6.0	9.9
P9	2.1	5.8	2.4	6.1	5.5	9.3
P10	3.7	9.6	1.6	3.9	7.2	22.4

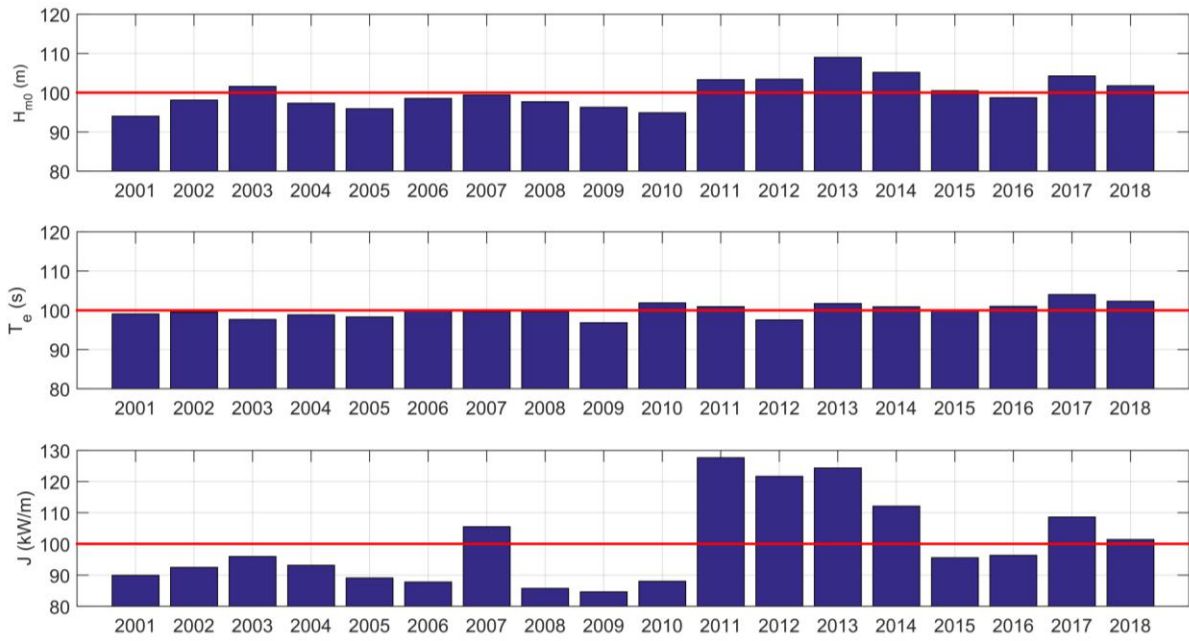


Figure G.1: Annual H_{m0} , T_e and J variations of P1

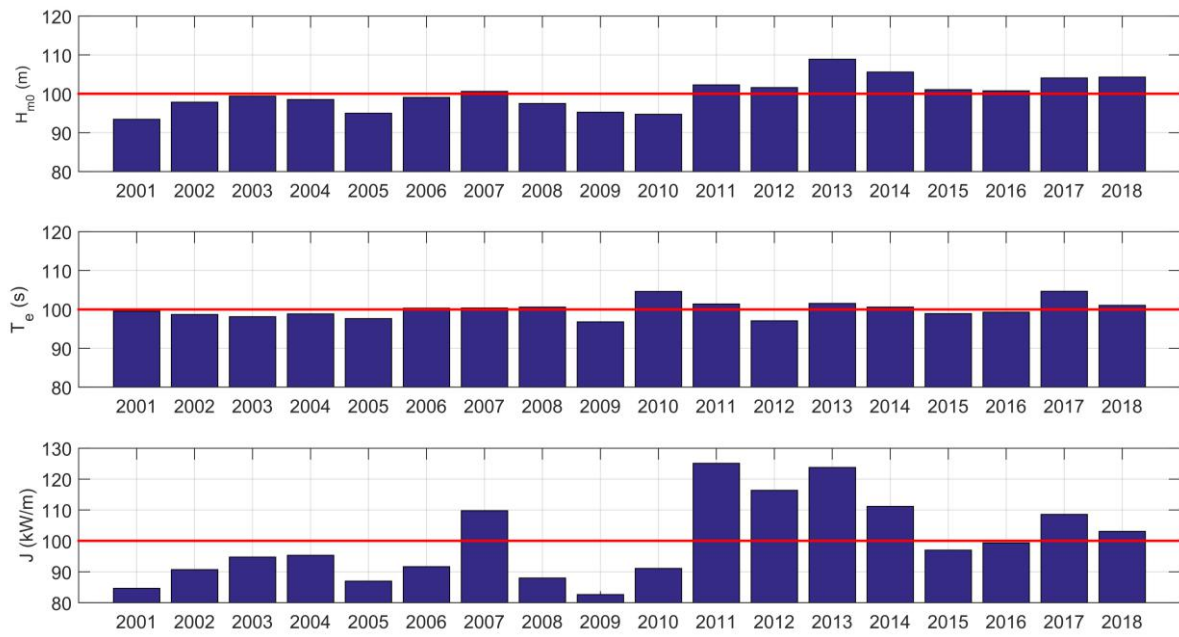


Figure G.2: Annual H_{m0} , T_e and J variations of P2

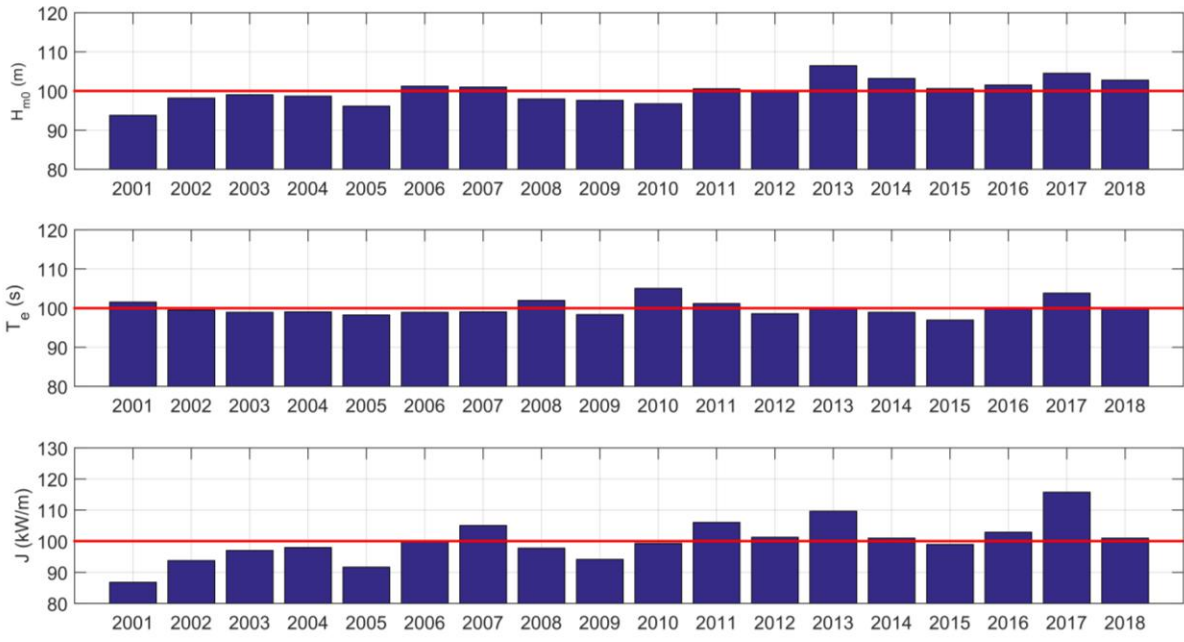


Figure G.3: Annual H_{m0} , T_e and J variations of P3

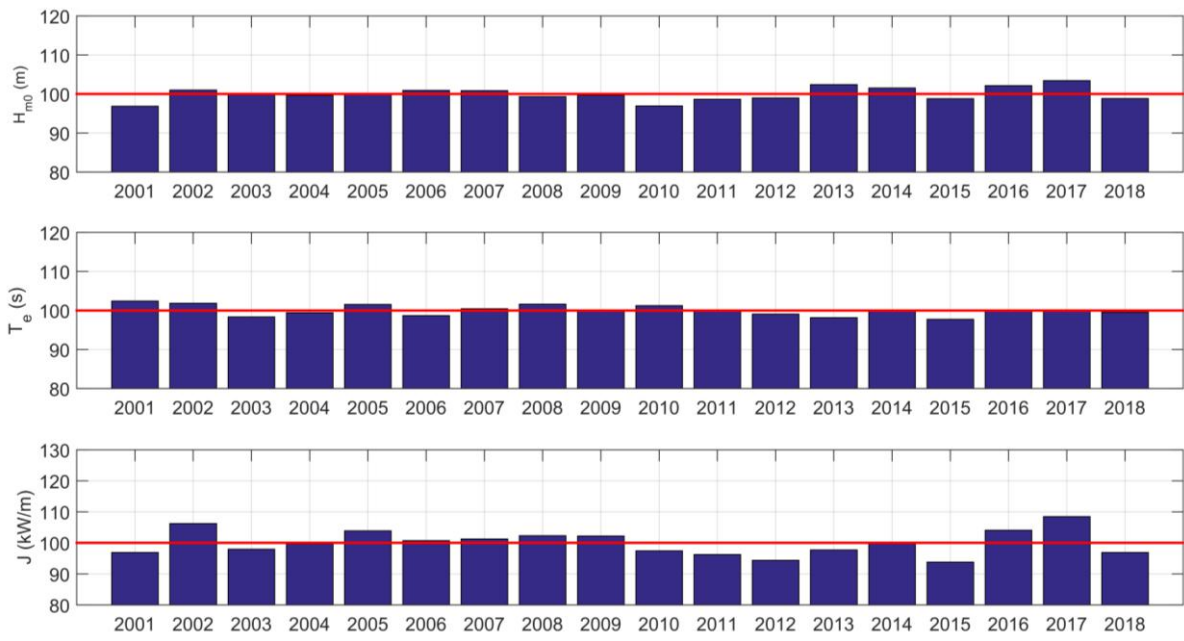


Figure G.4: Annual H_{m0} , T_e and J variations of P4

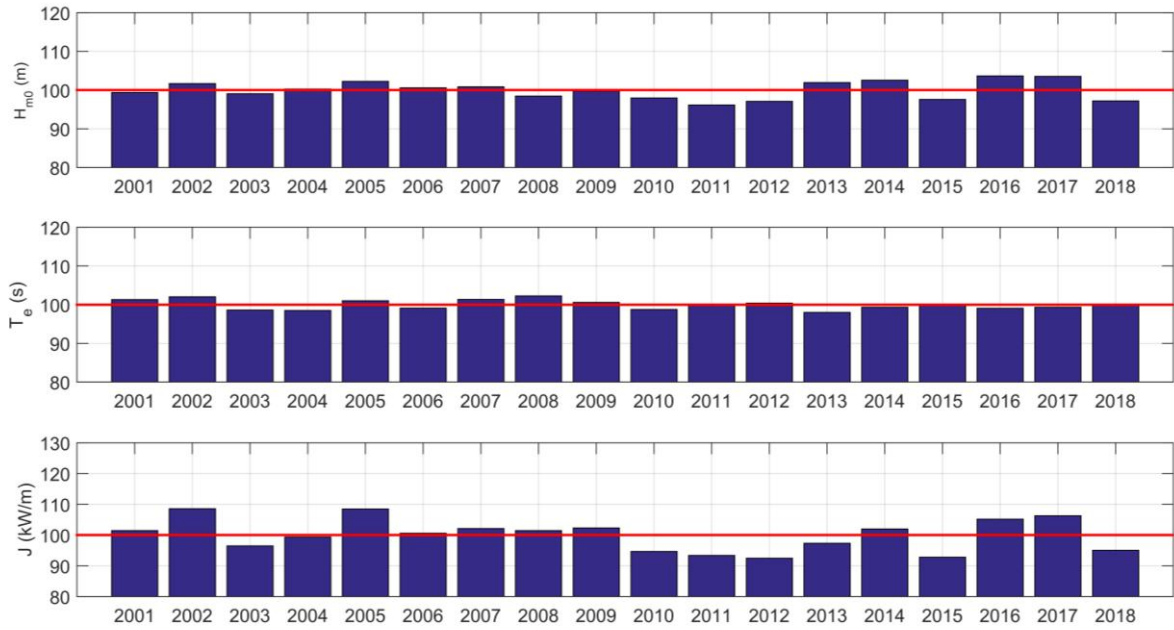


Figure G.5: Annual H_{m0} , T_e and J variations of P5

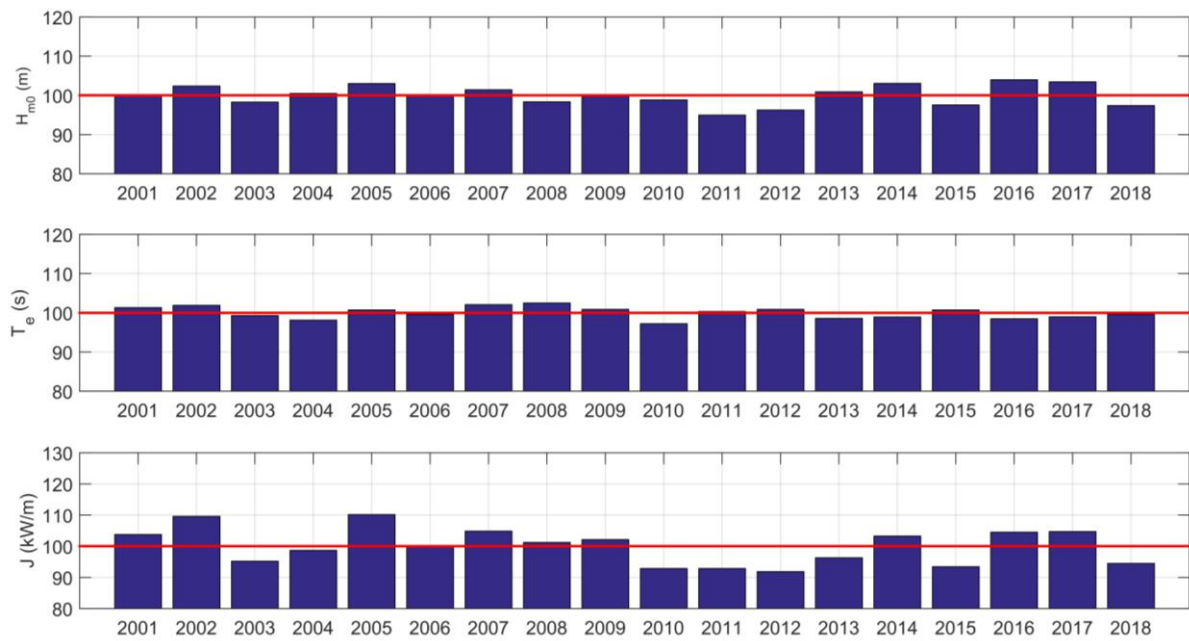


Figure G.6 : Annual H_{m0} , T_e and J variations of P6

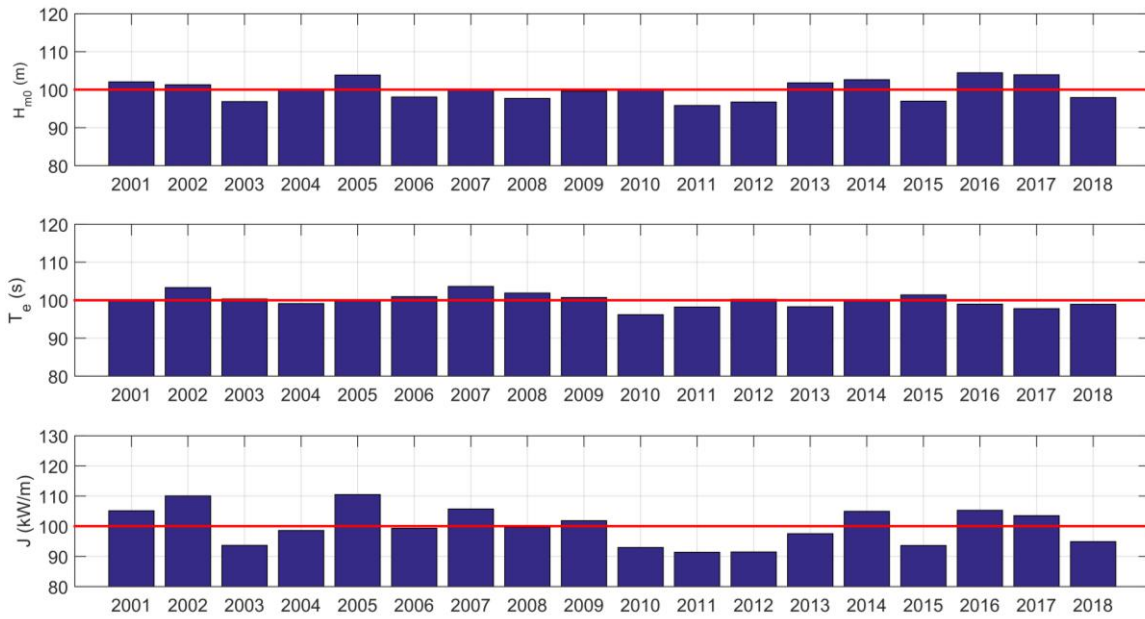


Figure G.7 : Annual H_{m0} , T_e and J variations of P7

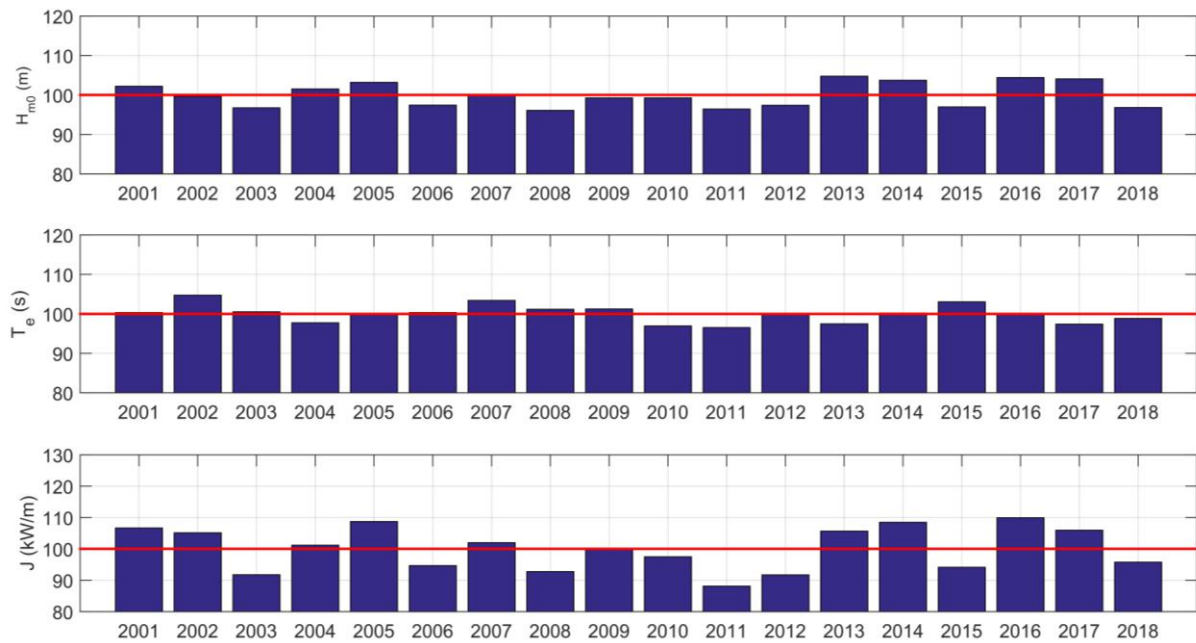


Figure G.8 : Annual H_{m0} , T_e and J variations of P8

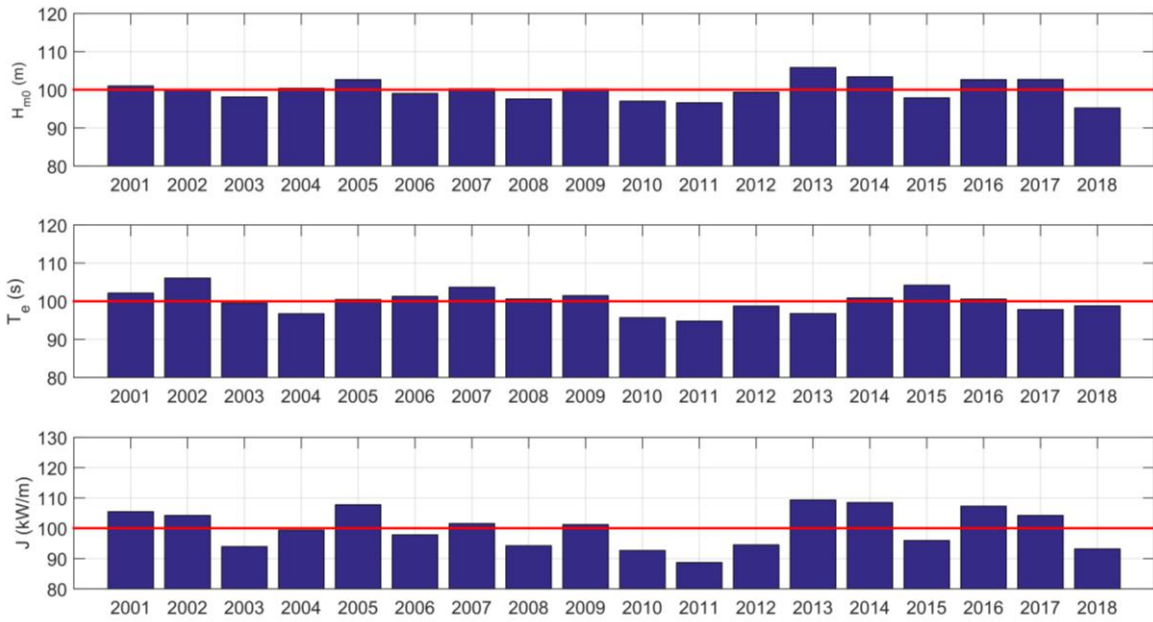


Figure G.9: Annual H_{m0} , T_e and J variations of P9

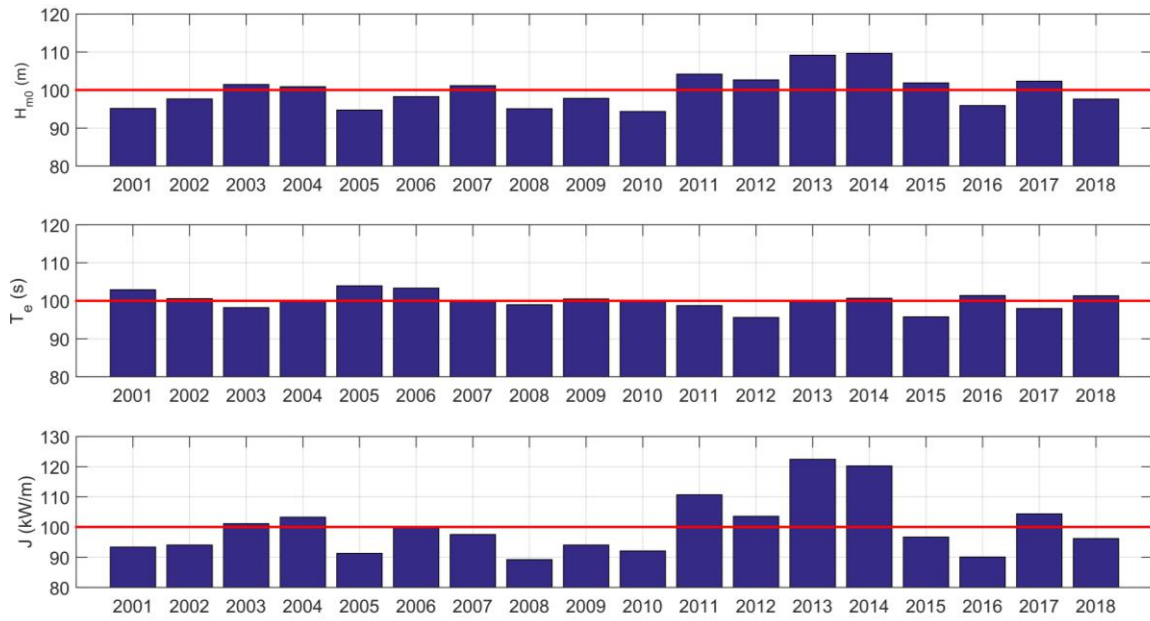


Figure G.10: Annual H_{m0} , T_e and J variations of P10

Annex H

Model Setup and Implementation

User Manual

Note : Authors are recommended to use softcopy of this annex which included in the attached DVD

General Information

About this manual

This User Manual describes all the steps that need to follow for the initial model running. As described in the report, the third-generation wave model SWAN 41.20A used for the model construction. This distribution can be implemented on Microsoft Windows, Linux, Unix and macOS, provided a Fortran90 compiler is available. In this manual, SWAN 41.20A on Microsoft Windows has described with relevant references. In addition, user should install compatible Matlab version (2014a or higher) to visualize the outputs of SWAN.

System configuration

To install SWAN for serial runs on Windows PC, download and run the [Setup Wizard](#) (size: 3.17 MB) or download and run another [Wizard](#) (size: 3.14 MB) that follow the OpenMP 2.0 standard. This will be particularly useful for those users who have a multiple core PC.

Note that the distributions have been compiled using the Intel Fortran Compiler 18.0 (as part of Intel Parallel Studio XE 2018 for Windows). If desired, user may need to install the redistributable libraries, which can be downloaded from [this page](#). User should download the appropriate version, which is Parallel Studio XE 2018 (all Editions). Next, use this [link](#) to download the redistributable packages and click on the of Update 1 of Intel Fortran Compiler 2018 for Windows. Install the redistributable package, either 32-bit or 64-bit, depending on the installed SWAN executable. This ensure the proper use of the OpenMP directives.

SWAN Manuals

The information about the SWAN package is distributed over four different documents. The [User Manual](#) describes the complete input and usage of the SWAN package. This document is also

available in [PDF](#) format. The [Implementation Manual \(PDF\)](#) explains the installation procedure of SWAN on a single- or multi-processor machine with shared or distributed memory. This document is also available in [PDF](#) format. The [Programming rules \(PDF\)](#) is meant for programmers who want to develop SWAN. The [Scientific/technical documentation \(PDF\)](#) discusses the physical and mathematical details and the discretizations that are used in the SWAN program.

Model files

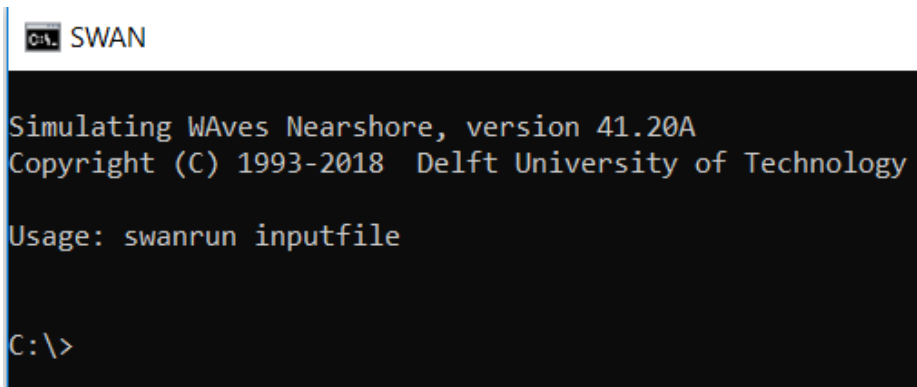
The attached DVD has consisted with a **.zip** file (e.g. Test_SL.zip). Unzip the file first and copy those files into your working directory. The .zip file consists with

1. unstructured grid data files generated by Triangle grid generator (.pole, .node and .ele),
2. bathymetric data file (.bot).
3. wind data file (.dat) and
4. spectral files (.spc)

The details of these datasets are described in WERSL-R-181031RL-B Model Construction Report.

Implementation steps

Step 01: After installation of SWAN setup, open the swan.exe 



```
SWAN
Simulating WAVes Nearshore, version 41.20A
Copyright (C) 1993-2018 Delft University of Technology
Usage: swanrun inputfile
C:\>
```

After following the steps of SWAN installation, this step allows user to open SWAN command line interface.

Step 02: After copying files from attached .zip file, go to the working directory by typing “cd <space> file path” (e.g: cd C:\Users\XXXX\Desktop\Test_SL)

```
C:\> SWAN

Simulating WAVes Nearshore, version 41.20A
Copyright (C) 1993-2018 Delft University of Technology

Usage: swanrun inputfile

C:\>cd C:\Users\Ravindu Lokuliyana\Desktop\Test_SL
```

With this step, user specifies the working directory of SWAN model to perform all computations. All required input files with SWAN command file (TestSL.swn) should be contained in this directory.

Step 03: To run the model, type “swanrun TestSL” on the command prompt

```
C:\> SWAN - swanrun TestSL

Simulating WAVes Nearshore, version 41.20A
Copyright (C) 1993-2018 Delft University of Technology

Usage: swanrun inputfile

C:\>cd C:\Users\Ravindu Lokuliyana\Desktop\Test_SL
C:\Users\Ravindu Lokuliyana\Desktop\Test_SL>swanrun TestSL

SWAN is preparing computation

+SWAN is processing output request 1
+SWAN is processing output request 2
+SWAN is processing output request 3
+time 20130401.010000 , step 1; iteration 1
+time 20130401.020000 , step 2; iteration 1
+time 20130401.030000 , step 3; iteration 1
+time 20130401.040000 , step 4; iteration 1
+time 20130401.050000 , step 5; iteration 1
```

This is the step when SWAN starts the computations under the defined conditions of .swn file (TestSL.swn).

Step 04: After finishing all iterations model will create the output files of **.mat** and **.dat** files (TestSL.mat, P1x1.dat, P2x1.dat). Other than that, SWAN also creates a **.prt** file (TestSL.prt)

In this initial model running, two types of output files can be obtained as discussed under the Section 3.2.6 in WERSL-R-181031RL-B Model Construction Report. TestSL.mat consists with the spatial outputs of significant wave height, mean wave direction, mean absolute wave period and directional spreading. In addition P1x1.dat and P2x1.dat files are isolated location outputs, consist with the same spatial output parameters. The **.prt** file is an overview of the actual physical and numerical parameters to be used in the simulation run, and possibly warning and error messages.

Visualizing results

After completion of model running, the results can be visualized through the developed Matlab functions (attached in DVD). Mainly, these results can be implemented as spatial and location outputs. Following are the used Matlab

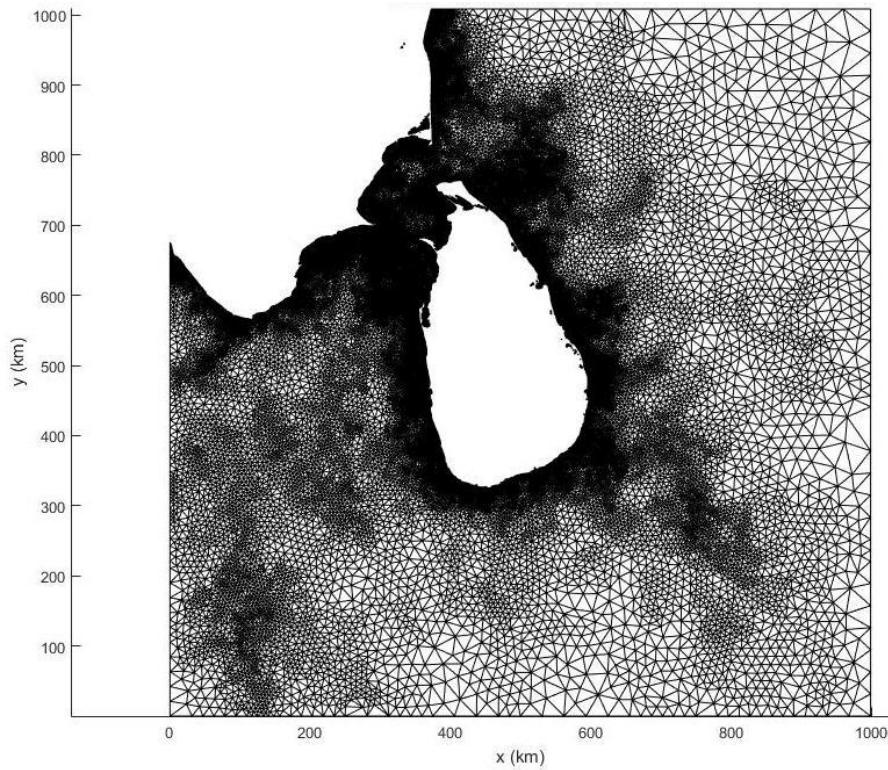
01. Plotgrid.m

This Matlab function plots unstructured grid generated by TRIANGLE grid generator.

With the use of TRIANGLE generated files with basename 'TestSL.2', ('TestSL.2.node' and 'TestSL.2.ele'), this Matlab function has the ability of plotting unstructured grid of SWAN computational area.

e.g. To make a plot of the unstructured grid, give the following command in Matlab command prompt:

plotgrid ('TestSL.2')



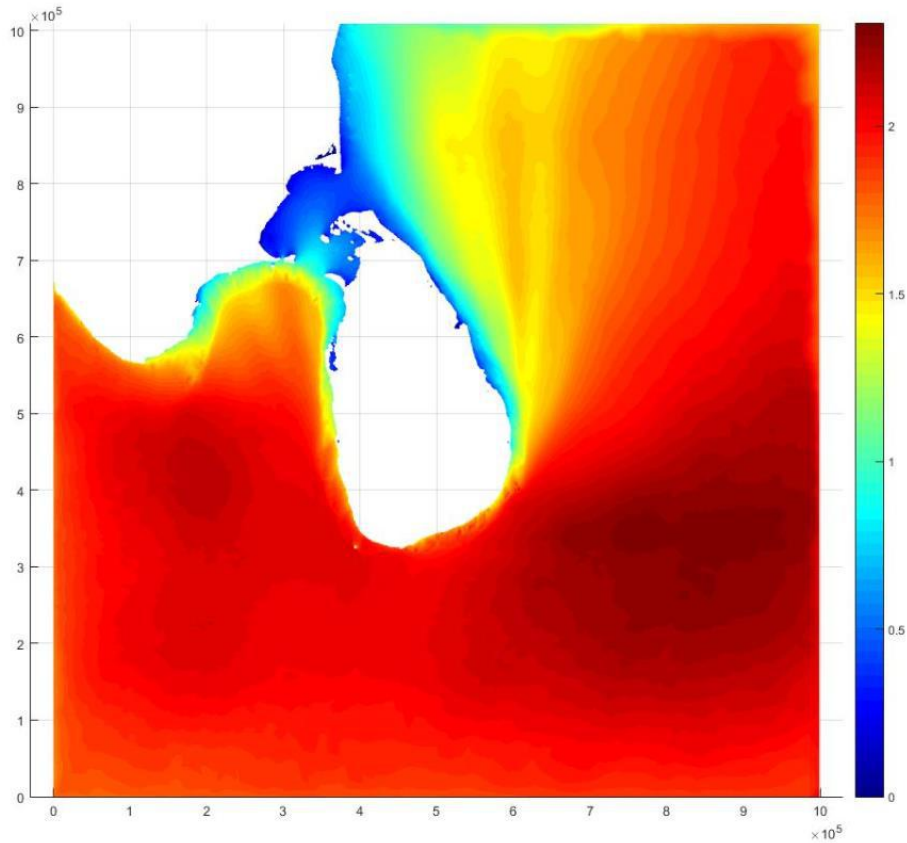
02. Plotswan.m

This Matlab function plots **a wave parameter on unstructured grid**

With the use of SWAN generated binary Matlab file called 'TestSL.mat' and 'TRIANGLE' generated files with basename 'TestSL.2', ('TestSL.2'.node' and 'TestSL.2.ele'), this Matlab function has the ability of plotting any defined output wave parameter.

e.g. To make a plot of the significant wave height for 01.10.2013 00:00h, give the following command in Matlab:

```
plotunswan('TestSL','TestSL.2','Hsig_20131001_0000')
```



03. Plotlocation.m

This Matlab function plots the location outputs of significant wave height and wave period of the SWAN model outputs.

With the use of SWAN generated binary Matlab file called 'P1x1.dat' and 'P1x1.dat' , this Matlab function has the ability of plotting any defined output location wave parameters of significant wave height and wave period.

e.g. To make a plot of the significant wave height from the starting date 01.04.2013, give the following command in Matlab:

plotlocation ('P1x1.dat','SWH', 20130401)

Example

SWAN model setup for the final validation

```
PROJ 'Test_SL' 'TSL'

SET LEVEL 0.0
SET NOR 90.0
SET DEPMIN 0.0
SET RHO 1025.0
SET CARTESIAN

MODE NONSTATIONARY TWODIMENTIONAL
COORDINATES CARTESIAN

CGRID UNSTRUCTURED CIRCLE 24 0.0345 0.5473 29
READ UNSTRUCTURED triangle 'Test_SL.2'

INPGRID BOTTOM -276991.4 -167068.1 0.0 2885 2691 500.000 500.000
READ BOTTOM 1.0 'Test_SL.2.bot' 3 0 FREE

INPGRID WIND -277453.4 -166605.5 0.0 52 48 27745.500 28519.500 EXC -99
NONSTAT 20130401.000000 6.0 HR 20140401.000000
READ WIND 1.0 'Test_SL_wind.dat' 2 0 0 0 FREE

INPGRID CURRENT -138727.4 -194358.0 0.0 23 23 55491.008 56838.063 EXC -99
NONSTAT 20130901.000000 3.0 HR 20140301.000000
READ CURRENT 1.0 'Test_SL_current.dat' 2 0 0 0 FREE

BOU SHAP JONSWAP PEAK DSPR DEGREES

BOU SIDE 5 CLOCKW VAR FILE &
499416.6 'N_81_12_N.spc' 1 &
665889.6 'N_82.5_12_N.spc' 1

BOU SIDE 3 CCW VAR FILE &
166835.0 'E_85.5_4.5_E.spc' 1 &
334012.7 'E_85.5_6_E.spc' 1 &
501651.8 'E_85.5_7.5_E.spc' 1 &
669869.4 'E_85.5_9_E.spc' 1 &
838786.7 'E_85.5_10.5_E.spc' 1 &
1008526.1 'E_85.5_12_E.spc' 1

BOU SIDE 2 CLOCKW VAR FILE &
166835.0 'W_76.5_4.5_W.spc' 1 &
334012.7 'W_76.5_6_W.spc' 1 &
501651.8 'W_76.5_7.5_W.spc' 1

BOU SIDE 4 CCW VAR FILE &
-0.4 'S_76.5_3_S.spc' 1 &
166471.6 'S_78_3_S.spc' 1 &
332944.6 'S_79.5_3_S.spc' 1 &
499416.6 'S_81_3_S.spc' 1 &
```

```
665889.6 'S_82.5_3_S.spc' 1 &
832360.6 'S_84_3_S.spc' 1 &
998833.6 'S_85.5_3_S.spc' 1

GEN3 KOMEN 2.36e-05 3.02e-03 AGROW 0.0015

WCAPPING KOMEN 2.36e-05 3.02e-03 2.0 1.0 1.0

QUADRUPL 1 0.25 3.00e+07 5.5 0.833333 -1.25

BREAKING CONSTANT 1.00 0.73

FRICTION JONSWAP CONSTANT 0.038

TRIAD 1 0.8 2.5 0.95 0.00

DIFFRACTION 1 0.00 0.00 1.00

POINTS 'P1x1' 450585.0 323970.2
TABLE 'P1x1' NOHEAD 'PN1.dat' HSIGN DIR TMM10 FSPR DSPR TM01 TM02 BOTLEV
OUTPUT 20130901.000000 1.0 HR

POINTS 'P2x1' 508295.4 345173.1
TABLE 'P2x1' NOHEAD 'PN2.dat' HSIGN DIR TMM10 FSPR DSPR TM01 TM02 BOTLEV
OUTPUT 20130401.000000 1.0 HR

TEST 1,0
COMPUTE NONSTAT 20130401.000000 1.0 HR 20140401.000000
STOP
```

Note: Above SWAN model setup has only considered the validation of SCSIO buoy location.

Descriptions of SWAN commands

PROJECT 'name' 'nr'

PROJECT	with this command, user defines a number of strings to identify the SWAN run
'name'	the name of the project, at most 16 characters long. 'TestSL' used as the name of the project
'nr'	the run identification to distinguish this run among other runs for the same project; it is at most 4 characters long. It is the only required information in this command. (e.g. 'TSL')

SET [level] [nor] [depmin] [rho]
SET CARTesian

SET	with this optional command the user assigns values to various general parameters. All default values of the 'SET' command are used for final validation.
[level]	increase in water level that is constant in space and time can be given with this option, [level] is the value of this increase (in m). Default: [level] = 0.
[nor]	direction of North with respect to the x-axis (measured counterclockwise); Default [nor] = 90°
[depmin]	threshold depth (in m). Default: [depmin] = 0.05
[rho]	is the water density ρ (in kg/m ³). Default: [rho] = 1025

CARTesian	CARTESIAN indicates that the Cartesian convention for wind and wave direction (SWAN input and output) is used.
-----------	--

MODE NONSTATIONARY TWODIMENTIONAL

COORDINATES CARTESIAN

MODE	Model run has set to nonstationary and two-dimensional (2D-mode).
COORDINATES CARTESIAN	Cartesian coordinates system has used for the model

CGRID UNSTRUCTURED CIRCLE [mdc][flow][fhig][msc]

READ UNSTRUCTURED TRIAngle 'fname'.

CGRID	With this required command the user defines the geographic location, size, resolution and orientation of the computational grid in the problem coordinate system
UNSTRUCTURED	this option indicates that the computational grid is to be taken as unstructured
CIRCLE	this option indicates that the spectral directions cover the full circle. This option is default.
[mdc]	number of meshes in θ space. In the case of CIRCLE, this is the number of subdivisions of the 360 degrees of a circle. [mdc] = 24 i.e. no of directions used in ECMWF ERA-Interim two-dimensional spectral dataset
[flow]	lowest discrete frequency that is used in the calculation (in Hz). [flow] = 0.0345 i.e. lowest discrete frequency that is used in ECMWF ERA-Interim two-dimensional spectral dataset
[fhig]	highest discrete frequency that is used in the calculation (in Hz).

	[fhigh] = 0.5473 i.e. highest discrete frequency that is used in ECMWF ERA-Interim two-dimensional spectral dataset
[msc]	one less than the number of frequencies. This defines the grid resolution in frequency-space between the lowest discrete frequency [flow] and the highest discrete frequency [fhigh]. [msc]= 29 i.e. one less than the number of frequencies that is used in ECMWF ERA-Interim two-dimensional spectral dataset
READ UNSTRUCTURED	With this command (required if the computational grid is unstructured; not allowed in case of a regular or curvilinear grid) the user controls the reading of the (x, y) co-ordinates of the vertices including boundary markers and a connectivity table for triangles (or elements).
TRIANGLE	the necessary grid information is read from two files as produced by Triangle. The .node and .ele files are required. The basename of these files must be indicated with parameter 'fname'.
'fname'	basename of the required files, i.e. without extension. fname = TestSL

INPGRID BOTTOM REG [xpinp] [ypinp] [alpinp] [mxinp] [myinp] [dxinp] [dyinp]

INPGRID	With this required command the user defines the geographic location, size and orientation of bathymetry grid.
BOTTOM	defines the input grid of the bottom level.
[xpinp]	geographic location (x-coordinate) of the origin of the input grid in problem coordinates (in m) xpinp = -276991.4 m i.e. used bathymetric grid has larger spatial area than computational grid

[ypinp]	geographic location (y-coordinate) of the origin of the input grid in problem coordinates (in m) ypinp = -167068.1 m i.e. used bathymetric grid has larger spatial area than computational grid
[alpinp]	direction of the positive x-axis of the input grid alpinp = 0 i.e. no change of direction
[mxinp]	number of meshes in x-direction of the input grid [mxinp] = 2885
[myinp]	number of meshes in y-direction of the input grid [myinp] = 2691
[dxinp]	mesh size in x-direction of the input grid [dxinp] = 500 m i.e. distance of interpolated regular bathymetry grid (x-direction)
[dyinp]	mesh size in y-direction of the input grid [dyinp] = 500 m i.e. distance of interpolated regular bathymetry grid (y-direction)

READ BOTTOM [fac] 'fname1' [idla] [nhedf] ([nhedt]) ([nhedvec]) FREE

READ	With this required command the user controls the reading of values of the indicated variables from bathymetry data file.
BOTTOM	with this option the user indicates that bottom levels (in m) are to be read from file.
[fac]	SWAN multiplies all values that are read from file with [fac] Default [fac] = 1
'fname1'	name of the bathymetric data file. fname1 = Test_SL.2.bot

[idla]	prescribes the order in which the values of bottom levels and other fields should be given in the file. [idla] = 3 i.e. SWAN reads the map from left to right starting in the lower-left-hand corner of the map.
[nhedf]	is the number of header lines at the start of the file. alpinp = 0 i.e. no header files are involved
[nhedt]	only if variable is time dependent: number of header lines in the file at the start of each time level
[nhedvec]	for each vector variable: number of header lines in the file at the start of each component [nhedvec] = 0
FREE	With this option the user indicates that the values are to be read with free format.

INPGRID WIND [xpinp] [ypinp] [alpinp] [mxinp] [myinp] [dxinp] [dyinp] NONSTAT
[tbeginp] [deltinp] SEC|MIN|HR|DAY [tendinp]

INPGRID	With this required command the user defines the geographic location, size and orientation of bathymetry grid.
WIND	defines the input grid of the wind data.
[xpinp]	geographic location (x-coordinate) of the origin of the input grid in problem coordinates (in m) xpinp = - 277453.4 m i.e. used wind grid has larger spatial area of computational grid
[ypinp]	geographic location (y-coordinate) of the origin of the input grid in problem coordinates (in m) ypinp = - 166605.5 m i.e. used wind grid has larger spatial area of computational grid

[alpinp]	direction of the positive x-axis of the input grid alpinp = 0 i.e. no change of direction
[mxinp]	number of meshes in x-direction of the input grid [mxinp] = 52
[myinp]	number of meshes in y-direction of the input grid [myinp] = 48
[dxinp]	mesh size in x-direction of the input grid [dxinp] = 27745.5 m i.e. distance of interpolated regular wind grid having 0.25° longitude space (x-direction)
[dyinp]	mesh size in y-direction of the input grid [dyinp] = 28519.5 m i.e. i.e. distance of interpolated regular wind grid having 0.25° latitude space (y-direction)
NONSTAT	wind variable is nonstationary (given in a time sequence of fields)
[tbeginp]	begin time of the first field of the variable [tbeginp] = 20130401.000000 (ISO-notation)
[deltinp]	time interval between wind fields [deltinp] = 6.0 HR
[tendinp]	end time of the last field of the variable [tendinp] = 20140401.000000 (ISO-notation)

```
READ WIND [fac] 'fname1' idla] [nhedf] ([nhedt]) (nhedvec]) FREE
```

READ	With this required command the user controls the reading of values of the indicated variables from wind data file.
WIND	With this option SWAN reads first all x-components and then all y-component.

[fac]	SWAN multiplies all values that are read from file with [fac] Default[fac] = 1
'fname1'	name of the wind data file. 'fname1' = 'Test_SL_wind.dat'
[idla]	prescribes the order in which the values of bottom levels and other fields should be given in the file. [idla] = 1 i.e. SWAN reads the map from left to right starting in the upper-left-hand corner of the map
[nhedf]	is the number of header lines at the start of the file.
[nhedt]	only if variable is time dependent: number of header lines in the file at the start of each time level [nhedt] = 0
[nhedvec]	for each vector variable: number of header lines in the file at the start of each component [nhedvec] = 0
FREE	With this option the user indicates that the values are to be read with free format.

INPGRID CURRENT [xpinp] [ypinp] [alpinp] [mxinp] [myinp] [dxinp] [dyinp] NONSTAT
[tbeginp] [deltinp] SEC|MIN|HR|DAY [tendinp]

INPGRID	With this required command the user defines the geographic location, size and orientation of bathymetry grid.
CURRENT	defines the input grid of the current data.
[xpinp]	geographic location (x-coordinate) of the origin of the input grid in problem coordinates (in m) xpinp = -138727.4 m i.e. used current grid has larger spatial area of computational grid

[ypinp]	<p>geographic location (y-coordinate) of the origin of the input grid in problem coordinates (in m)</p> <p><code>ypinp = -194358.5 m</code> i.e. used current grid has larger spatial area of computational grid</p>
[alpinp]	<p>direction of the positive x-axis of the input grid</p> <p><code>alpinp = 0</code> i.e. no change of direction</p>
[mxinp]	<p>number of meshes in x-direction of the input grid</p> <p><code>[mxinp] = 23</code></p>
[myinp]	<p>number of meshes in y-direction of the input grid</p> <p><code>[myinp] = 23</code></p>
[dxinp]	<p>mesh size in x-direction of the input grid</p> <p><code>[dxinp] = 27745.5 m</code> i.e. distance of interpolated regular current grid having 0.5° longitude space (x-direction)</p>
[dyinp]	<p>mesh size in y-direction of the input grid</p> <p><code>[dyinp] = 28519.5 m</code> i.e. i.e. distance of interpolated regular current grid having 0.5° latitude space (y-direction)</p>
NONSTAT	<p>current variable is nonstationary (given in a time sequence of fields)</p>
[tbeginp]	<p>begin time of the first field of the variable</p> <p><code>[tbeginp] = 20130401.000000</code> (ISO-notation)</p>
[deltinp]	<p>time interval between wind fields</p> <p><code>[deltinp] = 6.0 HR</code></p>
[tendinp]	<p>end time of the last field of the variable</p> <p><code>[tendinp] = 20140401.000000</code> (ISO-notation)</p>

READ CURRENT [fac] 'fname1' [idla] [nhedf] ([nhedt]) (nhedvec) FREE

READ	with this required command the user controls the reading of values of the indicated variables from current data file.
CURRENT	with this option SWAN reads first all x-components and then all y-component.
[fac]	SWAN multiplies all values that are read from file with [fac] Default[fac] = 1
'fname1'	name of the current data file. 'fname1' = 'Test_SL_current.dat'
[idla]	prescribes the order in which the values of bottom levels and other fields should be given in the file. [idla] = 1 i.e. SWAN reads the map from left to right starting in the upper-left-hand corner of the map
[nhedf]	is the number of header lines at the start of the file.
[nhedt]	only if variable is time dependent: number of header lines in the file at the start of each time level [nhedt] = 0
[nhedvec]	for each vector variable: number of header lines in the file at the start of each component [nhedvec] = 0
FREE	With this option the user indicates that the values are to be read with free format.

BOUnd SHAP JONswap [gamma] PEAK DSPR DEGREES

BOUnd SHAP	defines the shape of the spectra (both in frequency and direction) at the boundary of the computational grid
JONswap	JONSWAP spectrum will be used. This is default

[gamma]	peak enhancement parameter of the JONSWAP spectrum.
PEAK	the peak period is used as characteristic wave period
DSPR	option for expressing the width of the directional distribution
DEGREES	the directional width is expressed in terms of the directional standard deviation

BOUndspec SIDE [k] CCW|CLOCKwise VAR FILE < [len] 'fname' [seq] >

BOUndspec	defines parametric spectra at the boundary.
SIDE	the boundary is one full side of the computational grid
[k]	indicates on which side of the unstructured grid the boundary condition is applied. In the initial model: [k] = 2 ; Western boundary [k] = 3 ; Eastern boundary [k] = 4 ; Southern boundary [k] = 5 ; Northern boundary
CCW CLOCKwise	The length along a SIDE is measured in clockwise or counterclockwise direction, depending on the options CCW or CLOCKwise
VAR	with this option the wave spectra can vary along the side.
FILE	means that the incoming wave data are read from a file.
[len]	is the distance from the first point of the side
'fname'	name of the file containing the boundary condition e.g. 'N_81_12_N.spc', 'E_85.5_4.5_E.spc'
[seq]	sequence number of geographic location in the file.

GEN3 KOMEN [c_{ds2}] [st_{pm}]

GEN3	With this command the user indicates that SWAN should run in third-generation mode for wind input, quadruplet interactions and whitecapping.
KOMEN	linear growth
[c _{ds2}]	coefficient for determining the rate of whitecapping dissipation Default: [c _{ds2}] = 2.36e-5.
[st _{pm}]	value of the wave steepness for a Pierson-Moskowitz spectrum Default: [st _{pm}] = 3.02e-3.

WCAP KOMen [c_{ds2}] [st_{pm}] [pow_{st}] [delta] [pow_k]

WCAPping	With this command the user can influence whitecapping which is usually included in the computations.
KOMEN	whitecapping according to Komen et al. (1984) is applied
[c _{ds2}]	coefficient for determining the rate of whitecapping dissipation Default: [c _{ds2}] = 2.36e-5.
[st _{pm}]	value of the wave steepness for a Pierson-Moskowitz spectrum Default: [st _{pm}] = 3.02e-3.
[pow _{st}]	power of steepness normalized with the wave steepness of a Pierson-Moskowitz spectrum. Default: [pow _{st}] = 2
[delta]	coefficient which determines the dependency of the whitecapping on wave number. Default: [delta] = 1
[pow _k]	power of wave number normalized with the mean wave number. Default: [pow _k] = 1.

QUADrupl [iquad] [lambda] [cn₁₄] [csh₁] [csh₂] [csh₃]

QUADrupl	With this option the user can influence the computation of nonlinear quadruplet wave interactions.
----------	--

[iquad]	the quadruplets can be integrated by four different numerical procedures [iquad] = 2 (fully explicit computation of the nonlinear transfer with DIA per sweep)
[lambda]	coefficient for quadruplet configuration in case of DIA. Default: [lambda]= 0.25.
[cnl4]	proportionality coefficient for quadruplet interactions in case of DIA. Default: [cnl4] = 3×10^7 .
[csh1]	coefficient for shallow water scaling in case of DIA. Default: [csh1] = 5.5.
[csh2]	coefficient for shallow water scaling in case of DIA. Default: [csh2] = 0.833333.
[csh3]	coefficient for shallow water scaling in case of DIA. Default: [csh3] = -1.25.

BRE CON [alpha] [gamma]

BRE	With this command the user can influence depth-induced wave breaking in shallow water.
CON	indicates that a constant breaker index is to be used
[alpha]	proportionality coefficient of the rate of dissipation. Default: [alpha]= 1.0.
[gamma]	the breaker index, i.e. the ratio of maximum individual wave height over depth. Default: [gamma]= 0.73.

FRICtion JONswap CONstant [cfjon]

BRE	With this optional command the user can activate bottom friction
JONswap	indicates that the semi-empirical expression derived from the JONSWAP results for bottom friction dissipation should be activated

CONStant	this default option indicates that the JONSWAP coefficient is constant
[cfjon]	coefficient of the JONSWAP formulation. Default: [cfjon]= 0.038.

TRIad [itriad] [trfac] [cutfr]

TRIad	With this command the user can activate the triad wave-wave interactions using either the LTA method or the SPB method.
[itriad]	indicates the approximation method for the triad computation: [itriad] = 1 the LTA method of Eldeberky (1996)
[trfac]	proportionality coefficient. Its value is 0.8 in case of LTA [trfac]= 0.8.
[cutfr]	controls the maximum frequency that is considered in the LTA computation. The value of [cutfr] is the ratio of this maximum frequency over the mean frequency. Default: [cutfr] = 2.5.

TURBulence [ctb]

TURBulence	With this optional command the user can activate turbulent viscosity
[ctb]	the value of the proportionality coefficient appearing in the energy dissipation term. Default: [ctb]= 0.01

DIFFRac [idiffr]

DIFFRac	If this optional command is given, the diffraction is included in the wave computation.
[idiffr]	indicates the use of diffraction. Default: [idiffr] =1.

BLOCK 'sname' HEADER | NOHEADER 'fname' (LAY-OUT [idla] XP YP HSIGN DIR TMM10
 FSPR DSPR OUTPUT ([unit]) (OUTPUT [tbegblk] [deltblk] SEC|MIN|HR|DAY)

POINTS 'sname' < [xp] [yp] >

TABLE 'sname' HEADER | NOHEADER 'fname' HSIGN DIR TMM10 FSPR DSPR OUTPUT
 ([unit]) (OUTPUT [tbegblk] [deltblk] SEC|MIN|HR|DAY)

BLOCK	With this optional command the user indicates that one or more spatial distributions should be written to a file.
'sname'	name of frame or group 'sname' = 'COMPGRID'
HEADER	with this option the user indicates that the output should be written to a file with header lines.
NOHEADER	with this option the user indicates that the output should be written to a file without header lines.
'fname'	name of the data file where the output is to be written to. 'fname' = 'TESTSL.mat'
LAY-OUT	with this option the user can prescribe the lay-out of the output to file with the value of [idla]
[idla]	in case of a generated binary MATLAB file option 3 is recommended
XP	user instructs SWAN to write the x-coordinate in the problem coordinate system of the output location
YP	user instructs SWAN to write the y-coordinate in the problem coordinate system of the output location
HSIGN	output of significant wave height (in m).
DIR	output of mean wave direction
TMM10	mean absolute wave period (in s).
FSPR	the normalized width of the frequency spectrum.

DSPR	directional spreading of the waves (in degrees).
OUTPUT	the user requests output at various times
[tbegblk]	begin time of the first field of the variable [tbeginp] = 20130401.000000 (ISO-notation)
[deltblk]	time interval between wind fields [deltinp] = 6.0 HR
POINTS	With this optional command the user defines a set of individual output locations (points).
'sname'	name of the points
[xp] [yp]	problem coordinates of one output location
TABLE	With this optional command the user indicates that for each location of the output location set 'sname' one or more variables should be written to a file.
'sname'	name of the set of POINTS, CURVE, FRAME or GROUP

TEST [itest] [itrace]

TEST	If SWAN produces unexpected results, this optional command can be used to instruct the program to produce intermediate results during a SWAN run
[itest]	the level of test output. For values under 100 the amount is usually reasonable, Default: [itest]=1
[itrace]	SWAN writes a message (name of subroutine) to the PRINT file at the first [itrace] entries of each subroutine Default: [itrace]=0

COMPUte NONSTAT [tbegc] [deltc] HR [tendc]

STOP

COMPUte	This command orders SWAN to start the computation(s).
NONSTAT	a nonstationary computation is to be made
[tbegc]	the start date and time of the nonstationary computation [tbegc]= 20130401.000000
[deltc]	the time step of the nonstationary computation, the unit is indicated in the next option, [deltc] = 24.0 HR
[tendc]	the end time of the nonstationary computation [tendc] = 20140401.000000
STOP	This required command marks the end of the commands in the command file